



# LUND UNIVERSITY

## Hydrological Seasonal Forecasting

Foster, Kean

2019

*Document Version:*

Publisher's PDF, also known as Version of record

[Link to publication](#)

*Citation for published version (APA):*

Foster, K. (2019). *Hydrological Seasonal Forecasting*. Water Resources Engineering, Lund University.

*Total number of authors:*

1

### General rights

Unless other specific re-use rights are stated the following general rights apply:

Copyright and moral rights for the publications made accessible in the public portal are retained by the authors and/or other copyright owners and it is a condition of accessing publications that users recognise and abide by the legal requirements associated with these rights.

- Users may download and print one copy of any publication from the public portal for the purpose of private study or research.
- You may not further distribute the material or use it for any profit-making activity or commercial gain
- You may freely distribute the URL identifying the publication in the public portal

Read more about Creative commons licenses: <https://creativecommons.org/licenses/>

### Take down policy

If you believe that this document breaches copyright please contact us providing details, and we will remove access to the work immediately and investigate your claim.

LUND UNIVERSITY

PO Box 117  
221 00 Lund  
+46 46-222 00 00

# Hydrological Seasonal Forecasting

KEAN FOSTER

FACULTY OF ENGINEERING | LUND UNIVERSITY





# Hydrological Seasonal Forecasting

Kean Foster



**LUND**  
UNIVERSITY

DOCTORAL DISSERTATION

by due permission of the Faculty of Engineering, Lund University, Sweden.  
To be defended publically at the Department of Building and Environmental  
Technology, John Erikssons väg 1,

In room V:D at 10:15, on the 27<sup>th</sup> September 2019.

*Faculty opponant*

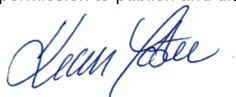
Dr. Michael Butts

RnD programme manager – Water Resources at DHI, Denmark

|   |                             |   |       |
|---|-----------------------------|---|-------|
| <b>Organization</b><br>LUND UNIVERSITY<br>Water Resources Engineering<br>Box 118<br>SE-221 00 Lund, Sweden  |                             | <b>Document name</b><br>Doctoral Dissertation           |       |
|   |                             | <b>Coden:</b> LUTVDG/TVVR-1066 (2019)                   |       |
| <b>Author:</b> Kean Foster  |                             | <b>Date of issue:</b> 2019-09-19                        |       |
|   |                             | <b>Sponsoring organizations:</b> Formas, SMHI, and HUVA |       |
| <b>Title and subtitle:</b> Hydrological seasonal forecasting  |                             |   |       |
| <b>Abstract</b><br>In Sweden, almost half of the electricity produced comes from hydropower. However, the amount of water in the reservoir catchments is not evenly distributed throughout the year. During the colder months, precipitation usually falls as snow and accumulates into a snowpack. This frozen water is not available to the energy producers until the spring snow melt when as much as 70% of the annual discharge will be generated. This can create a situation where there is a shortage of water resources during the winter when demand and energy prices are high, and a surplus during the spring and summer when demand and prices are lower. Hydropower plant operators try to minimize this asymmetric distribution through regulation of reservoir storages and hydrological forecasts are crucial for this.<br><br>However, the predominant method for hydrological seasonal forecasting the spring flood period in Scandinavia is the Ensemble Streamflow Prediction (ESP) approach. ESP uses historical observations of precipitation and temperature from previous years (a so-called historical ensemble) to force the hydrological model. The problem is that these forecasts are climatological in character, i.e. it performs well when the weather during the forecast period evolves normally, however if the development of weather conditions is not "normal", the season forecast will be more or less wrong.<br><br>The thesis of this work is that this is possible to improve seasonal forecasts so that they still have skill even when the weather deviates from the normal climate during the forecast period. By better understanding what affects the variability in the hydrology and using that information to inform how to modify or replace the ESP forecasting approach, it is possible to real skilful improvements over the ESP.<br><br>In this work it is shown that selected teleconnection patterns are the leading source of variability in the seasonal river discharge volumes in Sweden. In the case of the spring flood period in northern Sweden, these are the North Atlantic Oscillation, Arctic Oscillation, and Scandinavian pattern. With the help of information garnered by investigating these connections it is possible to modify different forecast modelling chains, that on their own show limited (if any) skill over ESP, and combine them into a multi-chain forecast system that does show skill over the ESP. A Multi-model ensemble of modelling chains made up of three different individual modelling chains, using a simple weighting scheme to combine them, is able to improve the general skill of spring flood volume forecasts and improve their ability to predict non-normal events. |                             |   |       |
| <b>Key words</b>  |                             |   |       |
| Classification system and/or index terms (if any)   |                             |   |       |
| Supplementary bibliographical information   |                             | <b>Language:</b> English                                |       |
| <b>ISSN and key title</b>   |                             | <b>ISBN:</b> 978-91-7623-986-5                          |       |
| Recipient's notes   | <b>Number of pages:</b> 218 |   | Price |
|   | Security classification     |   |       |

I, the undersigned, being the copyright owner of the abstract of the above-mentioned dissertation, hereby grant to all reference sources permission to publish and disseminate the abstract of the above-mentioned dissertation.

Signature



Date 2019-09-19

# Hydrological Seasonal Forecasting

Kean Foster



**LUND**  
UNIVERSITY

Cover photo: “Umeälven at E45 near Storuman” by Lars Falkdalen Lindahl,  
used under CC BY-SA 3.0/Cropped and colour processed.

© Kean Foster, 2018, unless otherwise stated

Water Resources Engineering  
Department of Building and Environmental Technology  
Faculty of Engineering  
Lund University  
P.O. Box 118  
SE-221 00 LUND  
Sweden

CODEN: LUTVDG/TVRL-1066 (2018)  
ISBN: 978-91-7623-986-5  
ISSN: 1101-9824  
Report 1066

Printed in Sweden by Media-Tryck, Lund University  
Lund 2019



Intertek

MADE IN SWEDEN 

Media-Tryck is an environmental-  
ly certified and ISO 14001 certified  
provider of printed material.  
Read more about our environmental  
work at [www.mediatryck.lu.se](http://www.mediatryck.lu.se)

*In regione caecorum rex est luscus*

- Desiderius Erasmus



# Content

|  |           |
|--|-----------|
| Acknowledgements .....   | 8         |
| Populärvetenskaplig Sammanfattning .....                           | 9         |
| Abstract .....   | 11        |
| Papers .....   | 12        |
| Appended Papers .....  | 12        |
| Author's contributions to appended papers .....                    | 12        |
| Publications not included .....                                    | 13        |
| Journal Papers .....   | 13        |
| Conference papers and proceedings .....                            | 13        |
| Co-supervised Master thesis .....                                  | 14        |
| Abbreviations .....  | 15        |
| <b>Introduction .....</b>  | <b>17</b> |
| Background .....   | 17        |
| Objective and Scope .....  | 19        |
| Dissertation Structure .....                                       | 19        |
| <b>Literature Review .....</b>                                     | <b>21</b> |
| Seasonal Forecasting .....   | 21        |
| Meteorological seasonal forecasting .....                          | 21        |
| Hydrological seasonal forecasting .....                            | 24        |
| Teleconnection Patterns and Indices .....                          | 27        |
| North Atlantic Oscillation (NAO) and Arctic Oscillation (AO) ..... | 27        |
| East Atlantic Pattern (EA) .....                                   | 28        |
| East Atlantic-Western Russia Pattern (EAWR) .....                  | 30        |
| Scandinavian Pattern (SCA) .....                                   | 31        |
| Polar/Eurasia Pattern (POL) .....                                  | 32        |
| <b>Study Area and Datasets .....</b>                               | <b>33</b> |
| Study area .....   | 33        |
| Datasets .....   | 37        |
| Observation data .....   | 37        |
| Reanalysis data .....  | 40        |
| Seasonal hindcast data .....                                       | 41        |

|   |           |
|---|-----------|
| <b>Models and Methods .....</b>   | <b>45</b> |
| Rainfall-runoff model based ensemble modelling chains .....                                       | 45        |
| HBV .....   | 45        |
| Historical ensemble modelling chain (HE) .....  | 47        |
| Analogue ensemble modelling chain (AE) .....  | 49        |
| Dynamic ensemble modelling chain (DE) .....   | 52        |
| Statistically downscaled ensemble modelling chain (SE) .....                                      | 53        |
| Multi-model ensemble of modelling chains (ME) .....   | 56        |
| Bootstrapping .....   | 57        |
| Cross Validation .....  | 57        |
| Principal Component Analysis .....  | 58        |
| Cluster Analysis .....  | 59        |
| Wavelet Analysis .....  | 60        |
| Validation metrics .....  | 62        |
| <b>Results and Discussion .....</b>   | <b>63</b> |
| The individual modelling chains .....   | 63        |
| Historical ensemble .....   | 63        |
| Analogue ensemble .....   | 65        |
| Dynamical ensemble .....  | 67        |
| Statistical downscaling .....   | 68        |
| The spatio-temporal influence of atmospheric teleconnection patterns on hydrology in Sweden ..... | 71        |
| Clustering of Swedish hydrology .....   | 71        |
| Climate-streamflow connections .....  | 73        |
| Multi modelling chain ensembles (ME) .....  | 76        |
| The operational prototype .....   | 83        |
| Year-round forecasting: preliminary assessment .....  | 84        |
| <b>Conclusions and Outlook .....</b>  | <b>87</b> |
| <b>References .....</b>   | <b>89</b> |

# Acknowledgements

There are numerous people without whom this thesis may never have been written and to whom I am incredibly grateful. They are the proverbial giants upon whose shoulders I have been allowed to stand to see a little bit further.

I owe my deepest gratitude to Professor Cintia Bertacchi Uvo and Dr. Jonas Olsson, my supervisors. Without your guidance I would still be very lost in the academic wilderness. You have both been incredible mentors and role models for me during this work. Thank you for sharing your experience and knowledge with me, for guiding me when I was lost, for your patience when I was struggling, and for your enthusiasm and genuine desire to see me succeed.

I would also like to acknowledge the support I received from my many colleagues, both at SMHI and Lund University, thank you. You were there for me as a source of guidance, inspiration, and someone to talk to when things needed perspective.

Thanks are also due to the Swedish Research Council FORMAS and the Energiforsk programme HUCA (hydrologiskt utvecklingsarbete) for financial support without which much of this work would not have been possible.

Thank you to all my friends who have journeyed life with me. It is a great source of comfort to know that you are just a phone call or message away, ready and willing

Lastly, but by no means least, to my family. In particular Åsa, Troy, and Bailey, I owe you everything! Without you none of this would have been possible. You are the foundation upon which I have been able to build any and all of my successes. Your love, understanding, and support have been invaluable, especially during this work. To my parents, Chris and Norma, I am eternally grateful for your love and support and regret not being able to share this with you in person. To Carrie, Murray, and Shannon thank you for being who you are and for keeping me grounded like only siblings can. To my extended family thank you for helping to shape me into the person that I am today.

Thank you!

# Populärvetenskaplig Sammanfattning

I Sverige kommer nästan hälften av den elektricitet som produceras från vattenkraft. Dock är mängden vatten i kraftverksdammarnas tillrinningsområden inte jämnt fördelad över hela året. Under de kalla vintermånaderna faller nederbörden oftast i form av snö som samlas på marken. Detta frusna vatten blir inte tillgängligt för energiproducenterna förrän snön smälter på våren, under vårfloden. Detta kan skapa en situation där det finns brist på vatten för att producera el under vintern, då både behovet och energipriset är högt, och ett överskott under våren och sommaren då behovet och priset är lägre. Kraftverksoperatörer försöker därför minimera denna asymmetriska fördelning genom att lagra så mycket som möjligt av vattnet från vårfloden i sina reservoarer för att kunna använda det för elproduktion under det kommande vinterhalvåret.

Hydrologiska säsongsprognoser, dvs. vattenflödesprognoser som är längre än två veckor men kortare än ett år, är viktiga för kraftbolagen när de planerar sin verksamhet. De måste veta hur mycket lagringsutrymme som de måste göra tillgängligt och när detta måste ske, så att de kan maximera sin användning av de vattenresurser som frigörs under vårfloden. SMHIs nuvarande hydrologiska säsongsprognoser använder en klimatologisk strategi. Detta innebär att historiska observationer av nederbörd och temperatur från tidigare år (en s.k. historisk ensemble), oftast för perioden från början av februari till slutet av juli, används som drivdata för en hydrologisk datormodell. Hydrologiska modeller använder främst nederbörd och temperatur som indata för att beräkna hur det vatten som når markytan, via nederbörd eller snösmältning, transporteras genom marken för att så småningom nå en sjö eller ett vattendrag och påverka flöden och vattenstånd. Om antalet år i den historiska ensemblen är tillräckligt stort blir den resulterande prognosen klimatologisk (normal) till sin karaktär, d.v.s. den presterar bra om vädret under prognosperioden avspeglar klimatet, är " normalt ". Men om utvecklingen av väderförhållandena inte är " normalt " kommer säsongsprognosen att slå mer eller mindre fel.

Målet med denna avhandling är att ta fram säsongsprognoser som kan presera bra även när vädret under prognosperioden avviker från det normala klimatet. Detta kan antas vara möjligt genom förekomsten av s.k. klimatmönster. Klimatmönster är tillfälliga men långvariga och återkommande fenomen i atmosfären som påverkar vädret på långa avstånd. Antagandet är att olika klimatmönster styr variationerna i Sveriges vattenflöden under olika perioder av året och att information om dessa mönster kan användas för att förbättra hydrologiska säsongsprognoser. Genom att använda information om hur, var och när dessa klimatmönster påverkar flöden runtom i Sverige är det möjligt att utveckla ett nytt säsongsprognossystem. I detta

system kombineras tre nya metoder för säsongsprognoser till en multi-metod. De tre metoderna är:

- Beräkna och använd statistiska samband som direkt kopplar vårflodens totala volym till klimatmönstren för att göra prognoser. I denna metod används alltså ingen hydrologisk modell.
- Leta upp historiska år som kan antas representera vädret under det år prognosen gäller, t.ex. via likartade klimatmönster. Använd därefter uppmätt nederbörd och temperatur enbart från dessa år som indata till en hydrologisk modell.
- Numera finns väderprognoser som sträcker sig upp till ett år framåt i tiden. Använd dessa meteorologiska säsongsprognoser på nederbörd och temperatur som indata till en hydrologisk modell.

Fördelen med att använda olika modeller är att du utnyttjar principen 'massans vishet'. En enskild modell kan vara fel ibland men påverkan av detta fel minskar när prognosen kombineras med de från andra modeller. Detta resulterar i ett prognosystem som är mindre benäget att göra prognoser som är mycket felaktiga.

Genom att jämföra det nya multi-modell prognosystemet med den nuvarande verksamhetsmodellen är det möjligt att testa det tidigare nämnda antagandet. Resultaten visar att det nya systemet presterar bättre än det nuvarande systemet över sextio procent av tiden. Dessutom visar det nya multi-modell prognosystemet en förbättrad förmåga att förutse "icke-normala" händelser och det kan även minska volymfelet med i genomsnitt två procentenheter. Dessa och andra resultat i denna avhandling tyder på att detta arbete har betydande fördelar för vattenkraftindustrin genom att leverera förbättrade prognoser för att stödja deras verksamhet.

# Abstract

In Sweden, almost half of the electricity produced comes from hydropower. However, the amount of water in the reservoir catchments is not evenly distributed throughout the year. During the colder months, precipitation usually falls as snow and accumulates into a snowpack. This frozen water is not available to the energy producers until the spring snow melt when as much as 70% of the annual discharge will be generated. This can create a situation where there is a shortage of water resources during the winter when demand and energy prices are high, and a surplus during the spring and summer when demand and prices are lower. Hydropower plant operators try to minimize this asymmetric distribution through regulation of reservoir storages and hydrological forecasts are crucial for this.

However, the predominant method for hydrological seasonal forecasting the spring flood period in Scandinavia is the Ensemble Streamflow Prediction (ESP) approach. ESP uses historical observations of precipitation and temperature from previous years (a so-called historical ensemble) to force the hydrological model. The problem is that these forecasts are climatological in character, i.e. it performs well when the weather during the forecast period evolves normally, however if the development of weather conditions is not "normal", the season forecast will be more or less wrong.

The thesis of this work is that this is possible to improve seasonal forecasts so that they still have skill even when the weather deviates from the normal climate during the forecast period. By better understanding what affects the variability in the hydrology and using that information to inform how to modifying or replace the ESP forecasting approach, it is possible to real skilful improvements over the ESP.

In this work it is shown that selected teleconnection patterns are the leading source of variability in the seasonal river discharge volumes in Sweden. In the case of the spring flood period in northern Sweden, these are the North Atlantic Oscillation, Arctic Oscillation, and Scandinavian pattern. With the help of information garnered by investigating these connections it is possible to modify different forecast modelling chains, that on their own show limited (if any) skill over ESP, and combine them into a multi-chain forecast system that does show skill over the ESP. A Multi-model ensemble of modelling chains made up of three different individual modelling chains, using a simple weighting scheme to combine them, is able to improve the general skill of spring flood volume forecasts and improve their ability to predict non-normal events.

# Papers

## Appended Papers

- I. **Foster, K.L.** and Uvo, C.B., 2010. Seasonal streamflow forecast: A GCM multi-model downscaling approach. *Hydrology Research*, 41(6), pp.503-507.
- II. **Foster, K.**, Olsson, J. and Uvo, C.B., 2010. New approaches to spring flood forecasting in Sweden. *Vatten*, 66, pp.193-198.
- III. Olsson, J., Uvo, C.B., **Foster, K.** and Yang, W., 2016. Initial assessment of a multi-method approach to spring-flood forecasting in Sweden. *Hydrology and Earth System Sciences*, 20(2), pp.659-667.
- IV. **Foster, K.**, Uvo, C.B., and Olsson, J., 2016. The spatio-temporal influence of atmospheric teleconnection patterns on hydrology in Sweden. *Submitted to Climate Dynamics*.
- V. **Foster, K.**, Uvo, C.B. and Olsson, J., 2018. The development and evaluation of a hydrological seasonal forecast system prototype for predicting spring flood volumes in Swedish rivers. *Hydrology and Earth System Sciences*, 22(5), pp.2953-2970.

## Author's contributions to appended papers

**Paper I:** The author planned the work together with the co-author, performed the modelling and statistical analysis works, and wrote all sections of the paper. The author participated in discussions and technically revised the paper together with the co-author.

**Paper II:** The author planned and wrote the paper with contributions from the co-authors.

**Paper III:** The author helped to design and implemented the TCI and SE approaches and contributed to writing parts of the paper. The author participated in discussions and assisted in technically revising the paper with the other authors.

**Paper IV:** The author planned and wrote the paper together with the first co-author. The author performed the modelling and statistical analysis. The author participated in discussions and assisted in technically revising the paper with the other authors.

**Paper V:** The author planned the work, performed the modelling experiments and wrote all sections of the paper. The author participated in discussions and technically revised the paper together with the co-authors.

## Publications not included

### Journal Papers

- I. Rana, A., **Foster, K.**, Bosshard, T., Olsson, J. and Bengtsson, L., 2014. Impact of climate change on rainfall over Mumbai using Distribution-based Scaling of Global Climate Model projections. *Journal of Hydrology: Regional Studies*, 1, pp.107-128.
- II. Olsson, J. and **Foster, K.**, 2013. Short-term precipitation extremes in regional climate simulations for Sweden. *Hydrology Research*, 45(3), pp.479-489.
- III. Olsson, J., Arheimer, B., Borris, M., Donnelly, C., **Foster, K.**, Nikulin, G., Persson, M., Perttu, A.M., Uvo, C., Viklander, M. and Yang, W., 2016. Hydrological climate change impact assessment at small and large scales: key messages from recent progress in Sweden. *Climate*, 4(3), p.39.

### Conference papers and proceedings

- I. Olsson, J., Willén, U., and **Foster, K.**, 2011. Extreme short-term rainfall in regional climate model simulations for Sweden. *IUGG General Assembly, International Association of Hydrological Sciences (IAHS), 28 June-7 July, Melbourne, Australia.*
- II. **Foster, K.**, Olsson, J., Uvo, C.B., Yang, W. and Södling, J., 2012. A comparison of different approaches for forecasting spring floods in Sweden. *EGU General Assembly, 22-27 April, Vienna, Austria.*
- III. **Foster, K.**, Siergieieva, O., Correl, D., and Uvo, C.B., 2012. Long term variability of Swedish river runoff as represented by EC-EARTH in past and future climates. *XXVII Nordic Hydrological Conference (Nordic Water), 13-15 August, Oulu, Finland.*
- IV. **Foster, K.**, Olsson, J., Uvo, C.B., Yang W. and Södling, J., 2012. A comparison of different approaches for forecasting spring floods in Sweden and the feasibility of a multi-model forecast system, *XXVII Nordic Hydrological Conference (Nordic Water), 13-15 August, Oulu, Finland.*
- V. **Foster, K.**, Olsson, J., and Uvo, C.B., 2013. Climate and hydrology – understanding the engine that powers our rivers to improve seasonal forecasts. *2nd International Conference Energy & Meteorology, 25-28 June, Toulouse, France.*



- VI. Strömbäck, L., **Foster, K.**, and Rosberg, J., 2013. Data and Provenance Management for Climate Effect Studies. Adaption of Climate Data with Distribution Based Scaling for Hydrological Simulations. *Proceedings of the Fifth International Conference on Advances in Databases, Knowledge, and Data Applications, 27 Jan – 1 Feb, Seville, Spain.*
- VII. **Foster, K.**, and Uvo, C.B., 2013. A new approach to calibrating hydrological models: Using cross wavelet transforms to select calibration and validation periods. *IAHS - IAPSO - IASPEI Joint Assembly, 22-26 July Gothenburg, Sweden.*
- VIII. Bosshard T., **Foster K.**, Pechlivanidis I.G., Olsson, J., 2013. ‘Bias-correction of regional CORDEX projections over the Indian sub-continent’. *International Conference on Regional Climate, CORDEX2013, 4-7 November, Brussels, Belgium.*
- IX. **Foster, K.**, Uvo, C.B., Olsson, J., Bosshard, T., Berg, P., and Södling, J., 2015. A Climate Service Prototype for the Hydropower Industry: Using a Multi-Model Approach to Improve Seasonal Forecasts of the Spring Flood Period in Sweden. *AGU Fall Meeting, 14-18 December, San Francisco, USA.*
- X. **Foster, K.**, Uvo, C.B. and Olsson, J., 2016. The spatio-temporal impacts of selected climate circulation patterns on Swedish hydrology. *XXIX Nordic Hydrological Conference, 8-10 August 2016, Kaunas, Lithuania.*
- XI. **Foster, K.**, Uvo, C.B., Olsson, J., and Södling, J., 2016. The development and testing of a climate service prototype for the hydropower industry in Sweden. *XXIX Nordic Hydrological Conference, 8-10 August 2016, Kaunas, Lithuania*

### **Co-supervised Master thesis**

- I. Lidén, A. and Persson, K., 2012. Evaluation of Long-term Discharge in Swedish Rivers. Master Thesis TVVR-12/5005, Lund University.
- II. Diaz, D.C., and O. Siergieieva (2012). Corral Díaz, D. and Siergieieva, O., 2012. Long term variability of Swedish river discharge as represented by EC-Earth in the past and future climates. Master Thesis TVVR 12/5013, Lund University.

# Abbreviations

|                 |  |
|-----------------|--|
| 2t              | 2 metre temperature  |
| 10u             | 10 metre zonal wind component  |
| 10v             | 10 metre meridional wind component   |
| AE              | Analogue ensemble modelling chain  |
| AO              | Arctic Oscillation   |
| AP              | Accumulation period  |
| CCA             | Canonical Correlation Analysis   |
| CP              | Circulation Pattern  |
| CPC             | Climate Prediction Center, College Park, Maryland, United States                             |
| CWT             | Continuous wavelet transform   |
| DE              | Dynamic ensemble modelling chain   |
| EA              | East Atlantic Pattern  |
| EAWR            | East Atlantic West Russia pattern  |
| ECMWF           | European Centre for Medium Weather Forecasting, Reading, United Kingdom                      |
| ESP             | Ensemble streamflow prediction   |
| FY <sup>+</sup> | Frequency of Years (%) in which the new approach performs better                             |
| GCM             | General Circulation Model or Global Climate Model  |
| HBV             | Hydrologiska Byråns Vattenbalansavdelning hydrological model                                 |
| HE              | Historical ensemble modelling chain  |
| HFP             | High flow period   |
| HP              | Hydrological period e.g. accumulation period, low flow period etc.                           |
| HUVA            | Hydrologiskt utvecklingsarbete programme, EnergiForsk, Sweden                                |
| IRI             | International Research Institute for Climate and Society, Columbia University, United States |
| IQRSS           | Interquartile range skill score  |
| LFP             | Low flow period  |
| LT              | Lower tercile  |
| LOOCV           | Leave-one-out cross validation   |
| MAE             | Mean Absolute Error  |
| MAESS           | Mean Absolute Error skill score  |
| mslp            | Mean sea level pressure  |
| MT              | Middle tercile   |
| n <sup>+</sup>  | Percentage of sub-basins where that perform better   |
| NAO             | North Atlantic Oscillation   |
| NCAR            | National Center for Atmospheric Research, Boulder, Colorado, United States                   |
| NOAA            | National Oceanic and Atmospheric Administration, Silver Spring, Maryland, United States      |

|  |   |
|--|---|
| NSC  | Normalised square covariance  |
| NSE  | Nash–Sutcliffe efficiency   |
| NVE  | Norwegian Water Resources and Energy Directorate, Oslo, Norway                                  |
| NWP  | Numerical Weather Predictor   |
| p  | p-value or probability  |
| P  | precipitation   |
| PCA  | Principal Component Analysis  |
| PFP  | Post flood period   |
| POL  | Polar/Eurasia Pattern   |
| PTHBV  | Precipitation and temperature for Hydrologiska Byråns Vattenbalansavdelning                     |
| q  | Specific humidity at 850 hPa  |
| Q  | Inflows   |
| R <sup>1</sup> and R <sup>2</sup>                  | The clusters in the southern region where hydrological regimes are dominated by rain processes. |
| ROCSS  | Relative Operating Characteristic Skill Score   |
| S <sup>1</sup> , S <sup>2</sup> and S <sup>3</sup> | The clusters in the northern region where hydrological regimes are dominated by snow processes. |
| SCA  | Scandinavian Pattern  |
| SFP  | Spring flow period  |
| SFV  | Spring Flood Volume   |
| SMHI   | Swedish Meteorological and Hydrological Institute, Norrköping, Sweden                           |
| SST  | Sea surface temperature   |
| SVD  | Singular Value Decomposition  |
| t850   | temperature at 850 hPa  |
| T  | Temperature   |
| TCI  | Teleconnection pattern index (or indices)   |
| tp   | Total precipitation   |
| TP   | Teleconnection pattern  |
| u850   | Zonal wind component at 850 hPa   |
| u  | Zonal wind component  |
| U  | Uncertainty sensitivity score   |
| UT   | Upper tercile   |
| v850   | Meridional wind component at 850 hPa  |
| WTC  | Wavelet transform coherence   |
| XWT  | Cross-wavelet transform   |
| z850   | Geopotential at 850 hPa   |

# Introduction

## Background

The Scandinavian Peninsula has an abundance of water resources (e.g. Angelin, 1981; Henriksen et al., 1998) and people have been exploiting these resources in numerous ways for centuries. The use of water as a source of energy first appears in the Swedish historical records around the 12th century with the introduction of the water wheel (e.g. Angelin, 1981; Greve, 2016). At first these were the relatively inefficient vertical axis ‘Norse mills’, used predominantly for small scale milling activities, but over time more efficient vertically mounted water wheels were introduced allowing for endeavours of a more commercial nature (e.g. Greve, 2016). With the increased energy demand and varied nature of the activities being powered by the water wheels there was an increased need to regulate the flow of water. Mill ponds and weirs allowed operators to modulate the flow to the water wheel and also permitted the limited storage of water for use when supply would otherwise be inadequate. These water regulation solutions were sufficient for local mill types e.g. grain, spinning, and sawmills, but they would not be suitable for the next technological jump in the exploitation of running water as an energy source – hydroelectric power or simply hydropower.

The first hydroelectric installation in Sweden was at a spinning mill on the river Viskan in 1882 (Rundgren and Martna, 1989) where a water powered dynamo was used to provide the company with electric lighting (Vattenfall, 2019). Adoption was swift with many industries building their own plants very soon thereafter. However, it was not until the introduction of three-phase technology, allowing the transmission of electrical power over great distances, that hydropower became commercialised. At the end of the 19<sup>th</sup> century over 50 industrial hydropower plants were operating around Sweden (Vattenfall, 2019). Today, nearly half of Sweden’s electrical energy, approximately 65 TWh during a ‘normal’ year (Statistiska centralbyrån, 2018), comes from hydropower. However, out of today’s more than 2100 hydroelectric power plants, with a total installed capacity of 16200 MW, just 200 account for 94% of the total production. The vast majority of these are located in the northern part of the country and require large regulation reservoirs to operate efficiently.

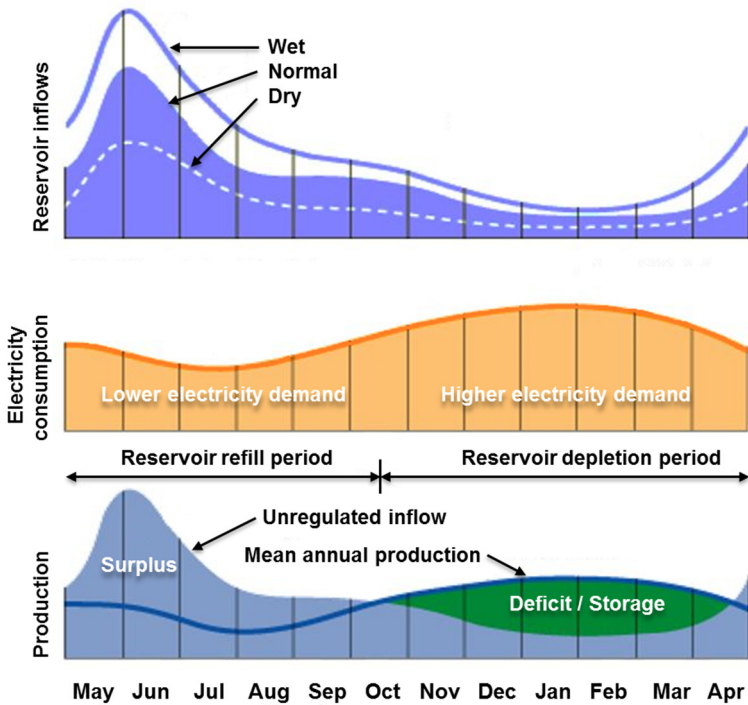


**Figure 1.** Idealised schematic showing the typical inflows to reservoirs (top panel), generalised electricity demand (middle panel), and the normal annual production together with the inflows highlighting the phase shift between water resources and planned production (lower panel). (Modified with permission – translated text, Vattenregleringsföretagen, 2016).

Managing hydropower production is highly complex in snow dominated regions like Sweden as the water resources are not distributed evenly throughout the year. Figure 1 summarises the overarching challenge operators are faced with, a mismatch between the natural supply and demand. During the colder months a large fraction of the precipitation falls as snow which is stored in the form of a snowpack. This water is not available for energy production until it melts in the spring when the temperature begins to rise again. This means that there is a potential lack of water to produce electricity during the winter when the demand is high and a surplus in the spring and summer when demand is low. Between 55 and 70% of the annual inflows to reservoirs in the larger hydropower producing rivers occur during the spring flood period which is typically between mid-April/early-May and the end of July. Hydropower operators try to minimize this asymmetric distribution and maximise their earning potential by storing water from the spring flood period in reservoirs for later use when demand is higher.

The typical strategy in Sweden is to have reservoirs at around 90% capacity at the end of the spring flood while maintaining a balance between a sufficiently large

volume of water for optimal production and enough remaining capacity in the reservoirs for safe flood risk management (e.g. Olsson et al., 2016). This means that sufficient capacity needs to be made available in the reservoirs to store as much of the spring flood as possible. Hydrological seasonal forecasts are indispensable to water regulators both for estimating the volume of the coming spring flood and the onset date. However, in practice most of the reservoirs (not those with multi-year regulation capacity) are run down to the legally allowable level in preparation for the spring flood as the seasonal forecasts are not deemed to be reliable enough to estimate a more appropriate level. The industry would rather maximise the production leading up to the spring flood and risk not filling their reservoirs than running the risk of having to spill water due to insufficient available capacity. This strategy minimises the risk rather than maximises the potential and has been reasonably successful so far. However, market forces are compelling hydropower operators to be even more flexible in their strategies. In addition to their base supply role, hydropower is being called on to help modulate the inconsistent supply from other sources of production such as solar and wind power.

## Objective and Scope

In light of the issues discussed in the previous chapter, the principal objective of this research is to improve upon the quality of operational hydrological seasonal forecasts in Sweden. To this end the following research goals are addressed:

- To investigate whether the seasonal forecasts can be improved by modifying the current approach or substituting it for another.
- To investigate whether there are any benefits of a multi-model approach to forecasting the spring flood volume (SFV) in Sweden.
- To investigate whether Sweden can be divided into sub regions to which the seasonal forecasts can be optimised.
- To investigate, identify, and understand the climatic drivers responsible for local hydrological variability.
- To develop and evaluate a hydrological seasonal forecast prototype for operational forecasting of the SFV in Sweden.

## Dissertation Structure

This dissertation is a “thesis by article” consisting of a summary and five appended papers. The summary begins with an introductory chapter that briefly presents the

background, objectives and scope of this dissertation. The second chapter is a literature review that provides the theoretical background for the dissertation. An overview of the study area, data and methods used in this research are presented in the third and fourth chapters. In chapter five the main results from the appended papers, together with a few findings not included in them, are summarised and discussed. The conclusions, implications, unresolved questions and future outlook are presented in chapter six. Finally, a post scriptum gives a summary of plans to operationalise the hydrological seasonal forecast prototype at the Swedish Meteorological and Hydrological Institute (SMHI).

The research of this dissertation is distributed as follows in the appended papers:

- Paper **I** investigates the predictability of the spring flood season at 29 selected gauging stations across Norway using a multi-model statistical downscaling approach. Hindcasts of large scale climate variables from two General Circulation Models were downscaled to accumulated streamflows using a Canonical Correlation Analysis based linear regression. Three predictors are individually downscaled and pooled into a multi-model forecast for each station.
- In Paper **II** selected hydrological seasonal forecast approaches and their benefits for making hydrological forecasts of the spring flood period in Sweden are briefly reviewed. Then, in this context, plans for a multi-model approach is discussed and a framework to achieve this is outlined.
- Paper **III** is a preliminary assessment of the multi-model approach outlined in paper **II**. The different individual methods that would make up the multi-model approach are compared to the climatological approach that is used operationally.
- In Paper **IV** the relationships between the seasonal and interannual variability in Swedish streamflow and different climate circulation patterns are systematically investigated. This is done to identify, understand and quantify the climatic drivers behind this variability. Sweden is divided into five homogeneous regions of hydrological variability by hierarchical clustering.
- Paper **V** presents the development and testing of a prototype hydrological seasonal forecast model. This paper utilises the knowledge gained from Papers **I-IV** and uses it to develop a hydrological seasonal forecast prototype which is tested by making hindcasts for the spring floods at 84 gauging stations for the period 1981-2015. These hindcasts are evaluated against climatology and hindcasts made using the current operational forecast system at SMHI, by comparison with observations.

# Literature Review

## Seasonal Forecasting

Seasonal forecasts apply to predictions over intermediate time scales; longer than two weeks on the low end and out to about a year on the upper end (Doblas-Reyes et al., 2013). In meteorology this time scale bridges the gap between weather forecasting and decadal/climate predictions. People have long used environmental indicators such as climatic conditions, animal behaviour and celestial observations as predictors of changes in coming seasons (Inwards, 1892). Many such relationships were fanciful speculation but some were without a doubt the result of keen observations that have since been corroborated by science (e.g. Goddard et al., 2001; Orlove et al., 2000). However, it is only with our ever growing understanding of these climate-environmental relationships that we have been able to progress from speculations to skilful predictions.

### **Meteorological seasonal forecasting**

There is a common adage that states, “If you want to know what the weather will be like (*insert time frame here*), just look outside”. Frivolity aside, this phrase alludes to a core principle in forecasting, that initial conditions are a good source of predictability (e.g. Lorenz, 1969; Palmer and Anderson, 1994; Thompson, 1957; Wood et al., 2015; Wood and Lettenmaier, 2008; Yossef et al., 2013). However, ‘memory’ in the atmosphere is short lived and any influence of these initial conditions will have greatly deteriorated within 5-10 days (Goddard et al., 2001). The main sources of predictability at longer time scales are the low frequency variations in boundary conditions like sea surface temperatures (SST), stratospheric processes, sea ice, snow cover and soil moisture (e.g. Miller and Wang, 2019; Shukla and Kinter, 2006; Smith et al., 2016; Yang et al., 2016). Anomalies in these boundary conditions, if large enough, can affect atmospheric circulations leading to atmospheric anomalies both locally and elsewhere (e.g. Doblas-Reyes et al., 2013; Miller and Wang, 2019). The time scales in the frequency of these boundary conditions offers a source of predictability that can extend far beyond that offered by the atmosphere alone (Charney and Shukla, 1981).



The two leading approaches to seasonal forecasting are statistical and dynamical modelling.

- Regression models are the most commonly used statistical techniques and they are generally contingent on the SST boundary (Goddard et al., 2001). This approach, using SST as a predictor, has been successfully applied to numerous regions, e.g. South America (e.g. Ward and Folland, 1991; Uvo et al., 1998), North America (e.g. DelSole and Banerjee, 2017; Dias et al., 2018; Fuentes-Franco et al., 2018), Europe (e.g. Gerlitz et al., 2016; Johansson et al., 1998; Colman and Davey, 1999), Africa (e.g. Landman and Mason, 1999a, 1999b; Mutai et al., 1998; Sittichok et al., 2016; Tuel and Eltahir, 2018), Middle East (e.g. Choubin et al., 2018; Shirvani and Landman, 2018), and South East Asia and Australia (e.g. Deo et al., 2017; Qian et al., 2019; Wu and Yu, 2016; Yu et al., 2018).
- Physical or dynamical models are predominantly based on numerical representations of physical processes which are either resolved at each of the model grid points or spectrally. Initially these types of models were applied regionally (e.g. Cane et al., 1986) but as our understanding of the climate system improved and computational capacity increased they began to be applied globally. Early generations of general circulation models (GCM) use prescribed SSTs that have been derived from statistical or dynamical predictions prior to their use in the GCM (e.g. Roeckner et al., 1996). With time these later evolved to using modelled boundary conditions, an ocean model is coupled with the GCM which allows the boundary conditions and the atmosphere to evolve together (e.g. Johnson et al., 2019; Saha et al., 2014).

A number of institutions around the world offer seasonal meteorological forecasts. These include, but not limited to, ECMWF, IRI, Météo France, the MetOffice and NCAR. These forecasts are generally initialised with observational information. This initial state is then perturbed to give an ensemble of initial states from which the model will evolve (e.g. Molteni et al., 1996; Molteni et al., 2011). This is done to better sample the uncertainties in the chaotic nature of the atmosphere. These forecasts are typically issued once a month and have a forecast horizon of several months (typically up to 15 months). These forecasts are of great benefit to a number of different fields and end-users including hydrological seasonal forecasters.

However, GCM seasonal forecast skills are variable for different regions of the world, in particular seasonal forecasts for Scandinavia are not very skilful (e.g. Doblas-Reyes, 2010; Doblas-Reyes 2013). Weisheimer and Palmer (2014) investigated the reliability of the seasonal climate forecasts from the system 4 version of the ECMWF seasonal forecast system (Figure 2). They developed a five category system for ranking the reliability of GCM forecasts based on reliability

diagrams. Their results show that overall the reliability performance of the ECMWF seasonal forecast system is poorer for precipitation forecasts than for temperature forecasts. The reliability category of precipitation forecasts over the Scandinavian region range from “not useful” to “dangerous” for dry winter and summer events, respectively, and “marginally useful” for wet winter and summer events. The reliability category of temperature forecasts for the same region range from “marginally useful” to “perfect” for cold winter and summer events, respectively, and “marginally useful” for warm winter and summer events. There is systematic evaluation of system 5, to this thesis author’s knowledge, at the time of writing.

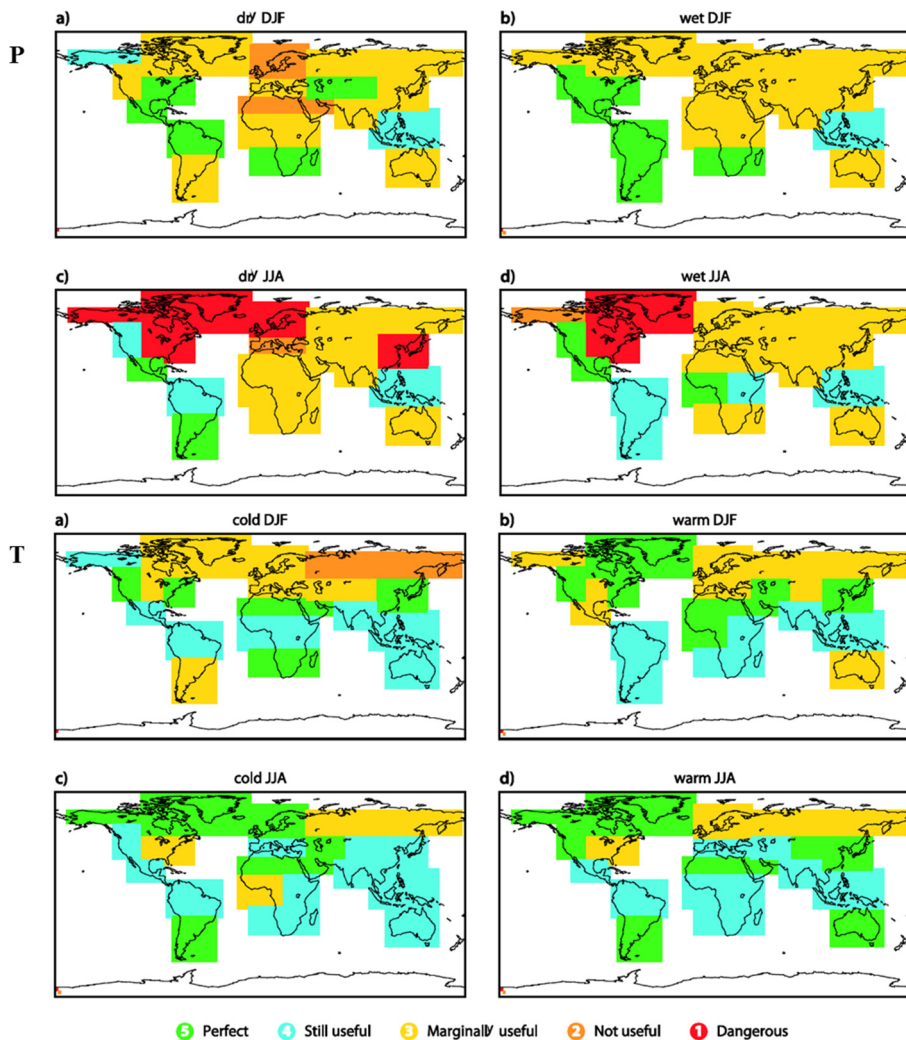


**Figure 2.** Reliability of system 4 seasonal forecasts for precipitation (the top four panels) and temperature (the lower four panels). (Composite of figures 4 and 5 taken from Weisheimer and Palmer, 2014)

## Hydrological seasonal forecasting

Society's ever increasing demand and pressure on water resources over time has created a need for improved hydrological forecasts, both from a quality and forecast lead time perspective. Unlike the atmospheric system, the hydrological system has a 'memory' which is derived from the different storages within the system e.g. groundwater, lakes, snowpacks and glaciers. The sources of predictability for hydrological seasonal forecasts come from these initial hydrological conditions (e.g. Wood and Lettenmaier, 2008; Wood et al., 2016; Yossef et al., 2013), and also from knowledge of the climate during the forecast period i.e. seasonal meteorological forecasts (e.g. Bennet et al., 2016; Doublas-Reyes et al., 2013; Wood et al., 2016; Yossef et al., 2013). Hydrological seasonal forecasts attempt to leverage at least one of these sources of predictability to make skilful predictions of future streamflow. In practice there are two predominant approaches to making hydrological forecasts at the seasonal scale; statistical approaches and dynamical approaches.

### *Statistical approaches*

Statistical approaches utilise empirical relationships between predictors and a predictand, typically streamflow or a derivative thereof (e.g. Garen, 1992; Pagano et al., 2009). These predictors can vary greatly in type from local hydrological storage variables like snow and groundwater storages (e.g. Robertson et al., 2013; Rosenberg et al., 2011), to local and regional meteorological variables (e.g. Còrdoba-Machado et al., 2016; Olsson et al., 2016), to large scale climate data such as El Niño-Southern Oscillation indices (e.g. Schepen et al., 2016; Shamir, 2017). For the better part of the 20th century most operational seasonal forecasts in Europe and North America were directed to the elevated flows during the spring caused by snow melt and were made by the regression of seasonal streamflow volume on antecedent indicator variables like snow water equivalent or accumulated precipitation (e.g. Melin, 1937; Garen, 1992; Wood and Lettenmaier, 2002; Pagano et al., 2009).

Around the beginning of the 21st century researchers began to link the seasonal variability of local streamflows to the variability in SSTs (e.g. Garen, 1992; Sadeghi et al., 2019; Seibert et al., 2017; Uvo and Graham, 1998). These studies found that anomalies in SSTs in different locations exhibited a teleconnection with streamflows in the US, China, Southern Africa and northern South America. For example, using this knowledge Uvo and Graham (1998) were able to construct a statistical model that regress monthly streamflow anomalies to monthly anomalies of Atlantic and or Pacific SSTs. Their results showed skill in predicting streamflows one season in advance. A study by Ionita et al. (2008) connected antecedent winter SSTs, land temperatures and precipitation anomalies to spring flood discharge in the Elbe River. Their findings showed that by combining the three predictands it

was possible to improve the forecast skill by considering the different predictands together instead of individually.

Other studies have investigated the influence of remote climate drivers on local hydrometeorological variability (e.g. Álvarez-García et al., 2019; Ionita et al., 2015; Ionita et al., 2017; Kingston et al., 2006a and 2006b; Kingston et al., 2009). According to Kingston et al. (2009), the links between large scale climate patterns, land surface and hydrologic variability in regions like Sweden are not well understood. However, the effects of meteorological variables locally on streamflow are well understood and changes in precipitation and temperature at the seasonal scale over Sweden are connected to the low-frequency variations in some large scale climate circulation patterns (e.g. Wallace and Gutzler, 1981; Barnston and Livezey, 1987; Hurrell, 1995). Work done in this thesis utilises information from these circulation patterns to modify and combine some of the approaches discussed above to improve the quality of hydrological seasonal forecasts in Sweden.

### *Model-based approaches*

Dynamical approaches use a hydrological model, typically initialised with observed data up to the date the forecast should be issued so that the model state is a reasonable approximation of the initial hydrological conditions. The model is then forced with either historical observations or using data representative of the future meteorological conditions such as GCM forecasts (e.g. Crochemore et al., 2016; Olsson et al., 2016; Yuan, 2016; Yuan et al., 2013a, 2015, 2016). Some variations of the dynamical approach for seasonal hydrological forecast, used in this work, are described here.

### *Historical ensembles*

The so-called ensemble streamflow prediction approach (ESP) where a hydrological model is forced using an ensemble of historical data (e.g. Day, 1985; Arheimer et al., 2011) is perhaps one of the most widely used methods of hydrological seasonal forecasting and is still the subject of new research. The hypothesis is that a well initialised and calibrated model forced with an ensemble of historical data is able to make skilful hydrological forecasts. This is typically true, by evolving the initial hydrological conditions into the future with historical forcing data it is possible to estimate the range of possible outcomes that represent a typical progression of events. However, this approach suffers if the conditions during the forecast period deviate from the normal (long-term average), especially for longer lead-times.

Recent work has looked at conditioning the historical ensembles before using them. This means that time series, representing specific years, are selected out of the historical ensemble to make up a reduced ensemble of driving data before being used to force the hydrological model. The hypothesis is that it is possible to select a subset from the historical driving data, based on some objective selection criteria,

that is more representative of how the meteorological conditions will evolve over the forecast period. This conditioning can be done using GCM outputs (e.g. Crochemore et al., 2016), and climate indices or circulation pattern analysis (e.g. Beckers et al., 2016; Candogan Yossef et al., 2016). The consensus is that with appropriate selection criteria and a sufficiently large ensemble of historical data it is possible to improve forecast skill with respect to the ESP approach.

### *Forecasted ensembles*

A related approach that has become common employs the outputs from GCMs to force the hydrological model. A successful system requires both accurate initial conditions such as soil moisture, snow cover (e.g. Koster et al., 2010) and upstream river flows (e.g. Yossef et al., 2013) and skilful seasonal predictions of the meteorological forcing data, typically precipitation and temperature, for the hydrological model (e.g. Yuan et al., 2013b). A typical forecast system that employs GCM outputs to drive a hydrological model consists of GCM input data (often downscaled or bias corrected), a hydrological model that is well initialised using observations, and some form of post processing to derive the seasonal forecast product.

One of the earliest attempts at using GCM outputs for hydrological forecasting was by Kim et al. (2000) who found overall decent agreement between simulated and observed discharge. However, low (high) flows were systematically overestimated (underestimated); this was primarily attributed to biases in the GCM forecasts for precipitation. Wood et al. (2002) proposed bias correction of the GCM forecasts by percentile-based mapping to minimise the effects of these biases.

Since then the GCM based hydrological seasonal forecast systems have been extensively evaluated through a number of case studies (e.g. Wood and Lettenmaier, 2006; Li et al., 2008) and hindcast experiments (e.g. Wood et al., 2005; Mo et al., 2012; Yuan et al., 2013; Bastola et al., 2013). Initially the use of GCM forecasts as inputs showed little to no improved skill over the historical approach (e.g. Wood et al., 2005) nevertheless as newer and more improved GCM products have become available so the skill of these GCM-hydrological seasonal forecast systems has improved (e.g. Luo et al., 2007; Yuan et al., 2011; Yuan et al., 2013). Additional techniques to improve the skill of these GCM-hydrological seasonal forecast systems have included using multi-model GCM ensembles as inputs to hydrological models (e.g. Yuan et al., 2011; Yuan et al., 2015; Ma et al., 2016), using multiple hydrological models to generate an ensemble of hydrological forecasts (e.g. Duan et al., 2007; Mo and Lettenmaier, 2014), bias correction of the GCM data before being used in the hydrological models (e.g. Wood et al., 2002; Yoon et al., 2012; Trambauer et al., 2015 e.g. Crochemore et al., 2016, Lucatero et al., 2017; Wood et al., 2002; Yuan et al., 2015), bias adjusting the hydrological model outputs (e.g. Lucatero et al., 2017) or a combination of both (e.g. Yuan et al., 2012).

# Teleconnection Patterns and Indices

Teleconnection patterns (TP) are large scale persistent and recurring patterns of circulation or air pressure anomalies that affect the intensity and location of the jet stream patterns (and other storm tracks), rainfall and temperature over a large geographical area. Consequently, teleconnection patterns have a significant correlation with the variability in some hydro-meteorological variables in geographically separated regions (Panagiotopoulos et al., 2002). Teleconnection pattern indices (TCI) are a numerical representation of the phase and relative strength of a TP.

A common procedure used to identify teleconnection patterns and indices is the Rotated Principal Component Analysis used by Barnston and Livezey (1987). For each of the twelve calendar months, the leading unrotated empirical orthogonal functions are first determined from reanalysis geopotential height anomaly fields in the three-month period centred on the month in question. These are then rotated, using a Varimax rotation, to yield the rotated modes (TP) and their time series for that calendar month. The TCIs are calculated using a Least Squares solution on these time series after any spurious modes/TP, those with no apparent physical meaning, have been filtered out. The solution to this system of equations give the respective teleconnection indices which represent the combination of teleconnection patterns that account for the most spatial variance of the observed standardized anomaly field in the month.

## **North Atlantic Oscillation (NAO) and Arctic Oscillation (AO)**

AO is the dominant variability pattern of sea level pressure, north of 20°N, if seasonality is disregarded. It is characterized by a centre of atmospheric pressure action over the Arctic and another one, of opposite sign, centred at about 35-45°N zonally distributed (Thompson and Wallace, 1998, among many others). The NAO is defined as an oscillation of the atmospheric mass between the Iceland subpolar low and the Azores subtropical high (see Figure 3; Hurrell et al., 2003). There is a debate in the scientific community as to whether NAO is a regional expression of AO or not as there are large similarities in their spatial patterns and climate impacts over the Atlantic-European region (e.g. Ambaum et al., 2001; Deser, 2000; Thompson and Wallace, 1998, 2001). Nevertheless, over the North Atlantic AO is nearly indistinguishable from NAO (Polyakov and Johnson, 2000).

AO and NAO are positively correlated with precipitation and temperature over Sweden. During positive (negative) AO/NAO conditions, the north Atlantic storm track is shifted northwards (southwards) over Scandinavia and the polar jet is

stronger (weaker) and more zonal (meridional) in nature (D'Aleo and Easterbrook, 2016). This increases (reduces) the transport of mild and moist air masses from the Atlantic (Hurrell 1995) and limits (enhances) the intrusion of a cold polar trough over the region. During the summer (July-August) there is a westerly shift of the Azores high pressure centre which results in anticyclonic conditions over the Scandinavian Peninsula leading to a negative association with precipitation during these months (Bladé et al., 2012).

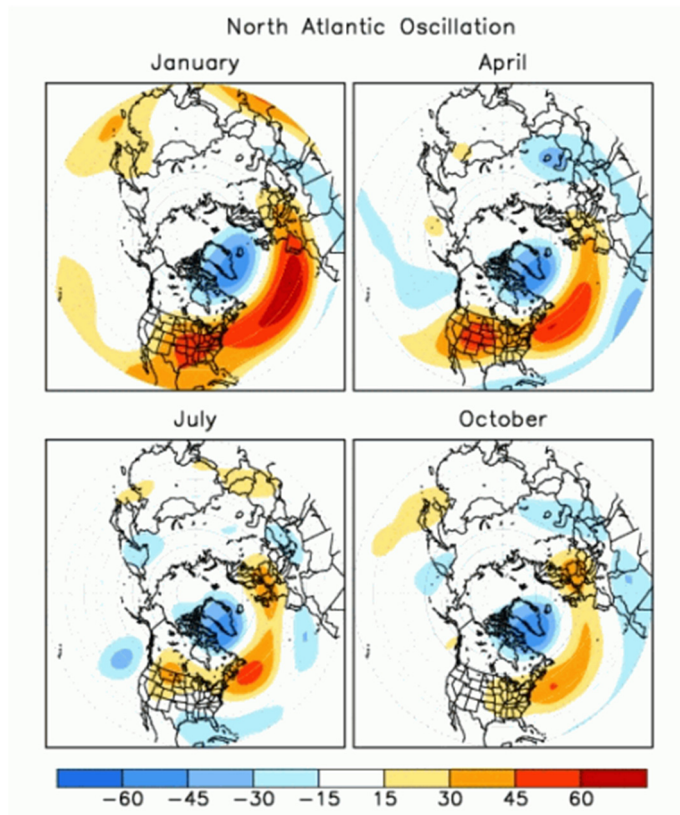


**Figure 3.** Map of the NAO loading patterns for January, April, July, and October. The loading patterns are expressed as the temporal correlation between the monthly standardized height anomalies at each grid point and the teleconnection pattern time series valid for the specified month. (Climate Prediction Center, 2005a)

### East Atlantic Pattern (EA)

The EA is structurally similar to NAO with south-eastwardly displaced centres of activity (see Figure 4; Barnston and Livezey, 1987). EA is generally positively correlated with precipitation and temperature over much of Sweden in most months. During positive EA conditions mild and moist air is drawn up from the Atlantic over

Europe and into Scandinavia. Furthermore, work by Comas-Bru and McDermott (2014) suggests that EA has a subtractive (additive) effect on the NAO-precipitation relationship over parts of central Sweden and lower half of the eastern seaboard (rest of the country) when the two teleconnection pattern indices (TPIs) have corresponding signs. When the TPIs have opposing signs there is a general additive effect on the NAO-precipitation relationship over the entire country. They argue that this is due to the shifting of their net centres of activity in the Atlantic-Eurasian domain EA appears to have little to no effect on the NAO-temperature relationship over Scandinavia.

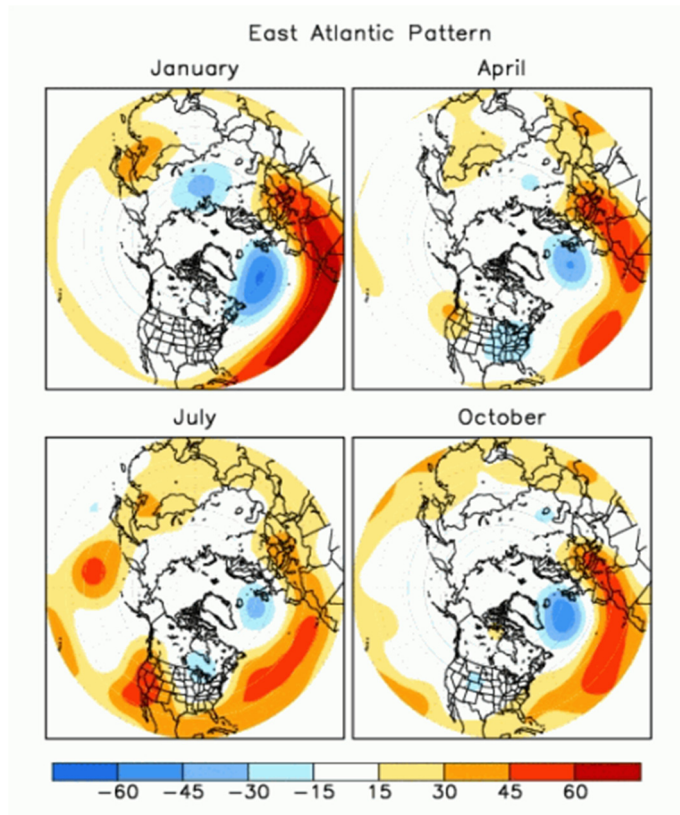


**Figure 4.** Map of the EA loading patterns for January, April, July, and October. The loading patterns are expressed as the temporal correlation between the monthly standardized height anomalies at each grid point and the teleconnection pattern time series valid for the specified month. (Climate Prediction Center, 2005b)



## East Atlantic-Western Russia Pattern (EAWR)

The EAWR consists of four anomaly centres of atmospheric pressure action located over the North Atlantic, Western Europe, the Caspian Sea/western Russia and northeast China respectively (see Figure 5; Climate Prediction Center, 2012a). It is positively correlated with temperature over most of Sweden during the winter and southern Sweden during the summer. EAWR is positively correlated with precipitation in the northern mountain region during the winter and negatively correlated with precipitation over southern Sweden and the coastal region in the north during winter and most of the country during the summer (e.g. Ionita, 2014; Lim, 2014). This is due to the blocking influence of the anticyclonic centre of activity over the North Sea between Scandinavia and the United Kingdom and the resulting north-westerly circulation over the Scandinavian Peninsula.

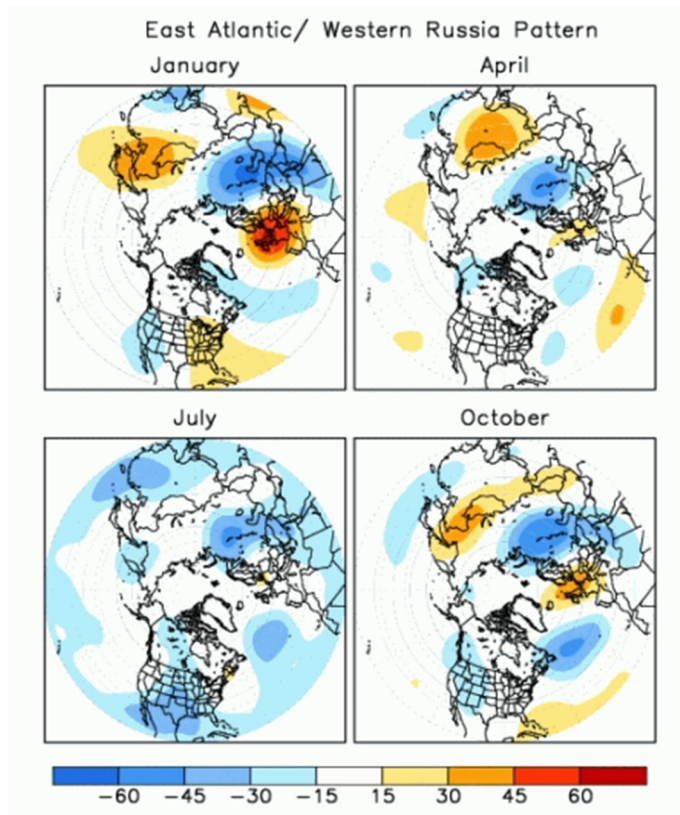


**Figure 5.** Map of the EAWR loading patterns for January, April, July, and October. The loading patterns are expressed as the temporal correlation between the monthly standardized height anomalies at each grid point and the teleconnection pattern time series valid for the specified month. (Climate Prediction Center, 2005c)

## Scandinavian Pattern (SCA)

The SCA consists of an anticyclonic centre over the Scandinavian Peninsula and two other centres of opposite sign located over the north-eastern Atlantic/western Europe and central Siberia, respectively (see Figure 6). SCA is negatively correlated with precipitation and temperature over Sweden (Bueh and Nakamura, 2007). Its positive phase is associated with a blocking anticyclone over the Fenno-Scandinavia region which not only negatively affects precipitation but can also draw cooler air masses down over southern Sweden from Siberia and the polar region (Barnston and Livezey 1987). Similarly to EA, the work by Comas-Bru and McDermott (2014) suggests that SCA has an additive (subtractive) interference effect on the NAO-precipitation relationship over the southwest coastal region of Sweden (rest of the country) when the TCIs have corresponding signs. When the TCIs have opposing signs there is a general additive effect on the NAO-precipitation relationship over the entire country due to the shifting of their net centres of activity in the Atlantic-Eurasian domain.

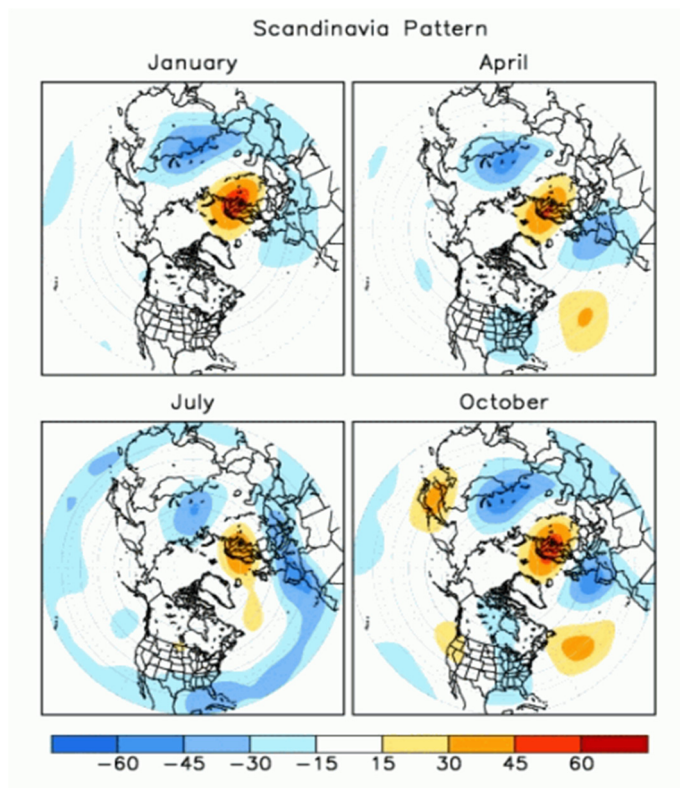


**Figure 6.** Map of the SCA loading patterns for January, April, July, and October. The loading patterns are expressed as the temporal correlation between the monthly standardized height anomalies at each grid point and the teleconnection pattern time series valid for the specified month. (Climate Prediction Center, 2005d)

## Polar/Eurasia Pattern (POL)

The POL (see Figure 7) is associated with variations in the circumpolar circulation and is positively correlated with the relative depth of the polar vortex and above normal air pressure values over most of the Eurasian region (Climate Prediction Center, 2012b; Panagiotopoulos et al., 2002). This above normal pressure suppresses precipitation due to reduced convective activity and possible blocking effects.

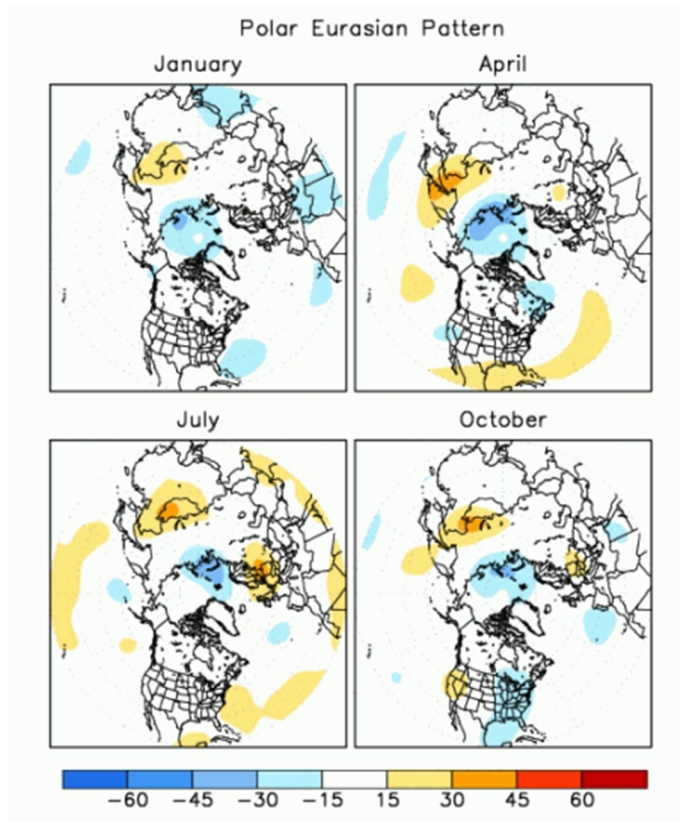


**Figure 7.** Map of the POL loading patterns for January, April, July, and October. The loading patterns are expressed as the temporal correlation between the monthly standardized height anomalies at each grid point and the teleconnection pattern time series valid for the specified month. (Climate Prediction Center, 2005e)

# Study Area and Datasets

## Study area

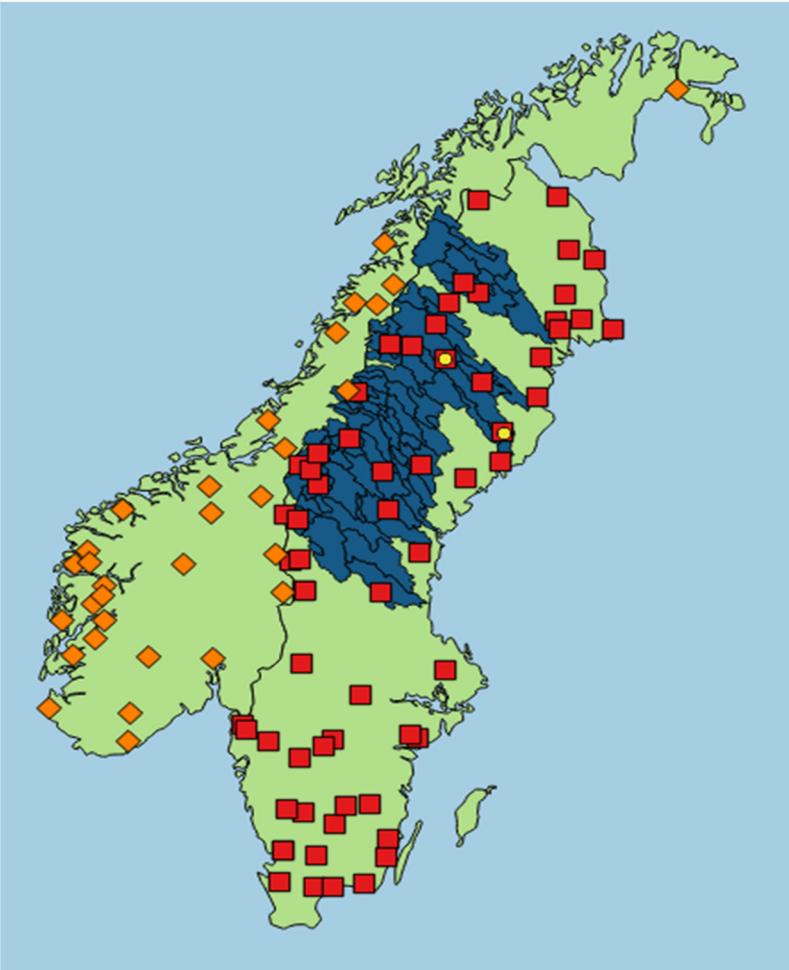


**Figure 8.** Map showing the location of the hydrological gauging stations and sub-basins used in this work. The gauging stations used in Paper I (orange diamonds), the gauging stations used in Paper III (yellow dots), the gauging stations used in paper IV (red squares), and the sub-basins used in Paper V.

The study areas of interest in this dissertation are a collection of river basins situated on the Scandinavian Peninsula (Figure 8). In Paper I the study area comprises basins associated with 30 gauging stations across Norway (see Figure 1 in paper I). In Papers III - V study areas of interest are two gauging stations on the Vindel River (see Figure 1 in paper III), 64 unregulated gauging stations across Sweden (see Figure 1 in paper IV), and 84 gauging stations in Northern Sweden (see Figure 3 in paper V) respectively. The following paragraphs give a brief summary of the hydro-meteorological climate of the study areas with special emphasis on Sweden.

The Scandinavian Peninsula is a relatively long and narrow region in northern Europe. It ranges from the mild Öre Sound and southern Baltic Sea in the south (55.3°N) to the icy Barents Sea in the north (71.2°N) from the Norwegian fjords to the east (4.6°E), over the Scandinavian mountains and down to the Swedish coastal plains to the west (31°E). The Scandinavian Peninsula enjoys a surprisingly milder climate than its northern latitudes might suggest with temperatures that are 5-10°C above the latitudinal means. This is predominantly due to heat from the tropics being transported to the region by the North Atlantic thermohaline and Atlantic meridional overturning circulations (e.g. Rahmstorf, 2006). The short to medium term variability in the climate is driven by the teleconnection effects caused by the interplay between a number of climate circulation patterns over the Euro-Atlantic domain regulating the transport of moist air masses over Scandinavia as well as other local meteorological conditions (e.g. Barnston and Livezey, 1987; Comas-Bru and McDermott, 2014; Hurrell et al., 2003; Rogers, 1997).

Temperatures in Sweden are a function of season, latitude, elevation, and proximity to the coast. For the majority of the country the mean annual temperature, for the period 1961-1990, is above freezing, ranging from 8°C in the south to around zero in the north. In the highlands of northwest Norrland and parts of the Scandinavian mountain range the mean annual temperature can be as low as -3°C. The pattern for the mean annual evaporation follows closely the general pattern for mean annual temperature and ranges from between 500-600 mm per year in the south to less than 100 mm per year in parts of the mountainous regions in the north. Winters tend to be long (shorter) and cold (milder) for much of the northern (southern) parts of the country while summers tend to be warm everywhere save some areas at high elevations.

Precipitation normals for Sweden for the period 1961-1990 (SMHI, 2019) show that precipitation in Sweden is highest in the mountain regions and can be as high as 2000 mm per year in some places. The interior of northern Sweden, the lowland areas of southern Sweden and the eastern seaboard are relatively dry in comparison due to the rain shadow effect caused by the Scandinavian mountains lying across the prevailing westerly airflow. Here the precipitation range is 500-700 mm per year. The south-western part of the country is less affected by this rain shadow effect

and the precipitation there can reach 1100 mm per year. In the south of Sweden, the amount of precipitation is highest in late summer and early autumn, and remains elevated until around February when there is a significant drop before slowly increasing again through to the end of summer. The intra-annual distribution of precipitation elsewhere in the country is similar to that in the south except that it does not remain elevated during the colder months but rather steadily declines until the end of winter.

All these aspects, together with other physical factors and processes, contribute to a very heterogeneous hydrology. The natural discharge differs greatly from river to river but in general the larger rivers, by discharge, tend to be found in the northern two thirds of the country (Figure 9; SMHI, 2017). The farther northwards one goes, or the higher the elevation, the greater the fraction of winter precipitation that falls as snow. This means that for gauging stations with higher fractions of solid winter precipitation the annual hydrograph is characterised by low flows in the winter followed by a relatively short period of extreme discharge during the spring when the snow melts due to the warmer temperatures. By contrast, the annual hydrographs for gauging stations in southern Sweden are characterised by high flows during winter and low flows during the summer which is predominantly driven by seasonal changes in evapotranspiration. A mild spring melt signal preceding the low summer flow period is common for gauging stations that are inland or farther north.

Discharge statistics for the larger rivers across Sweden are summarised in Figure 9. The width of the rivers denotes the magnitude of their discharge, the dark blue representing the mean annual discharge and the total width the mean annual maximum discharge. Additionally, boxes containing hydrographs show the 5<sup>th</sup>, 50<sup>th</sup> and 95<sup>th</sup> percentiles of selected annual hydrographs from unregulated gauging stations from five different regions across Sweden.

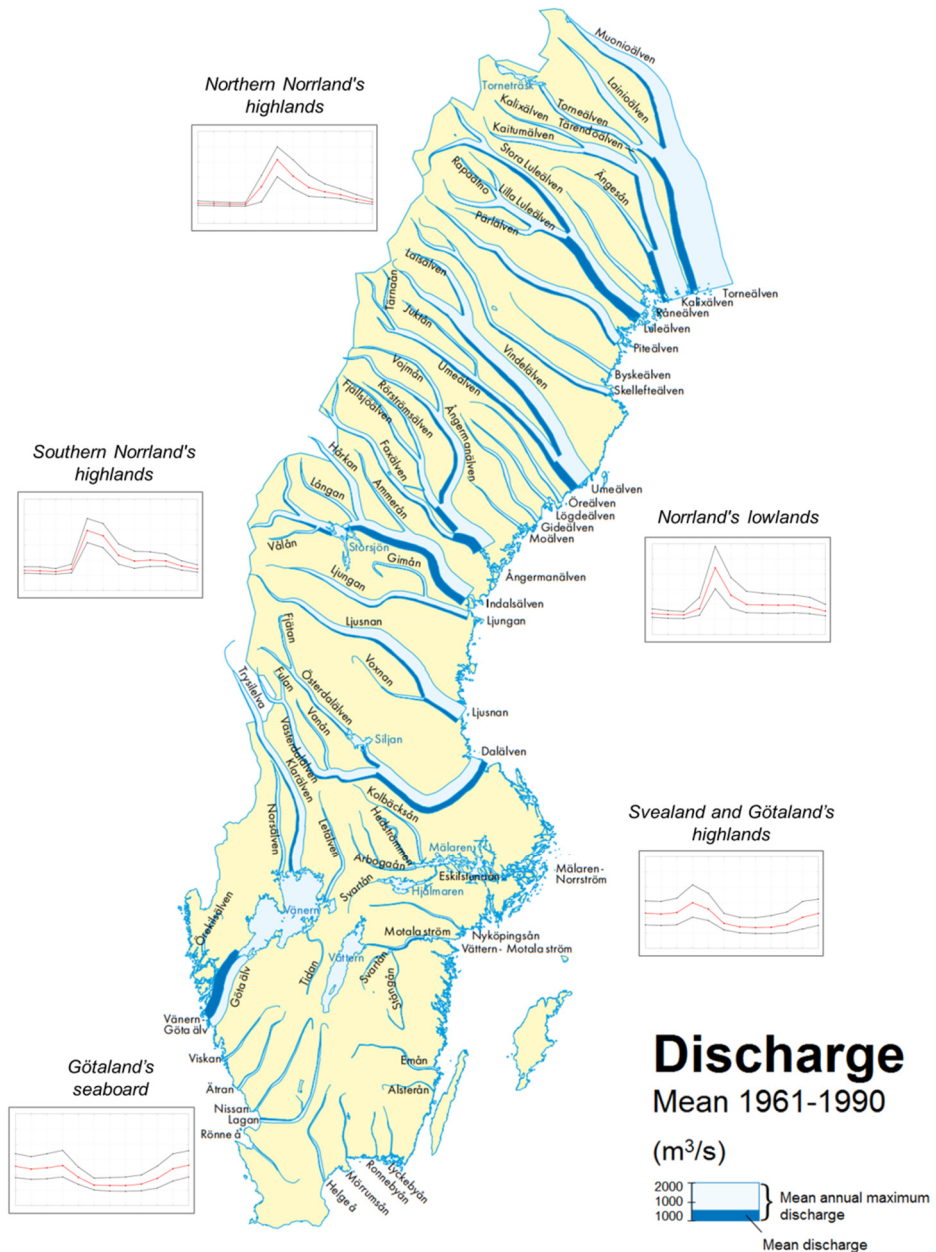


**Figure 9.** Map showing discharge statistics for the larger rivers across Sweden for the period 1961-1990. The total width of the rivers represents the mean annual maximum discharge and the dark blue sub-width the mean discharge (SMHI, 2017). Overlaid are the annual standardised hydrographs for unregulated rivers in five regions around the country, the median hydrograph is shown in red and the grey hydrographs represent the 5th and 95th percentiles.

# Datasets

For the sake of simplicity, the datasets used in this work are summarised in Table 1 and briefly reported by type, the reader is referred to the appended papers for more details.

**Table 1.** Summary of the data used in this work. (The reader is referred to the list of abbreviations, or relevant data sections, for the full variable names)

| Type         | Variables  | Dataset / Model | Format  | Resolution |  | Period    | Provider   |
|--------------|--|-----------------|---------|------------|--|-----------|--|
|              |  |                 |         | Temporal   | Domain   |           |  |
| Observations | P, T   | PTHBV           | Gridded | Daily      | Sweden   | 1961-2015 | Swedish Meteorological and Hydrological Institute            |
|              | NAO, AO, EA, EAWR, SCA, POL                                | –               | Indices | Monthly    | Northern Hemisphere                                    | 1951-2015 | Climate Prediction Center, US                                |
|              | Q  | –               | Point   | Daily      | Norway   | 1968-2003 | Norwegian Water Resources and Energy Directorate             |
|              |  | –               | Point   | Daily      | Sweden   | 1961-2015 | Swedish Meteorological and Hydrological Institute            |
| Reanalysis   | mslp   | ERA-40          | Gridded | Daily      | 60N to 70N and 5E to 25E                               | 1961-2002 | European Centre for Medium-Range Weather Forecasts           |
|              |  | ERA-Interim     | Gridded | Daily      | 60N to 70N and 5E to 25E                               | 2003-2010 | European Centre for Medium-Range Weather Forecasts           |
| Hindcasts    | v, 10u, tp   | ECHAM5          | Gridded | Daily      | 30N to 72N and -75E to 75E                             | 1968-2003 | International Research Institute for Climate and Society, US |
|              | t850, u850, v850, q850, sshf, slhf, mslp, 10u, 10v, 2t, tp | ARPEGE system 3 | Gridded | Daily      | 30N to 72N and -75E to 75E                             | 1982-2010 | European Centre for Medium-Range Weather Forecasts           |
|              |  | ECMWF system 3  | Gridded | Daily      | 30N to 72N and -75E to 75E / 55N to 70N and 11E to 23E | 1982-2010 | European Centre for Medium-Range Weather Forecasts           |
|              |  | ECMWF system 4  | Gridded | Daily      |  | 1981-2015 | European Centre for Medium-Range Weather Forecasts           |

## Observation data

### *Atmospheric*

Observed time-series of precipitation and temperature for Sweden are used in paper III and V. These data are sourced from the Precipitation and Temperature for Hydrologiska Byråns Vattenbalansavdelning (PTHBV) dataset maintained by



SMHI (Johansson, 2002). It is a gridded observation dataset created by optimal interpolation of meteorological station observations with elevation and wind taken into account.

|                      |  |
|----------------------|--|
| Data type:           | Gridded observations                                     |
| Period:              | 1961-2015  |
| Temporal resolution: | Daily  |
| Spatial resolution:  | 4km x 4km  |
| Domain:              | Sweden   |
| Variables:           | Precipitation (P)<br>Temperature (T)                     |
| Source:              | Swedish Meteorological and Hydrological Institute (SMHI) |

Teleconnection indices used in papers **III**, **IV**, and **V** are sourced from the CPC, a member of the National Oceanic and Atmospheric Administration of the United States of America. CPC calculates these teleconnection indices by applying a Rotated Principal Component Analysis, similar to the approach used by Barnston and Livezey (1987), to monthly mean standardized height anomalies (500 hPa) from the NCEP/NCAR reanalysis dataset.

|                      |   |
|----------------------|---|
| Data type:           | Teleconnection indices  |
| Period:              | 1951-2015   |
| Temporal resolution: | Monthly means   |
| Variables:           | North Atlantic Oscillation (NAO)<br>Arctic Oscillation (AO)<br>East Atlantic Pattern (EA)<br>East Atlantic/Western Russia pattern (EAWR)<br>Scandinavian pattern (SCA)<br>The Polar/Eurasia pattern (POL) |
| Source:              | Climate Prediction Center (CPC)   |

## *Hydrological*

The gauging stations used in this work are selected according to the following the four criteria:

1. Degree of regulation: Stations with the least regulation are preferred to ensure that the streamflow is as near to natural as possible.
2. Length of time series: Stations with longer time series are preferred to allow for more robust analyses.
3. Number of missing data: Stations with fewer missing data are preferred to minimise data filling effects influencing the study results.
4. Geographic location: Stations were selected to maximise the geographical coverage of Sweden.

Inflows measured at 30 selected gauging stations across Norway for the period 1968-2003. These data are available from the Norwegian Water Resources and Energy Directorate (NVE) who operate the gauging stations (more information visit <https://www.nve.no>). Homogenisation and quality control of the data was performed by NVE.

|                      |  |
|----------------------|--|
| Data type:           | Observations   |
| Period:              | 1968-2003  |
| Temporal resolution: | Daily  |
| Spatial resolution:  | 30 gauging stations across Norway (see Figure 8)       |
| Variables:           | Inflows (Q)  |
| Source:              | Norwegian Water Resources and Energy Directorate (NVE) |

Inflows measured at 142 selected gauging stations across Sweden for the period 1961-2015. These data are available from the Swedish Meteorological and Hydrological Institute (SMHI) who operate and or maintain the data from these gauging stations (more information visit <https://www.smhi.se> or <https://vattenweb.smhi.se>). Homogenisation and quality control of the data was performed by SMHI.

|                      |   |
|----------------------|---|
| Data type:           | Observations                                      |
| Period:              | 1961-2015   |
| Temporal resolution: | Daily   |
| Spatial resolution:  | 142 gauging stations across Sweden (see Figure 8) |
| Variables:           | Inflows (Q)                                       |

Source: Swedish Meteorological and Hydrological Institute (SMHI)

## Reanalysis data

Mean sea level pressure (mslp) from two different reanalysis datasets, ERA40 (Uppala et al., 2005) and ERA-Interim (Dee et al., 2011) are used in paper **III** to select analogue years. Data from these two datasets were appended to each other to obtain a single re-analysis dataset that spanned the whole period from 1961-2010. These data are available from the European Centre for Medium-Range Weather Forecasts (ECMWF), for more information visit <http://www.ecmwf.int>.

|                      |   |
|----------------------|---|
| Dataset:             | ERA-40  |
| Data type:           | Re-analysis   |
| Period:              | 1961–2002   |
| Temporal resolution: | Daily   |
| Spatial resolution:  | 0.75° x 0.75°   |
| Domain:              | 60°N to 70°N and 5°E to 25°E (see Figure 1a in Paper <b>III</b> ) |
| Variables:           | Mean sea level pressure (mslp)                                    |
| Dataset:             | ERA-Interim   |
| Data type:           | Re-analysis   |
| Period:              | 2003–2010   |
| Temporal resolution: | Daily   |
| Spatial resolution:  | 0.75° x 0.75°   |
| Domain:              | 60°N to 70°N and 5°E to 25°E (see Figure 1a in Paper <b>III</b> ) |
| Variables:           | Mean sea level pressure (mslp)                                    |
| Source:              | European Centre for Medium-Range Weather Forecasts (ECMWF)        |

## Seasonal hindcast data

### *ECHAM4.5 and ECHAM5*

Hindcasts of large scale circulation fields from the ECHAM4.5 (Roeckner et al., 1996) and ECHAM5 GCMs (Roeckner et al., 2003) are used as predictors in paper **I**. The International Research Institute for Climate and Society (IRI) at Columbia University maintains and runs their own versions of the ECHAM4.5 ECHAM5 models.

Available online from <http://iridl.ldeo.columbia.edu/index.html>

|                      |   |
|----------------------|---|
| Model:               | ECHAM5 and ECHAM5   |
| Boundary conditions: | Prescribed seas surface temperatures  |
| Data type:           | Hindcast  |
| Period:              | 1968-2003   |
| Season:              | Jan-Feb-Mar   |
| Temporal resolution: | Daily. These data are aggregated by taking the seasonal mean of the ensemble median             |
| Spatial resolution:  | 2.5° x 2.5°   |
| Domain:              | 30°N to 72°N and -75°E to 75°E (see Figure 1a in Paper <b>III</b> )                             |
| Variables:           | Meridional wind velocity at 850 hPa (v850)<br>Total precipitation (tp)<br>Zonal wind stress (u) |
| Source:              | International Research Institute for Climate and Society (IRI)                                  |

### *ARPEGE*

Hindcasts of large scale circulation fields from the ARPEGE atmospheric model (Déqué et al., 2004) are used as predictors in paper **III**. ARPEGE is developed and maintained by Meteo France, however these data were sourced through the ECMWF where copies of the data are hosted, for more information visit <http://www.ecmwf.int>.

|        |                 |
|--------|-----------------|
| Model: | ARPEGE system 3 |
|--------|-----------------|

|                      |   |
|----------------------|---|
| Boundary conditions: | The variable-resolution (0.33–2°) ORCA ocean model  |
| Data type:           | Hindcast  |
| Period:              | 1982-2010   |
| Season:              | Jan-Aug   |
| Temporal resolution: | Daily. These data are aggregated by taking the seasonal mean of the ensemble median.  |
| Spatial resolution:  | 0.75° x 0.75 °  |
| Domain:              | 30°N to 72°N and -75°E to 75°E (see Figure 1a in Paper III)   |
| Variables:           | 2 metre temperature (2t)<br>10 metre meridional wind velocity (10v)<br>10 meter zonal wind velocity (10u)<br>Mean sea level pressure (mslp)<br>Surface sensible heat flux (sshf)<br>Surface latent heat flux (slhf)<br>Total precipitation (tp)<br>Temperature at 850 hPa (t850)<br>Specific humidity at 850 hPa (q850)<br>Meridional wind velocity at 850 hPa (v850)<br>Zonal wind velocity at 850 hPa (u850)<br>Geopotential height at 850 hPa (z850) |
| Source:              | European Centre for Medium-Range Weather Forecasts (ECMWF)  |

### *ECMWF IFS*

Hindcasts of P and T as well as large scale circulation fields from the ECMWF IFS (Integrated Forecast System) are used as predictors in paper III and V. ECMWF IFS is developed and maintained by ECMWF, for more information visit <http://www.ecmwf.int>.

Model: ECMWF system 3 cycle 31r1

|                      |  |
|----------------------|--|
| Boundry conditions:  | The HOPE ocean model with 1° x 1° spatial resolution   |
| Data type:           | Hindcast   |
| Period:              | 1982-2010  |
| Season:              | Jan-Aug  |
| Temporal resolution: | Daily. Those data used as predictors in the SE modelling chain are aggregated by taking the seasonal mean of the ensemble median   |
| Spatial resolution:  | 1° x 1° (DE) and 2° x 2° (SE)  |
| Domain:              | 55°N to 70°N and 11°E to 23°E (DE) (see Figure 1a in Paper III)<br>30°N to 80°N and -75°E to 75°E (SE) (see Figure 1b in Paper III)  |
| Variables:           | 2 metre temperature (2t)<br>10 metre meridional wind velocity (10v)<br>10 meter zonal wind velocity (10u)<br>Mean sea level pressure (mslp)<br>Surface sensible heat flux (sshf)<br>Surface latent heat flux (slhf)<br>Total precipitation (tp)<br>Temperature at 850 hPa (t)<br>Specific humidity at 850 hPa (q)<br>Meridional wind velocity at 850 hPa (v)<br>Zonal wind velocity at 850 hPa (u)<br>Geopotential height at 850 hPa (z) |
| Model:               | ECMWF system 4 cycle36r4   |
| Boundary conditions: | The NEMO ocean model with 1° x 1° spatial resolution with equatorial refinement  |
| Data type:           | Hindcast   |
| Period:              | 1981-2015  |

|                      |  |
|----------------------|--|
| Season:              | Jan-Aug  |
| Temporal resolution: | Daily. Those data used as predictors in the SE modelling chain are aggregated by taking the seasonal mean  |
| Spatial resolution:  | 0.5° x 0.5° (DE) and 1° x 1° (SE)  |
| Domain:              | 55°N to 70°N and 11°E to 23°E (DE) (see Figure 3b in Paper V)<br>30°N to 80°N and -75°E to 75°E (SE) (see Figure 3a in Paper V)  |
| Variables:           | 2 metre temperature (2t)<br>10 metre meridional wind velocity (10v)<br>10 meter zonal wind velocity (10u)<br>Mean sea level pressure (mslp)<br>Surface sensible heat flux (sshf)<br>Surface latent heat flux (slhf)<br>Total precipitation (tp)<br>Temperature at 850 hPa (t)<br>Specific humidity at 850 hPa (q)<br>Meridional wind velocity at 850 hPa (v)<br>Zonal wind velocity at 850 hPa (u)<br>Geopotential height at 850 hPa (z) |
| Source:              | European Centre for Medium-Range Weather Forecasts (ECMWF)   |

# Models and Methods

Diverse methods for hydrological seasonal modelling, analysis, and evaluation were used in this work. This chapter presents and briefly describes these. The reader is referred to the appended papers for more detail.

## Rainfall-runoff model based ensemble modelling chains

In this section, the hydrological rainfall-runoff model used in this work and three different hydrological modelling chains that utilise it are presented. A modelling chain, for the purpose of this work, is the cascade of nested steps that need to be performed to produce a forecast. The hydrological model is presented first followed by the modelling chains.

### **HBV**

The rainfall-runoff model used in this work is the Hydrologiska Byråns Vattenbalansavdelning hydrological model (HBV). It is a semi-distributed conceptual rainfall-runoff model which includes numerical descriptions of hydrological processes at the basin scale. HBV was originally developed at SMHI in the early 1970s (Bergström, 1976) to assist hydropower operations and it is still the hydrological model of choice for the industry in Sweden. Since its development model has also proved itself to be a useful for work related to dam safety, water supply, flood warnings and climate change studies (SMHI, 2016). Operational or scientific applications of the HBV model have been reported from more than 40 countries around the world (SMHI, 2016). The general water balance in the HBV-96 model can be expressed as:

$$P - E - Q = \frac{d}{dt}(SP + SM + UZ + LZ + LV)$$



where,

P = precipitation

E = evapotranspiration

Q = runoff

SP = snow pack

SM = soil moisture

UZ = upper groundwater zone

LZ = lower groundwater zone

LV = lake volume

The model is normally forced with daily observations of P, T and monthly estimates of potential evapotranspiration. The model consists of subroutines for meteorological interpolation, snow accumulation and melt, evapotranspiration estimation, soil moisture accounting procedure, routines for runoff generation and finally, a simple routing procedure between sub-basins and in lakes. Basins with considerable elevation ranges can be subdivided into elevation zones which, if needed, can be further divided into different vegetation zones (e.g., forested and non-forested areas). These subdivisions are made for the snow and soil moisture routines only. The model structure of HBV-96, with the most important characteristics, is presented schematically in Figure 10. For a more comprehensive model description readers are referred to Lindström et al. (1997).

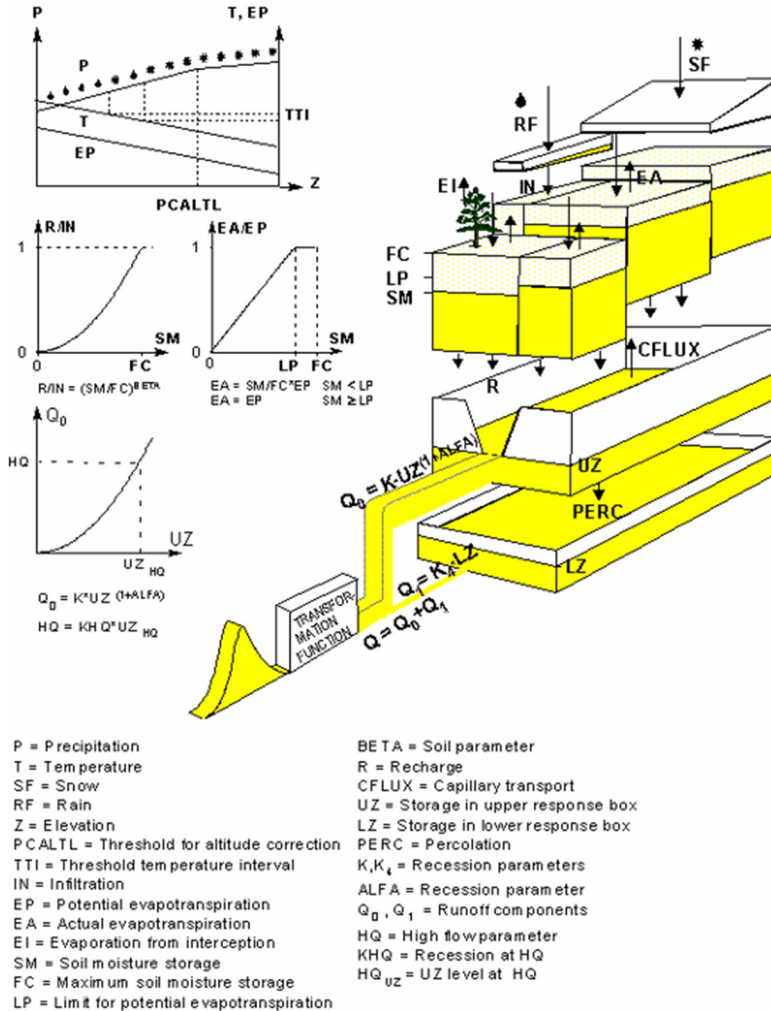
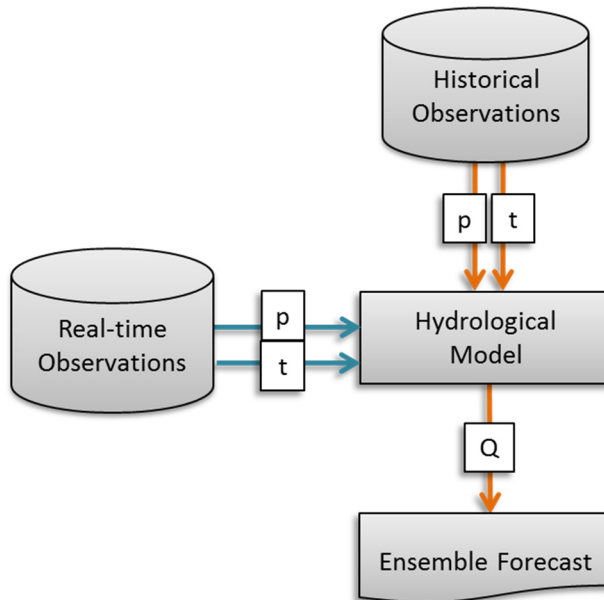


Figure 10. Schematic presentation of the HBV-96 model for a single basin (Lindström et al., 1997).

## Historical ensemble modelling chain (HE)

The HE, also referred to as ensemble streamflow prediction or ESP in the literature (e.g. Day, 1985), is the predominant modelling chain used for making operational seasonal forecasts of reservoir inflows within the hydropower sector in Sweden. Figure 11 shows a schematic of the HE modelling chain used in this work. The modelling chain follows three steps:

1. A well-calibrated set-up of the HBV rainfall-runoff model is initialized by running it up to the forecast issue date, typically in February, using observed meteorological data (T, P). This is done to ensure that the HBV model states reflect the current hydrological conditions in the basin with respect to e.g. streamflow, snow pack and soil moisture at the time of the forecast initialisation.
2. The initialised model from step 1) is then forced with catchment time series of T and P from all available historical years prior to the current one, which covers the period from the forecast issue date until the end of July. The time series of each historical year represents one possible weather evolution and results in one possible spring-flood volume (SFV) estimate.
3. The results from step 2) make up the HE. The nature of this modelling chain, using all available historical years of observations, means that the forecast evolution from the initial model states is climatological in nature. This climatological forecast which may be expressed in terms of percentiles with different probabilities. Though, in current practice, as well as in this study, the median value of SFV is considered as the spring flood forecast. The spin-up period used is from 01-01-1961 to “present”. As each new forecast is made, the initial conditions (i.e. model state) are saved and these are used when spin-up for the next forecast date is performed. In this work, the HE is thus made up of all historical years from 1961 to “present”. This means that the HE has 40 members in 2000 and increases in size by one member for each year thereafter (paper III). However, in paper V, a cross-validation protocol is used which results in a fixed sized ensemble using data from all available years excluding those data for the year for which the hindcast is being made.



**Figure 11.** Schematic diagram of the historical ensemble modelling chain.

### **Analogue ensemble modelling chain (AE)**

The use of analogues has been widely used as a downscaling methodology since Zorita and von Storch (1999). The hypothesis is that similar large-scale atmospheric patterns can result in similar meteorological conditions. The objective is to identify historical years with similar large-scale circulation conditions as the current year, up to the forecast issue date, and then assume that their subsequent weather evolutions are likely realisations over the coming forecast period. In this work a period of 1 to 8 months prior to the forecast initialisation date is used to identify the analogue years. The motivation for this is that this period covers the period when snow is accumulated in the catchments and that similar climate behaviour during this period could induce similar snow accumulation. With snow being the major contributor to the SFV, years that have similar large-scale circulation conditions during the winter period should have similar sized snowpacks and thus similar SFVs.

Compared with the HE modelling chain, this approach aims at identifying a reduced ensemble of data from analogue years with which the AE forecast will be made. To restrict the large number of degrees of freedom of the atmospheric circulation, that would require an unreasonable number of years in the historical data set, two methods are used for the selection of the analogue ensemble. The first one is based

on teleconnection climate indices and the second on circulation patterns. Thus, the AE is the same as the HE with the added step, after step 2), that once the historical ensemble forecasts is calculated, only those ensemble members corresponding to the identified analogue years are retained to make up the AE.

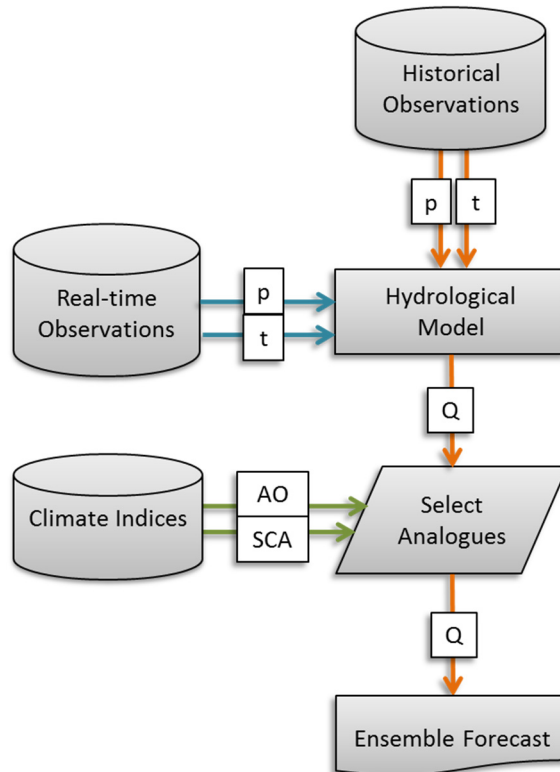


**Figure 12.** Schematic diagram of the AE modelling chain where TCIs are used for analogue selection.

### *Analogue selection based on teleconnection pattern indices (TCI)*

The prospect of using climate indices for identifying analogue years in a hydrological forecasting context is not a new one (e.g. Hamlet and Lettenmaier, 1999) but it is relatively rare. As mentioned in the previous section, the hypothesis is that it is possible to select analogue years from the historical driving dataset by comparing the TCIs in the period leading up to the forecast initialisation with the same period in previous years and selecting those that are similar to force a hydrological model. Other investigations in this work connects the following three TCIs with the SFV in northern Sweden (see section Climate-streamflow connections and paper **IV**):

- NAO/AO: positively correlated with P and T over Sweden for most of the year. For P, the relationship switches to a negative correlation during the months of July and August (see section North Atlantic Oscillation (NAO) and Arctic Oscillation (AO)).
- SCA: negatively correlated with P and T and has been shown to modify, strengthen or weaken, the teleconnection effects of AO/NAO on P over Scandinavia (see section Scandinavian Pattern (SCA)).
- EA: positively correlated with P and T for much of the year and has also been shown to modify the teleconnection effects of AO/NAO on P over Scandinavia (see section East Atlantic Pattern (EA)).

In Paper III, the analogue years are classified based on the indices' historical mean value  $TCI_M$  and standard deviation  $TCI_S$  for six months prior to the forecasts initialisation date. The current year, with its certain TCI-value, is classified as above normal if  $TCI > TCI_M + TCI_S$ , below normal if  $TCI < TCI_M - TCI_S$  and normal if  $TCI_M - TCI_S \leq TCI \leq TCI_M + TCI_S$ . The same classification is done for the corresponding periods in each of the years in the historical archive. If the classification of the three different indices is in agreement with the index classification for the year in question for the forecast, the specific historical year is selected as an analogue year. If no analogue years are identified, then analogue years are sought using an agreement with two indices. The number of identified analogue years range between 1 and 19 with the average number being 7.

In Paper V, an improved approach for selecting analogues is employed (Figure 12). The mean TCI of AO and SCA is calculated for the period from October to the forecast date minus one month, to replicate the delay in real-time teleconnection indices being published e.g. the period would be October-November-December-January if the forecast date was in March. This is done for all years in the climatological ensemble. If the values of these indices are considered to be coordinates then their positions can be plotted in Euclidean space. An analogue year is defined to be those years whose positions in the resulting AO-SCA Euclidean plane that are within a distance of 0.2 from the Euclidean position of the forecast year. The limit of 0.2 is an arbitrary value found, through an iterative process, to give a good balance between precision and the chance of finding an analogue. The analogues are replicated so that the number of ensemble members is the same as that in the HE. If no analogue years are identified then the HE is used instead.

#### *Analogue selection based on circulation patterns (CP)*

Circulation-pattern (CP) analysis is a commonly used tool in climatological and meteorological studies (Hay et al., 1991; Wilby and Wigley 1994). It was initially applied to explain climate variability at a large scale (Barry and Perry, 1973) and later on widely developed to downscale GCM output to local climate in e.g. climate

change studies (Wetterhall et al., 2006; Yang et al., 2010). The use of CP to select analogues is used in paper III only.

The method is generally applied to reliable upper-air data at multi-grid, e.g. sea level pressure and geopotential height, to explain recorded observations of e.g. P and T. By differentiating historical observations into several representative CPs, each CP is supposed to represent specific climate conditions in the study area. The CPs are defined based on either professional knowledge of atmospheric motions (subjective classification) or statistical characteristics derived from the observations (objective classification). As the subjective classification is only available in a limited number of regions, the objective classification has been widely developed and used. The objective classification is a semi-automated or automated technique that pertains to mathematical approaches, e.g. hierarchical methods (Johnson, 1967), k-means methods (Mac-Queen, 1967), cluster analysis (Kysely and Huth, 2005) and correlation methods (Yarnal, 1984).

The method used in this work uses fuzzy-rule-based classification, built on the concept of fuzzy sets (Zadeh, 1965), of MSLP reanalysis data (see Table 1) to determine the circulation patterns common to the region in the three or six months prior to the forecast initialisation date. An analogue year is defined as any historical year for which the two dominant CPs in the months prior to the forecast date are the same as those found for the year in question. (see paper III for more details). The analogues are then used in the same manner as the TCI analogue approach i.e. replicated so that the number of ensemble members is equal to those in the HE and the HE is used if no analogues can be identified.

## **Dynamic ensemble modelling chain (DE)**

The DE, Figure 13, is similar to the HE except that the hydrological model is not forced with historical data in step 2) but rather by an ensemble of seasonal forecasts of daily P and T from the ECMWF IFS (see Table 1). This is done by mapping the daily meteorological forecasts (see Table 1) from the GCM grid onto the HBV sub-catchments. The resulting sub-catchment average P and T forecasts are used to force the HBV model from the same initial state as used in the current HE procedure i.e. following the HE procedure but with forecasts instead of historical years in step 2. Again, the final forecast used in the evaluation is defined by the ensemble median.

In Paper V the P and T forecasts from the ECMWF IFS are bias adjusted before being used to force the HBV model. The bias adjustment method used is a version of the distribution based scaling approach (DBS; Yang et al., 2010) which has been adapted for use on seasonal forecast data. DBS is a quantile mapping bias adjustment method where meteorological variables are fitted to appropriate parametric distributions (e.g. Berg et al., 2015; Yang et al., 2010).

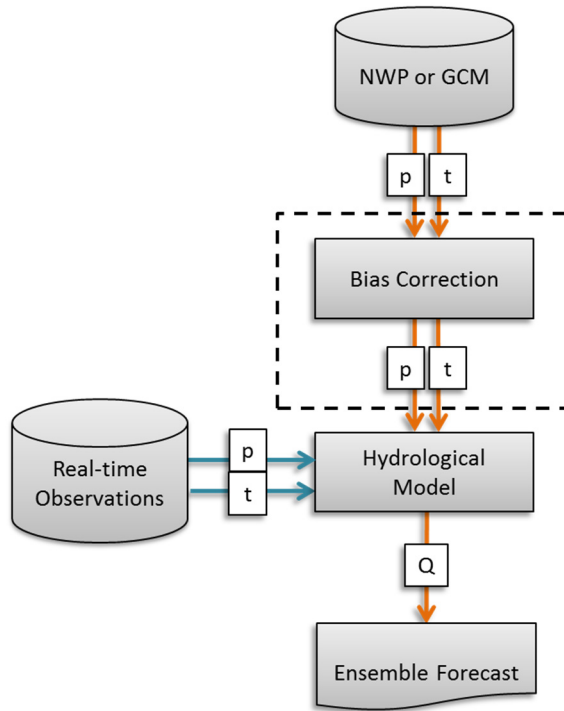


**Figure 13.** Schematic diagram of the dynamic ensemble modelling chain. The dashed box shows the bias correction step that is present in the modelling chain used in paper V but is not present in the modelling chain used in paper III.

## Statistically downscaled ensemble modelling chain (SE)

Statistical downscaling is a widely accepted methodology used to connect coarse-scale climate data output from GCM to local-scale variables. In this work, large-scale circulation variables are statistically connected to the SFV. The method employed to establish the statistical relationship among the variables are the multivariate procedures known as canonical correlation analysis (CCA; see section Canonical Correlation Analysis) and Singular Value Decomposition (SVD; see section Singular Value Decomposition) analysis. Both methods isolate sets of mutually orthogonal pairs of spatial patterns that maximize the squared temporal correlation (the former) or covariance (the latter) between two physical variables.

These analyses can be used to derive specific prediction or specification models for particular points in one variable's field (the predictand; SFV in this work) based on the spatial pattern and/or on the evolution patterns of the anomalous values in the other field (the predictor). From the singular vector pairs, the temporal expansion series of each field can be obtained by projecting the data onto the appropriate



singular vector (Bretherton et al., 1992). The relationship between the variables is generated by calculating the matrix of regression coefficients which relates the values of the predictor singular mode temporal amplitudes to the individual points in the predictand field.

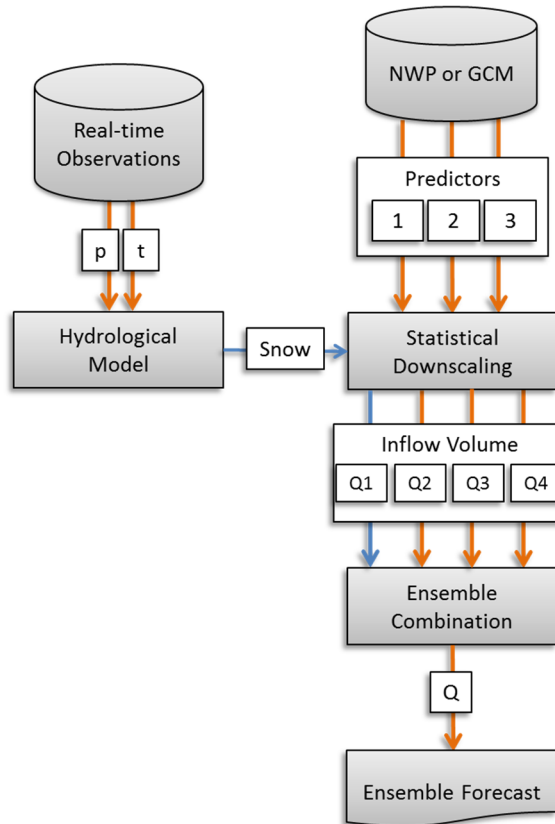


**Figure 14.** Schematic diagram of the statistical downscaled ensemble modelling chain.

In this work, hindcasts for the predictors and historical observations for the predictands are used to define the statistical relationship between them i.e. to calibrate the model. To maximise the robustness of the forecast, multiple forecasts are made with different predictors resulting in an ensemble forecast. In Paper I a CCA approach with three large scale climate variables is used; alternatively in Papers III and V the SVD approach is used with three and four predictors, respectively (Figure 14). The reader is referred to the relevant papers for more details.

It should be noted that whereas the other methods generate daily discharge time series over the spring flood period, from which SFV is estimated, the SE method directly forecasts the SFV. Therefore forecasts from the SE method give information about the volume of the spring flood only; they do not provide information about the evolution of the flood profile.

### *Canonical Correlation Analysis*

Canonical correlation analysis (CCA) is a statistical method, first developed by Hotelling (1936), for exploring the relationship between two multi-dimensional datasets. It estimates two linear transformation coefficients, one from each dataset, such that the data are maximally correlated in the transformed space (e.g. Barnett and Preisendorfer, 1987; Sun et al., 2009). In Paper I, CCA is used to construct a statistical regression model to downscale output fields from a GCM directly to seasonal streamflows for multiple gauging stations in Norway.

A CCA regression model can be constructed by first calculating the matrix of regression coefficients ( $S$ ) which relate the values of the predictor canonical mode temporal amplitudes ( $U$ ) to the individual values in the predictand field ( $Z$ ). These coefficients are given by the vector product  $S_{m,z} = (U_m Z_z)$ , where  $m$  is the canonical mode index and  $z$  is the spatial index of the elements. That is to say that  $S_{m,z}$  links the predictor side of the canonical mode  $m$  to point  $z$  in the predictand field ( $Z$ ). The CCA model regression equation can then be written in matrix notation as  $\hat{Z} = U'S$  (Uvo, 1998).

The three CCA models in paper I are constructed using the Climate Predictability Tool (CPT) developed at IRI. The CPT is a software package (Mason and Tippet, 2015) for constructing seasonal climate forecast models, performing model validation, and producing forecasts given updated data.

### *Singular Value Decomposition*

Singular value decomposition (SVD) is the generalization of the eigen decomposition of matrices that are not square or symmetrical. SVD isolates sets of mutually orthogonal pairs of spatial patterns that maximize the squared temporal covariance between two physical variables (e.g. Cheng and Dunkerton, 1995; Uvo et al., 1998). The SVD of the cross-covariance matrix ( $C_{yz}$ ) between the predictor and predictand fields is given by  $A = G_k \sigma H'_k$ , where  $\sigma$  are the eigenvalues,  $G_k$  and  $H_k$  are the predictor and predictand eigenvectors respectively, and  $k$  is the number of modes. The pair of eigenvectors describes spatial patterns for each field that have overall covariance given by the corresponding eigenvalue. SVD is used in paper V to identify which of the GCM output fields is suitable as predictors and to construct a regression model to downscale these predictors directly to SFV.

In order to identify which predictors to use they are first divided into one of three groups; pressure related fields, humidity related fields, and temperature related fields. Then the members of each group are ranked according to the strength of their relationship with the predictand (SFV). This ranking is based on the normalised squared covariance (NSC) which is defined by Wallace et al. (1993) as:

$$NSC_k = \sqrt{\frac{\sigma_k^2}{\sum_i \sum_j var_i var_j}}$$

where,  $var_i$  and  $var_j$  are the variances at the  $i^{th}$  and  $j^{th}$  grid points in the predictor field and predictand fields respectively and  $\sigma_k$  are the eigenvalues of the  $k^{th}$  mode.

The construction of the SVD regression model is similar to the construction of the CCA regression model described in the preceding section.

## Multi-model ensemble of modelling chains (ME)

The ME is the next step in the modelling chain concept hierarchy where individual modelling chains are combined into a single multi-chain forecast system. This falls under the umbrella of what is often referred to as multi-modelling in the literature. The hypothesis is that by applying the notion of the “wisdom of the crowd” to forecasting it is possible to improve forecast skill. Basically, it assumes that the larger errors in one model will be offset by smaller errors in the other models resulting in a forecast with better skill overall. This approach is not new in hydrological forecasting and has been successfully applied numerous times (e.g. Duan et al., 2007; Ma et al., 2016; Mo and Lettenmaier, 2014; Wanders et al., 2019; Yuan et al., 2011; Yuan et al., 2015).

In this work, the forecast ensembles from the individual modelling chains are combined into an ME in three different ways (see papers **III** and **V** for more details):

- Using the ensemble median of the middle ranked modelling chain as the forecast.
- Weighting the individual models using simple fractional weights, based on their individual performance, such that the weights added up to one.
- Simply pooling the individual modelling chain ensembles into one large ensemble.

The reason for using these simple techniques is due to the lack of data points, the longest series have a total of 35 spring flood events per sub-basin and forecast initialisation date (see paper V). This lack of data with which to derive informed weights excludes more sophisticated methods such as Bayesian model averaging (e.g. Kleiven and Steinsland, 2018) or machine learning (e.g. Zaherpour et al., 2019).

## Bootstrapping

Bootstrapping is a resampling technique that allows for the estimation of the precision of any sample statistic such as a validation metric. By calculating the validation metrics on randomly sampled subsets of the population data it is possible to calculate the confidence intervals for these metrics which are an inference of their true values for the population (Efro, 1992). In Papers I and V bootstrapping is used to ascertain whether the validation metrics from the cross validation hindcast experiments are significant or not. The rationale for doing this is that the length of the data series are limited and in the case of Paper I a simpler k-fold cross validation is employed and not a more complete leave-one-out cross validation, where the data is repeatedly divided up until all possible combinations have been explored (Kohavi, 1995), so resampling would be required to better estimate the distribution of the validation scores.

## Cross Validation

Model performance in Papers I and V are estimated using cross validation. K-fold cross validation divides the datasets up into  $k$  mutually exclusive subsets of roughly equal size. The modelling experiments are then carried out  $k$ -times, each time a different subset is used as the testing dataset while the remaining subsets are used as the training data. An estimation of model performance is then calculated on the results from the different modelling experiments. Leave-one-out cross validation (LOOCV) is the logical extreme of the  $k$ -fold cross validation where the number of subsets is equal to the number of data points. The advantages with this approach are that it is relatively easy to implement and that it offers a more robust method of evaluating model performances when the datasets are small. A drawback is that the procedure can be time consuming as the modelling must be performed many times. Figure 15 shows graphically how the data is divided into the training and testing subsets.

In Paper I the data is divided into seven subsets,  $k=7$ , and the regression model is repeatedly trained using the data from six of these subsets and the resulting models are used to make hindcasts for the remaining years. In Paper V a LOOCV protocol is used for the modelling experiments i.e.  $k=1$ .

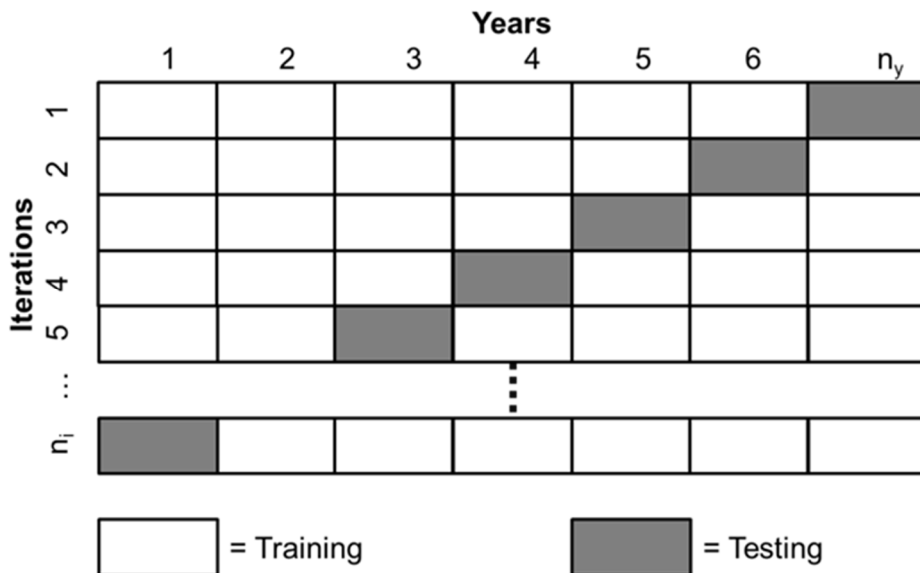


Figure 15. Division of the data into training and testing subsets. This example uses  $k=1$  i.e. a LOOCV protocol.

## Principal Component Analysis

Principal component analysis (PCA) is a multivariate technique developed by Pearson (1901), although Hotelling (1933) is often the one credited, that provides a way to convert complex data into simplified linearly uncorrelated principle components of variance using orthogonal transforms. If the PCA is performed successfully the resulting data will still retain much of the original information while the original dimensionality has been greatly reduced.

PCA was applied in Paper IV in two ways. The first is as a filter to increase the signal to noise ratio by retaining the components that contained 90% of the explained variance in the hydrological data before clustering; this use of orthogonal solutions as the input for the cluster analyses is common practice and convenient (e.g. Uvo and Berndtsson, 1996). The second is as a method to determine connections between the different teleconnection patterns and streamflow for every hydrological period and homogeneous hydrological region. For each homogeneous

hydrological region and hydrological period, a PCA was performed to the data matrix composed by the time series of the streamflow composite (average of the streamflow of all stations belonging to the homogeneous hydrological region) and the time series of the accompanying TP periods. A biplot of the first two PCA modes was used to identify within all TPs and TP periods, the ones that were most strongly related to the hydrological region and period in question.

## Cluster Analysis

The goal in Paper IV is to identify, quantify and understand the climatic drivers that govern the variability in seasonal hydrology in Sweden. To this end it is necessary to divide Sweden into homogeneous hydrological regions, and this is done by cluster analysis. This method groups variables that are linearly related to each other into subsets by developing ‘dendrograms’, tree-like hierarchical diagrams which show the familial relationships among all the variables in a dataset (Krumbein and Graybill 1965). The correlation matrix is used as a foundation for discriminating the levels of relatedness between the variables. Starting with one or more highly correlated pairs of attributes, the connections between these and the remaining variables are computed to develop a hierarchy of interrelations showing the degree of connection within the dataset.

The hierarchical cluster analysis is done using Ward’s algorithm (Ward, 1963). The clusters are validated by correlating the individual records with the cluster mean, by physical understanding of the geographical expression of the clusters and by using silhouettes. Silhouettes are a graphical aid based on the comparison of the dissimilarity of the members of each cluster and the mean silhouette width gives a measure for the clustering solution’s validity (Forgy, 1965; Rousseeuw, 1987).

A composite monthly series and a monthly hydrograph of long term average streamflow are created for each cluster. These composite time series, which are derived from the average of the normalised time series composing the cluster, are used as the representation of the streamflow for the correspondent cluster in later analyses. The benefit with using a composite is that it acts as a generalised time series for the entire cluster and thus is not biased toward any individual time series.

# Wavelet Analysis

In Paper IV the temporal variability of the hydrological periods (HP) and TP periods were analysed by means of continuous wavelet transform (CWT). The wavelet analysis (Morlet et al., 1982a and 1982b; Grossmann and Morlet, 1984; Grossmann and Morlet, 1985) can analyse both the time and frequency variations of a non-stationary time series. The wavelet analysis decomposes a time series into scale components which discriminate between the oscillations at different time scales. Wavelet analysis retains information regarding the occurrence of non-stationary events in both the time and frequency domains, unlike other spectral techniques such as the Fourier and Gabor transforms, highlighting localized intermittent periodicities. Furthermore, it is possible to provide information about the level of significance by varying the period in accordance to short or long time scale oscillations (Grinstead et al. 2004).

A wavelet function is characterized by a zero mean and its localization in both frequency and time. The Morlet ( $\Psi_0$ ) wavelet was used in this study since it is efficient in extracting features, maintaining a good balance between frequency and time information (Grinstead et al., 2004). It is defined as:

$$\Psi_0(\eta) = \pi^{-1/4} e^{i\omega_0\eta} e^{-\eta^2/2}$$

where,  $\eta$  and  $\omega_0$  are time and frequency respectively, both non-dimensional. The CWT of a discrete data series  $X$ , with  $N$  elements, is defined as the convolution of  $x_n$  with a scaled and translated version of the wavelet  $\Psi_0(\eta)$ . When normalized to have unit energy, it might be compared to the CWT of other variables and assumes the form:

$$W_n^X(s) = \sqrt{\frac{\delta t}{s}} \sum_{n'=1}^N x_{n'} \Psi^* \left[ \frac{(n' - n)\delta t}{s} \right]$$

where,  $s$  is the wavelet scale,  $n$  is the localized time index, and  $*$  indicates the complex conjugate (Torrence and Compo 1998; Grinstead et al., 2004). The wavelet spectrum is then defined as the square of the amplitude of the transform:  $|W_n(s)|^2$  (Torrence and Compo, 1998). The statistical significance level of the CWT is

estimated by comparing the calculated spectra with the spectrum of the red noise as suggested by Torrence and Compo (1998).

The relationships between the temporal variability of the TP periods and the HPs were investigated using Cross Wavelet Transforms (XWT). The XWT between two data series  $x_n$  and  $y_n$  is defined by Grinsted et al. (2004) as the product between the CWT of one variable and the complex conjugate of the CWT of the other variable ( $W^{XY} = W^X W^{Y*}$ ), and the cross-wavelet power as the absolute value of the XWT ( $|W^{XY}|$ ). The local relative phase between the TP period and the HP is represented by the complex argument of the XWT. The XWT shows the periods and frequencies in which the individual CWTs both have high power plus the local phase between them.

To avoid the pitfalls of XWT analysis identified by Maraun and Kurths (2004), the wavelet transform coherence (WTC) was used. This is a measure of the coherence between the signals from the individual CWT (Grinsted et al., 2004), and can be thought of as the local correlation between the wavelet transform of each time series used in the XWT. Therefore, while a XWT identifies periods and times when the two variables are oscillating, the WTC enhances the periods and time when the variables are locally correlated. As such, WTC is able to highlight periods and times when the two variables were correlated, even if the power of their oscillation is not strong. Results of these analyses are presented in form of a diagram Period vs Time with colours representing the power intensity and arrows representing the relative local phase. Horizontal arrows pointing to the right indicates that the TP period and the hydrological variability are in-phase and pointing to the left that they are in anti-phase. Vertical arrows indicate that one variable time series leads the others by  $90^\circ$  (Grinsted et al., 2004).



# Validation metrics

The validation metric used to estimate model performance in this dissertation are briefly presented in table below.

**Table 2.** The validation metrics used to evaluate the multi-model performance. The threshold for skill is 50 for FY+ and 0 for all the other metrics.

| Name  | Equation   | Description  |
|---|--|--|
| Mean absolute error skill score ( <b>MAESS</b> )                    | $MAESS = 1 - \frac{MAE_f}{MAE_r}$ <p>where <math>f</math> is the modelled forecast and <math>r</math> reference forecast.</p>  | Measure of the model's general performance; it quantifies the relative forecast error against a reference forecast.  |
| Frequency of Years ( <b>FY+</b> )                                   | $FY^+ = \frac{100}{n} \sum_{y=1}^n H^y,$ <p>where <math>y</math> is the timestep and <math>n</math> is the total number of timesteps. <math>H</math> is the Heaviside function defined by</p> $H^y = \begin{cases} 0, & AE_r^y < AE_f^y \\ 1, & AE_r^y > AE_f^y \end{cases}$ <p>where <math>AE</math> is the absolute error, <math>y</math> is the timestep, <math>f</math> is the modelled forecast, and <math>r</math> reference forecast.</p> | Measure of the model's general performance; it quantifies how often the forecast outperforms a reference forecast.   |
| Nash-Sutcliffe efficiency ( <b>NSE</b> ; Nash and Sutcliffe, 1970)) | $NSE = 1 - \frac{\sum_{y=1}^n (SFV_r^y - SFV_f^y)^2}{\sum_{y=1}^n (SFV_r^y - \overline{SFV_r})^2}$ <p>where <math>SFV</math> is the springflood volume, <math>y</math> is the timestep, <math>n</math> the total number of timesteps, <math>f</math> is the modelled forecast, and <math>r</math> reference forecast.</p>  | Measure of the model's general performance; it quantifies the model's residual variance against a reference forecast's variance.                                     |
| Relative operating characteristic skill score ( <b>ROCSS</b> )      | $ROCSS = 2 * AUC - 1,$ <p>where <math>AUC</math> is the area under the curve</p> $AUC = \sum_{y=1}^{n+1} \frac{(FR^y - FR^{y-1})(HR^y + HR^{y-1})}{2},$ <p>where <math>FR</math> is the false alarm rate, <math>HR</math> is the hit rate, <math>y</math> is the timestep, and <math>n</math> the total number of timesteps.</p>   | Measure of the model's probabilistic performance; it quantifies the model's ability of the discriminate between an event and a non-event given a specific threshold. |
| Interquartile range skill score ( <b>IQRSS</b> )                    | $IQRSS = 1 - \frac{IQR_f}{IQR_r}$ <p>where <math>IQR</math> is the interquartile range, <math>f</math> is the modelled forecast, and <math>r</math> reference forecast.</p>  | Measure of the forecast sharpness, it quantifies the relative spread in the forecast against a reference forecast.   |
| Uncertainty sensitivity ( <b>U</b> )                                | $U = 1 - \frac{6 \sum_{y=1}^n d^2}{n(n^2 - 1)},$ <p>where <math>d</math> denotes the difference in the ranks of the <math>IQR</math> and <math>AE</math>, <math>y</math> is the timestep, and <math>n</math> the total number of timesteps.</p>  | Measure of the model's sensitivity to uncertainty; it quantifies the correlation between forecast sharpness and absolute error                                       |

# Results and Discussion

Different forecasting approaches were investigated and developed in this work with the aim of improving the performance of seasonal forecasts of the spring flood inflow volumes to Swedish hydropower reservoirs. These approaches can be divided into two general categories: the individual modelling chains, and multi-models comprising combinations of these individual modelling chains. The main findings are presented in this chapter. For further details the reader is directed to the appended papers.

## The individual modelling chains

### **Historical ensemble**

Table 3 gives an overview of the HE approach's ability to predict the inflow volume of the spring flood in 84 sub-basins in Sweden (paper V). It presents skill scores and the number of sub-basins, as a percentage, where the HE performs better than climatology. The reported skill scores are the median results for the 84 sub-basins aggregated by cluster. The  $n^+$  values indicate the percentage of sub-basins where the HE exhibits skill over climatology and those in brackets show the percentage of sub-basins for which these results are significant at the 0.1 level.

These results show that the general performance of the HE approach is best when the lead times are shorter i.e. those forecasts which are initialised later in the year. The MAE skill scores (MAESS) and change in NSE ( $\Delta$ NSE) suggest the HE approach has little to no skill over climatology with respect to forecast error and interannual variability for forecasts initialised in January and February. However, the results typically improve with each initialisation.

There is a marked jump in the general skill going from forecasts initialised in February to those initialised in March. The interpretation for this is that the snow pack is more developed by this time. The skill achieved by such an approach is mainly leveraged from the initial hydrological conditions i.e. information relating to the water stores within the catchment at the time the forecast is initialised. In the

context of this work, it is information related to the snow pack that is of greatest value. Snow melt is a majority contributor to the inflow volumes during the spring melt period in Sweden. HE achieves similar results for all sub-basins with those results in  $S^2$  being the weakest.

**Table 3.** Cross-validated median skill scores, bootstrapped  $N = 10\,000$ , for HE with respect to climatology, aggregated by forecast initialisation month and cluster for the 84 sub-basin used in paper V. The  $n+$  values indicate the percentage of sub-basins where the HE performs better than climatology averaged over all 84 sub-basins.  $n+$  values in brackets show the percentages of the sub-basins for which these scores are statistically significant at the 0.1 level. The skill threshold is 0 for MAESS and  $\Delta NSE$ , while the skill threshold for  $FY+$  is 50.

|       |     | MAESS |          | FY+  |          | $\Delta NSE$ |          |
|-------|-----|-------|----------|------|----------|--------------|----------|
|       |     |       | $n+$ (%) |      | $n+$ (%) |              | $n+$ (%) |
| $S^1$ | Jan | -0.02 | 56 (0)   | 48.3 | 56 (0)   | -0.10        | 40 (0)   |
|       | Feb | 0.01  | 60 (0)   | 50.4 | 56 (0)   | -0.03        | 52 (4)   |
|       | Mar | 0.06  | 84 (0)   | 54.9 | 80 (0)   | 0.05         | 80 (0)   |
|       | Apr | 0.08  | 80 (20)  | 55.8 | 80 (0)   | 0.10         | 72 (16)  |
|       | May | 0.17  | 88 (36)  | 58.6 | 84 (24)  | 0.24         | 88 (36)  |
| $S^2$ | Jan | -0.15 | 5 (0)    | 42.6 | 5 (0)    | -0.32        | 0 (0)    |
|       | Feb | -0.08 | 26 (0)   | 44.5 | 26 (0)   | -0.20        | 26 (0)   |
|       | Mar | 0.02  | 68 (0)   | 49.6 | 37 (0)   | 0.03         | 58 (11)  |
|       | Apr | 0.09  | 84 (26)  | 52.8 | 63 (0)   | 0.14         | 74 (21)  |
|       | May | 0.16  | 89 (37)  | 57.4 | 26 (37)  | 0.24         | 89 (26)  |
| $S^3$ | Jan | -0.12 | 15 (0)   | 44.6 | 18 (0)   | -0.31        | 10 (0)   |
|       | Feb | 0.02  | 55 (13)  | 49.1 | 45 (3)   | -0.05        | 40 (10)  |
|       | Mar | 0.15  | 88 (33)  | 54.5 | 75 (15)  | 0.22         | 85 (43)  |
|       | Apr | 0.21  | 88 (50)  | 57.4 | 78 (20)  | 0.32         | 88 (50)  |
|       | May | 0.25  | 93 (60)  | 60.6 | 90 (33)  | 0.41         | 90 (65)  |

The ROCSS in Table 4 shows that the HE approach does show general skill over climatology at discriminating between below normal (lower tercile, LT), near normal (middle tercile, MT), and above normal (upper tercile, UT) events for all forecast initialisations. This suggests that HE already offers some, albeit limited, benefit over climatology for the early forecast initialisations by being better at discriminating between below, near, and above normal events. It is interesting to note that the HE has better skill at discriminating below normal events than above normal events. The probable explanation for this is that there is a cold and dry bias in the historical driving data. The typical precipitation and temperatures from the period that the historical data spans, 1961 to ‘present’, are lower than those for the period 1981-2010 or 1981-2015, the periods used in this work. The cause of this bias is not investigated in this work, however the working hypothesis is that it is due to some combination of climate change and NAO switching to positive trend in the early 1980s.

**Table 4.** Cross-validated median ROCSS, Bootstrapped (N = 10 000), aggregated by forecast initialisation month for the 84 sub-basin used in paper V. The n<sup>+</sup> values indicate the percentage of sub-basins where the HE performs better than climatology averaged over all 84 sub-basins. n<sup>+</sup> values in brackets show the percentages of the sub-basins for which these scores are statistically significant at the 0.1 level. LT = lower tercile, MT = middle tercile, UT = upper tercile, and the skill threshold is 0.

|       |    |                    | Jan     | Feb     | Mar      | Apr      | May      |
|-------|----|--------------------|---------|---------|----------|----------|----------|
| ROCSS | LT |                    | 0.23    | 0.42    | 0.57     | 0.63     | 0.69     |
|       |    | n <sup>+</sup> (%) | 90 (21) | 99 (56) | 100 (91) | 100 (95) | 100 (99) |
|       | MT |                    | 0.08    | 0.11    | 0.11     | 0.18     | 0.24     |
|       |    | n <sup>+</sup> (%) | 72 (0)  | 72 (1)  | 76 (5)   | 85 (8)   | 92 (9)   |
|       | UT |                    | 0.11    | 0.26    | 0.46     | 0.53     | 0.62     |
|       |    | n <sup>+</sup> (%) | 69 (9)  | 93 (28) | 99 (59)  | 100 (79) | 100 (95) |

## Analogue ensemble

When the skill of the two AE variants are tested for skill over HE, in two sub-basins, it is found that the approach which uses CP analysis as the selection criteria performs better than the other TCI-based version. Table 5 gives the relative improvement (RI; see paper 3 for more details) and FY<sup>+</sup> values of forecasts made for two unregulated sub-basins in the Ume River system. Although this is a study with a limited sample, the CP variant shows improved values for forecasts initialised in January and March for both sub-basins and validation measures. While the TCI variant is only able to show improved values in the FY<sup>+</sup> measures for one of the sub-basins.

**Table 5.** Relative improvement RI (%) and frequency of years with a better performance FY<sup>+</sup> (%) of the two different AE forecasting approaches TCI and CP for two sub-basins in the Vindel River. The results are with reference to the climatological ensemble HE (boldface indicates better performance than HE). The skill threshold is 0 for RI and 50 for FY<sup>+</sup>.

|     |                 | Jan        |           | Mar         |             | May       |         | Average    |
|-----|-----------------|------------|-----------|-------------|-------------|-----------|---------|------------|
|     |                 | Sorsele    | Vindeln   | Sorsele     | Vindeln     | Sorsele   | Vindeln |            |
| TCI | RI              | -6.6       | -9        | -1.2        | -10.4       | -6.6      | -21.9   | -9.3       |
|     | FY <sup>+</sup> | <b>55</b>  | 45        | <b>64</b>   | 45          | <b>55</b> | 45      | <b>52</b>  |
| CP  | RI              | <b>1.4</b> | <b>13</b> | <b>19.2</b> | <b>36.2</b> | -9.9      | -31.3   | <b>4.8</b> |
|     | FY <sup>+</sup> | <b>75</b>  | <b>75</b> | <b>70</b>   | <b>80</b>   | 33        | 33      | <b>61</b>  |

These results are encouraging in that they suggest that improvements are possible, especially for the longer lead-times. However, the CP variant of the AE is not easily implementable in an operational setting. The reanalysis data that are used to select the analogues have a two month delay in their release which makes a third of the period, on which the analysis is performed, unavailable. Additionally, the CP analysis would be more difficult to automate, due to its complexity, compared to the much simpler TCI analysis for selecting analogues.

**Table 6.** Cross-validated median skill scores, bootstrapped N = 10 000, for the TCI version of AE with respect to HE, aggregated by forecast initialisation month and cluster for the 84 sub-basin used in paper V. The n<sup>+</sup> values indicate the percentage of sub-basins where the HE performs better than climatology averaged over all relevant sub-basins. n<sup>+</sup> values in brackets show the percentages of the sub-basins for which these scores are statistically significant at the 0.1 level. The skill threshold is 0 for MAESS and  $\Delta$ NSE, while the skill threshold for FY<sup>+</sup> is 50.

|                |     | MAESS |                    | FY <sup>+</sup> |                    | $\Delta$ NSE |                    |
|----------------|-----|-------|--------------------|-----------------|--------------------|--------------|--------------------|
|                |     |       | n <sup>+</sup> (%) |                 | n <sup>+</sup> (%) |              | n <sup>+</sup> (%) |
| S <sup>1</sup> | Jan | -0.02 | 44 (0)             | 47.5            | 40 (4)             | -0.05        | 20 (0)             |
|                | Feb | -0.03 | 48 (0)             | 45.7            | 36 (8)             | -0.02        | 48 (0)             |
|                | Mar | -0.07 | 4 (0)              | 40.8            | 20 (0)             | -0.14        | 4 (0)              |
|                | Apr | -0.02 | 36 (0)             | 45.9            | 20 (0)             | -0.07        | 20 (0)             |
|                | May | -0.07 | 8 (0)              | 49.6            | 56 (4)             | -0.11        | 0 (0)              |
| S <sup>2</sup> | Jan | 0.01  | 37 (5)             | 39.9            | 32 (0)             | 0.01         | 53 (5)             |
|                | Feb | -0.03 | 21 (0)             | 42.1            | 26 (0)             | -0.04        | 26 (0)             |
|                | Mar | -0.05 | 5 (0)              | 42.1            | 37 (5)             | -0.11        | 0 (0)              |
|                | Apr | -0.03 | 26 (0)             | 40.6            | 26 (0)             | -0.04        | 37 (0)             |
|                | May | -0.01 | 26 (5)             | 46.3            | 26 (5)             | -0.02        | 42 (0)             |
| S <sup>3</sup> | Jan | -0.01 | 45 (0)             | 49.8            | 60 (10)            | -0.01        | 48 (3)             |
|                | Feb | -0.09 | 5 (0)              | 46.1            | 30 (3)             | -0.19        | 5 (0)              |
|                | Mar | -0.08 | 3 (0)              | 49.1            | 53 (3)             | -0.16        | 3 (0)              |
|                | Apr | -0.03 | 40 (0)             | 47.1            | 33 (3)             | -0.06        | 28 (5)             |
|                | May | -0.04 | 38 (0)             | 50.7            | 57 (5)             | -0.07        | 28 (0)             |

Table 6 show the results from a more systematic analysis of AE skill over 84 sub-basins, including those reported in Table 5. These results are limited to the TCI version of the AE approach as the CP version was not considered due to it not being ready for production. The results for the three different performance scores show a similar general trend for each type and in all clusters, the AE tends to perform best in forecasts initialised earlier or later in the season i.e. January and May, rather than those initialised mid-season. In general, AE does not appear to offer much improved skill over HE. The percentage of sub-basins for which the AE shows skill over the HE never exceeds 50% for MAESS, once for  $\Delta$ NSE (forecasts initialised in January for sub-basins in cluster S<sup>2</sup>), and four times for FY<sup>+</sup> (forecasts initialised in May and January, March, and May for sub-basins in cluster S<sup>1</sup> and S<sup>3</sup> respectively).

This would imply that the results in Table 5 should be seen as being either atypical or at the upper end of the result envelope. However, the fact that the CP analysis is related to the TCI analysis, where both endeavour to separate the atmospheric circulation into mutually exclusive subcomponents, it would suggest that there is scope for improvement in the TCI approach.

## Dynamical ensemble

Table 7 gives an overview of the DE approach's ability to predict the inflow volume of the spring flood in 84 sub-basins in Sweden. DE tends to outperform HE in all clusters for forecasts initialised early in the season with respect to FY<sup>+</sup>. This skill then drops as the season progresses. The entirely negative median MAESS results suggest that DE has no skill over HE with respect to forecast volume error in general. However, there appear to be a relatively high percentage of sub-basins for which DE has skill over HE, especially in cluster S<sup>3</sup>. Furthermore, there are a small percentage of sub-basins in all clusters and initialisation months, save March and April in cluster S<sup>2</sup>, where this skill is statistically significant. This pattern is similar for  $\Delta$ NSE albeit more so. This suggests that the DE performs well for some sub-basins while performing significantly worse for others. HBV is well calibrated and as such is not the cause of this conflicting results. This would indicate, predictably, that the fault is with the meteorological driving data from the GCMs.

**Table 7** Cross-validated median skill scores, bootstrapped N = 10 000, for DE with respect to HE, aggregated by forecast initialisation month and cluster for the 84 sub-basin used in paper V. The n<sup>+</sup> values indicate the percentage of sub-basins where the HE performs better than climatology averaged over all relevant sub-basins. n<sup>+</sup> values in brackets show the percentages of the sub-basins for which these scores are statistically significant at the 0.1 level. The skill threshold is 0 for MAESS and  $\Delta$ NSE, while the skill threshold for FY<sup>+</sup> is 50.

|                |     | MAESS |                    | FY <sup>+</sup> |                    | $\Delta$ NSE |                    |
|----------------|-----|-------|--------------------|-----------------|--------------------|--------------|--------------------|
|                |     |       | n <sup>+</sup> (%) |                 | n <sup>+</sup> (%) |              | n <sup>+</sup> (%) |
| S <sup>1</sup> | Jan | -0.09 | 36 (8)             | 50.3            | 48 (4)             | -0.16        | 40 (8)             |
|                | Feb | -0.08 | 32 (8)             | 48.9            | 48 (0)             | -0.17        | 36 (8)             |
|                | Mar | -0.16 | 20 (0)             | 46.1            | 32 (0)             | -0.27        | 16 (0)             |
|                | Apr | -0.09 | 20 (4)             | 50.6            | 56 (0)             | -0.14        | 28 (0)             |
|                | May | -0.02 | 40 (4)             | 40.7            | 16 (0)             | 0.01         | 64 (24)            |
| S <sup>2</sup> | Jan | -0.39 | 37 (5)             | 56.4            | 89 (16)            | -1.03        | 42 (16)            |
|                | Feb | -0.28 | 37 (5)             | 55.2            | 79 (11)            | -0.70        | 53 (21)            |
|                | Mar | -0.28 | 32 (0)             | 54.0            | 63 (11)            | -0.72        | 42 (11)            |
|                | Apr | -0.18 | 37 (0)             | 51.1            | 47 (16)            | -0.43        | 42 (11)            |
|                | May | -0.12 | 21 (11)            | 43.8            | 16 (5)             | -0.26        | 32 (11)            |
| S <sup>3</sup> | Jan | -0.03 | 68 (15)            | 52.6            | 65 (8)             | -0.05        | 65 (28)            |
|                | Feb | -0.02 | 50 (10)            | 52.3            | 50 (10)            | -0.05        | 63 (15)            |
|                | Mar | -0.04 | 43 (8)             | 47.1            | 33 (5)             | -0.08        | 40 (15)            |
|                | Apr | -0.05 | 33 (5)             | 47.4            | 40 (8)             | -0.14        | 30 (3)             |
|                | May | -0.01 | 55 (10)            | 44.1            | 25 (5)             | -0.03        | 48 (15)            |

These modest results are not uncommon in the literature but neither are they the norm. For example, Mackay et al. (2015) found no advantage over climatology using seasonal forecasts from the UK Met Office global seasonal forecast system (version 5) as forcing data to predict groundwater levels in the UK three months into the future. Whereas, Thober et al. (2015) were able to show skill over ESP when using the North American Multi-Model Ensemble (NMME) as forcing data for seasonal soil moisture and drought prediction over Europe. These, and other works, show that the forecast skill can vary considerably based on the target variable being forecasted, the geographical location for which the forecasts are made, and the source of the forcing data. This suggests that it may be possible to improve the performance of the DE modelling chain by using a different forcing dataset. However, this was not investigated further as model skills over the Scandinavian domain are known to be generally low in the current and past generations of GCMs (e.g. Doblas-Reyes, 2010; Doblas-Reyes 2013).

## **Statistical downscaling**

The predictability of forecasting the SFV in selected basins across Norway using CCA to downscale seasonal forecasts of large scale climate variables directly to SFV is investigated in paper I. Initially the models are applied to 30 stations concurrently however this has mixed success (Table 8; not shown in paper I). From the positive NSE values it can be seen that the performance of the multi-model statistical downscaling is better than climatology for 23 of the 30 stations; however only five of these results are significant at the 0.05 level. This suggests that trying to find a set of predictors that can be applied successfully to all stations is not feasible.

However, if the models, using the same predictors, are applied to a subset of 10 stations the results show a marked improvement in their performance (see Table 1 in paper I). The explanation for this is that the selected stations are predominantly situated close to the coast or on the windward side of the Scandinavian mountains i.e. an ad hoc clustering. Here the hydrology is heavily influenced by the westerly winds that transport moisture in from the Atlantic over the Scandinavian Peninsula. The performance results for the individual statistical downscaling models, those that use meridional velocity at 850 hPa and total precipitation from ECHAM5 as predictors, are often higher than those for the combined multi-model; however these results are not all statistically significant while the multi-model results mostly are. This would imply that although these individual models generally match the observed data, the use of these models alone may result in overfitting. The consequence for this being significantly reduced skill when the model is applied to new data.

**Table 8.** Cross-validated Spearman rank correlation ( $R^2$ ) and Nash-Sutcliffe Efficiency (E) scores, bootstrapped  $n=5000$ , for the multi-model statistical downscaling forecasts of the SFV in 30 unregulated sub-basins across Norway. Values statistically significant at the 0.05 level are marked with bold text.

| Sub-basin     | Area               | $R^2$       | NSE         | Sub-basin    | Area               | $R^2$       | NSE         |
|---------------|--------------------|-------------|-------------|--------------|--------------------|-------------|-------------|
|               | (km <sup>2</sup> ) |             |             |              | (km <sup>2</sup> ) |             |             |
| Austena       | 286                | 0.02        | 0.00        | Landbru      | 60                 | <b>0.37</b> | <b>0.29</b> |
| Berget        | 211                | 0.01        | -0.01       | Målset       | 8                  | 0.03        | 0.02        |
| Bulken        | 1100               | 0.23        | 0.21        | Myrkdalsvatn | 157                | 0.21        | 0.19        |
| Eggafors      | 653                | 0.17        | 0.15        | Nautsundvatn | 219                | 0.06        | 0.06        |
| Femundsanden  | 1770               | 0.01        | -0.02       | Nybergsund   | 4410               | 0.01        | -0.01       |
| Fetvatn       | 89                 | <b>0.32</b> | <b>0.27</b> | Oyungen      | 238                | 0.12        | 0.12        |
| Flakvatn      | 1790               | 0.00        | -0.04       | Polmak       | 14200              | 0.00        | -0.05       |
| Fustvatn      | 530                | 0.08        | -0.01       | Rinna        | 88                 | 0.13        | 0.13        |
| Grosettjern   | 7                  | 0.03        | 0.03        | Risefoss     | 738                | <b>0.29</b> | <b>0.25</b> |
| Grunnfoss     | 898                | <b>0.31</b> | <b>0.25</b> | Roeykenes    | 50                 | 0.02        | 0.02        |
| Haugland      | 135                | 0.01        | 0.00        | Sandvenvatn  | 464                | 0.17        | 0.16        |
| Holen         | 229                | <b>0.36</b> | <b>0.29</b> | Sjödalsvatn  | 473                | 0.11        | 0.11        |
| Hovefoss      | 232                | <b>0.27</b> | <b>0.22</b> | Stordalsvatn | 127                | 0.14        | 0.13        |
| Junkerdalselv | 422                | 0.19        | 0.17        | Strandå      | 23                 | 0.00        | -0.04       |
| Krinsvatn     | 205                | 0.06        | 0.06        | Viksvatn     | 505                | 0.23        | 0.22        |

These mixed results show that there is room for improvement. One conspicuous omission in these studies is the lack of initial condition information taken into account by the forecasts. Snow melt is a majority contributor to the SFV but any information regarding how much water is already stored in the snowpack prior to the forecast is not used. This omission becomes more pronounced the later in the season (see paper III) when the snowpack has developed and the initial conditions start to become the dominant source of predictability.

An overview of the SE approach's ability to predict the inflow volume of the spring flood in 84 sub-basins in Sweden are presented in Table 9. However, for these results the SE is applied to sub-basins that have been clustered, GCM predictors are from the ECMWF IFS (see Table 1), and data about the initial conditions are included as a predictor in the form of modelled snow depth. The SE tends to outperform the HE in forecasts initialised early on. The MAESS results show clear skill over the HE, with respect to volume error, in January-February-March and January-February for clusters  $S^2$  and  $S^3$  respectively. However, this is not true for cluster  $S^1$ . The pattern is similar for  $\Delta NSE$ . The  $FY^+$  results suggest that neither the SE nor the HE have the advantage over the other in clusters  $S^1$  and  $S^2$  while the SE does consistently outperform the HE in cluster  $S^3$  albeit modestly. These results are in agreement with the findings in paper III.



It can be seen that the SE performs best in the clusters where snow processes are more dominant i.e.  $S^2$  and  $S^3$ . The reason for this is that the relationship between the GCM predictors and the local hydrological processes are “persevered” through the snowpack. The evolution of the snowpack is relatively slow which means that any predictive teleconnection signal is long-lived and thus more exploitable. The poor performance results can, in part, be explained by the SE’s Achilles heel - training data. The SE is a regression based approach and as such requires a lot of data to properly train the models. The models used in this work are restricted to 34 years of training data, at the most, so it is likely that the full natural variability of the system has not been sampled. The SE has the tendency to produce forecasts that diverge considerably from the observations if the forecasted conditions are outside those encountered in the training period. This risk is not trivial due to the relatively short training datasets.

**Table 9.** Cross-validated median skill scores, bootstrapped  $N = 10\,000$ , for SE with respect to HE, aggregated by forecast initialisation month and cluster for the 84 sub-basin used in paper V. The  $n^+$  values indicate the percentage of sub-basins where the HE performs better than climatology averaged over all relevant sub-basins.  $n^+$  values in brackets show the percentages of the sub-basins for which these scores are statistically significant at the 0.1 level. The skill threshold is 0 for MAESS and  $\Delta NSE$ , while the skill threshold for  $FY^+$  is 50.

|                      |     | MAESS |           | FY <sup>+</sup> |           | $\Delta NSE$ |           |
|----------------------|-----|-------|-----------|-----------------|-----------|--------------|-----------|
|                      |     |       | $n^+$ (%) |                 | $n^+$ (%) |              | $n^+$ (%) |
| <b>S<sup>1</sup></b> | Jan | -0.02 | 40 (0)    | 54.1            | 56 (16)   | 0.00         | 44 (12)   |
|                      | Feb | -0.03 | 44 (0)    | 49.6            | 44 (8)    | -0.02        | 36 (4)    |
|                      | Mar | -0.07 | 32 (0)    | 45.9            | 44 (0)    | -0.06        | 44 (4)    |
|                      | Apr | -0.02 | 36 (4)    | 49.6            | 40 (0)    | -0.02        | 44 (8)    |
|                      | May | -0.22 | 8 (0)     | 52.8            | 72 (8)    | -0.38        | 20 (0)    |
| <b>S<sup>2</sup></b> | Jan | 0.10  | 95 (16)   | 49.3            | 42 (16)   | 0.22         | 100 (26)  |
|                      | Feb | 0.09  | 89 (5)    | 49.6            | 58 (5)    | 0.20         | 100 (11)  |
|                      | Mar | 0.01  | 58 (5)    | 48.3            | 58 (5)    | 0.01         | 58 (0)    |
|                      | Apr | -0.02 | 47 (11)   | 49.0            | 47 (5)    | -0.05        | 53 (0)    |
|                      | May | -0.14 | 16 (5)    | 51.4            | 58 (21)   | -0.29        | 21 (0)    |
| <b>S<sup>3</sup></b> | Jan | 0.08  | 80 (13)   | 54.5            | 70 (20)   | 0.20         | 88 (30)   |
|                      | Feb | 0.04  | 70 (5)    | 50.1            | 48 (8)    | 0.13         | 85 (8)    |
|                      | Mar | -0.06 | 33 (3)    | 52.9            | 65 (5)    | -0.03        | 48 (5)    |
|                      | Apr | -0.09 | 30 (8)    | 52.3            | 60 (8)    | -0.17        | 43 (8)    |
|                      | May | -0.20 | 13 (0)    | 53.8            | 65 (8)    | -0.45        | 13 (3)    |

# The spatio-temporal influence of atmospheric teleconnection patterns on hydrology in Sweden

The results from the individual modelling chains show that, although they have some promising performances, there was still scope for improvement. In line with the recommendations made in paper II, highlighted by the results from paper I and paper III, a systematic investigation of the relationship between large scale atmospheric circulation patterns and hydrological seasonal variability is carried out.

## Clustering of Swedish hydrology

To facilitate an investigation of these relationships a cluster analysis of monthly streamflow data from 64 gauging stations in unregulated systems across Sweden was performed. This is done to identify homogeneous hydrological regions to differentiate between the different hydrological processes involved which greatly simplify the task at hand by reducing the complexity of the analyses.

Standardised monthly data from 64 unregulated gauging stations, filtered for noise by means of a PCA so that 90% of the original variance is retained, is clustered by hierarchical cluster analysis. This resulted in the five unique clusters shown in Figure 16 which are in general agreement to solutions obtained by other studies (e.g. Gottschalk, 1985; Kingston et al., 2011). An average silhouette width of 0.52 and high correlations between the individual cluster members and their cluster mean ( $0.79 \pm 0.025$ ;  $p < 0.01$ ) further support the robustness of the clustering solution obtained.

The clusters can be divided into two general groups based on their annual hydrographs. The northern group ( $S^1$ ,  $S^2$  and  $S^3$ ), where the hydrological regimes are dominated by snow processes, have annual hydrographs that are characterised by a period of low flow during the winter months followed by the spring flood peak that recedes thereafter back down to the winter low flows. The southern group ( $R^1$  and  $R^2$ ), where the hydrological regimes are predominately dominated by rain processes, have annual hydrographs that are characterised by high flows during the winter months and low flows during the summer months. Although  $R^1$  has a distinct snow melt feature in the annual hydrograph, the general form is that of the rain-dominated southern group and is therefore classified as such.

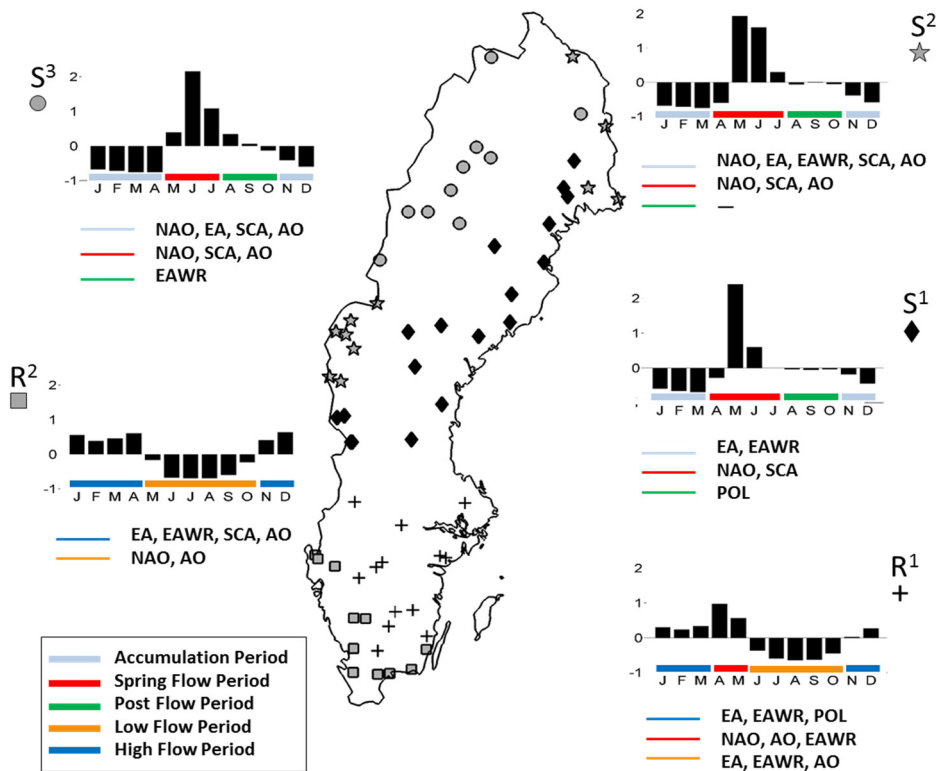


**Figure 16.** Location of the five clusters, composite annual hydrograph (black bars) for each cluster and the climate patterns that exhibit statistically significant correlation ( $p < 0.01$ ) with the seasonal streamflow for the individual seasons.

The annual hydrographs for each cluster are divided up into distinct hydrological periods with similar hydrological activity. This gives the following five different hydrological periods:

- Accumulation Period (AP): the low flow period, during the winter months, during which precipitation is accumulated in the basin in the form of a snowpack.
- Spring Flow Period (SFP): the months following winter where the streamflow is significantly elevated due to the melting snowpack.
- Post Flood Period (PFP): the months between the SFP and the AP where the streamflow is steadily declining from the elevated levels during the SFP.

- High Flow Period (HFP): the period of above average streamflow during the winter months due to relatively high amounts of precipitation, thaw and rain on snow processes, and depressed evapotranspiration rates.
- Low Flow Period (LFP): the period of below average streamflow during the summer months due to the elevated evapotranspiration rates.

## **Climate-streamflow connections**

Monthly teleconnection pattern indices are averaged into periods of differing lead times and persistence intervals, including one that is concurrent to the hydrological period. A PCA is performed on the data matrix comprised of a HP and the associated teleconnection pattern persistence periods (TP period). A biplot of the first two PCA modes is used to identify those TPs and their periods that are most related to the cluster and HP in question. The Spearman rank correlation coefficient between the time series of the selected TPs and that of the streamflow composite are calculated. Only TP periods with correlation coefficients significant at the 0.01 level are retained for further analysis. Figure 17 (also summarised in Figure 16) show which teleconnection patterns are related to each HP in the different clusters, the persistence and lead time of these TP periods and the correlation coefficients of these relationships.

For example, Figure 17 panel S<sup>3</sup> shows that for the S<sup>3</sup> cluster, the streamflow during the SFP is negatively correlated (-0.51) to the mean SCA index during the eight months prior to the SFP and positively correlated to the mean NAO (0.58) and AO (0.57) indices during the seven months prior to the SFP. The physical explanation for this is that it is during this time that the snowpack, a major contributor to the SFV, is being generated. These teleconnection patterns have a known impact on the local weather within the S<sup>3</sup> cluster which, in turn, has an impact on the evolution of the snowpack. It follows, therefore, that the mean of the teleconnection indices would offer information on the weather conditions that were prevalent during that period.

It is notable that only the PFP in all three snow dominated clusters (S<sup>1</sup>, S<sup>2</sup>, and S<sup>3</sup>) do not exhibit a significant correlation between the antecedent climatic conditions and the inflow volumes during the PFP. This is not because the inflow volumes are not contingent on the antecedent conditions but rather that the signal from these conditions are diluted by signals from the concurrent conditions. For example, the PFP in cluster S<sup>1</sup> shows a significant correlation with the concurrent POL teleconnection pattern suggesting that the weather conditions during the PFP have a greater impact on the inflow volumes during this period.

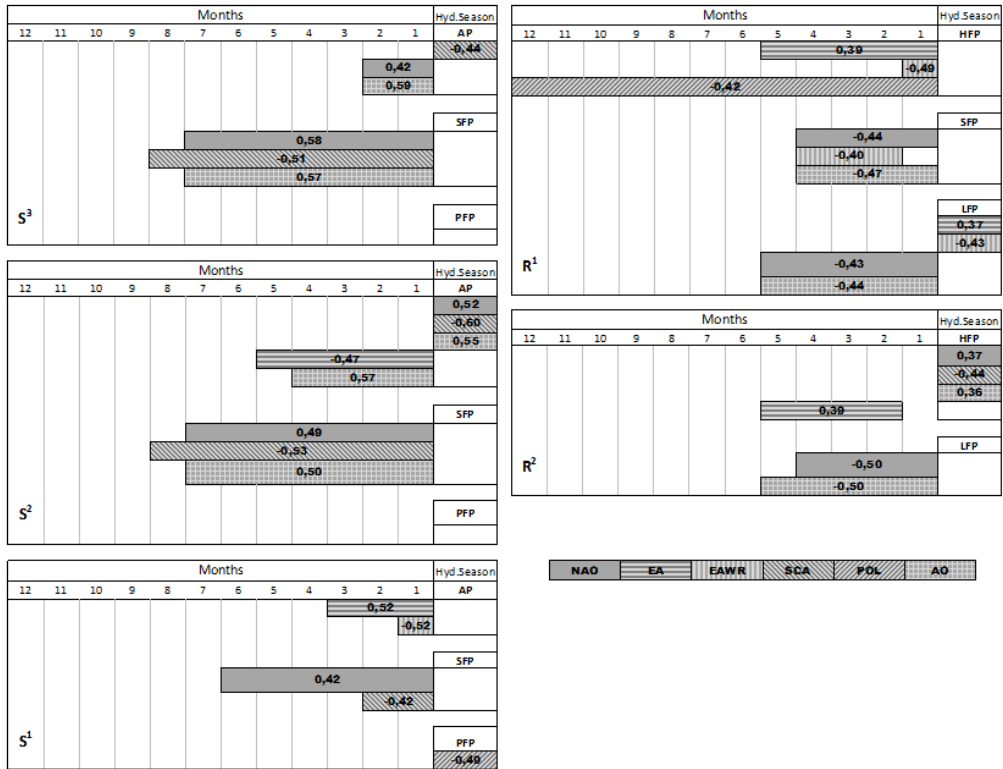


**Figure 17.** The Spearman rank-order correlation coefficients for the TP periods and the hydrological periods at the 0.01 level for  $S^3$ ,  $S^2$ ,  $S^1$ ,  $R^2$  and  $R^1$ . The gap between the hydrological period and the bars indicate the lead time in months (bars within the hydrological period are concurrent with the hydrologic season) and the length of the bars represent the persistence of the TP period in months.

### Time-Frequency Analysis

With the TP periods of interest identified in the previous section, a more complete understanding of the relationship between the teleconnection patterns and the streamflow variability is gained with the help of CWT, XWT, and WTC analyses. These clarify how and when the inter-annual flow variability may be associated to the variability in TPs.

For the sake of brevity, and in keeping in with the rest of this chapter, the results presented in this section concentrate on the SFP in the Northern Group, starting with a detailed presentation of the results from cluster  $S^3$  followed by a general summary for the three clusters making up the Northern Group. The reader is referred to paper **IV** for more results.

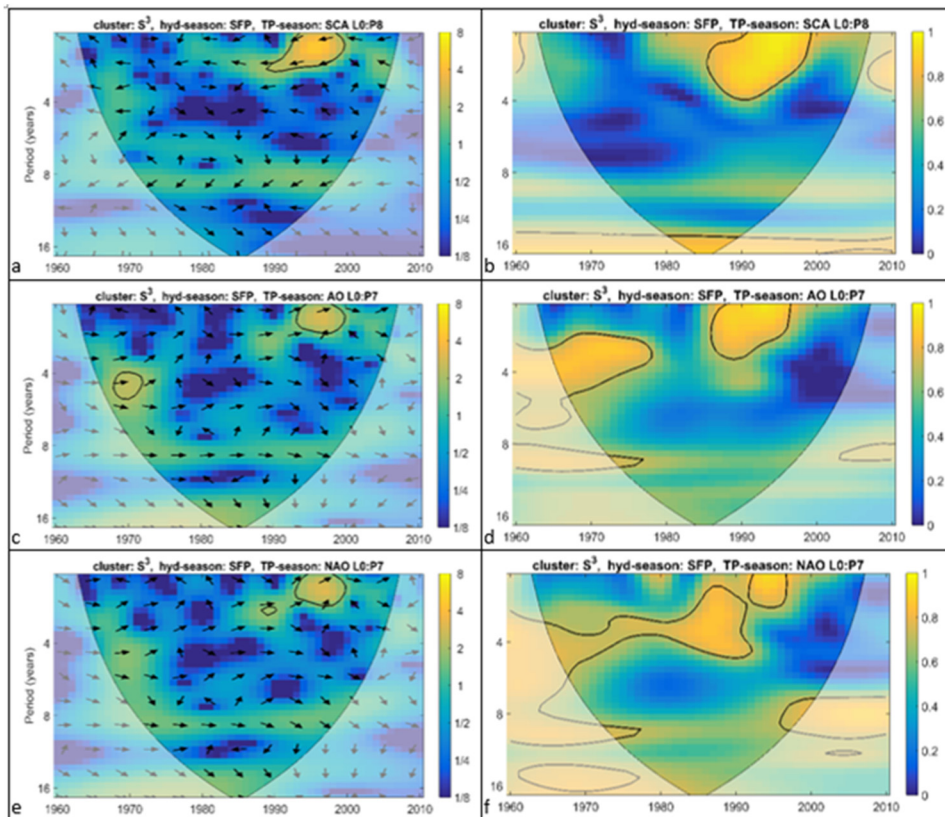


**Figure 18.** Plots of the Cross-Wavelet Transform (left column) and Wavelet Transform Coherence (right column) between the composite flows for cluster  $S^3$  during the spring flow period and the concomitant SCA (top row), AO (L0:P7) (central row) and NAO (L0:P7) (bottom row). Colours indicate power intensity in the left column and correlation in the right column as expressed in the bars to the right of each plot.

The CWT of the SFP in cluster  $S^3$  during the SFP (see Figure 6d in paper IV) shows two dominant active oscillation periods. The first has a period of about 2-year and is most active during the 1990's, the second has a period of 4 to 8-years and is most active between the late 1960's and the mid 1970's.

The XWT and WTC of the SFP and selected TP periods in  $S^3$  (Figure 18) show that both centres of action are connected (in-phase) to the AO L0:P7 (the seven months antecedent to the SFP – see Figure 17; see paper IV for more details) activity, likewise for NAO L0:P7. However, the concomitant SCA is only connected (in anti-phase) to the activity centre with a 2-year period. The phase indicates whether the variabilities in the TP and the HP are positively (in-phase) or negatively (in anti-phase) correlated.

The results of the wavelet analyses between annual flow variability and climate variability show that, in general, different climatic processes affect the river flows in different regions of Sweden at different periods. The variability of the SFP in clusters  $S^3$  and  $S^2$  is connected to AO, NAO and SCA variability up to eight months prior to the SFP. It is interesting to note that it is the preferred oscillation period (2 to 4-years) of NAO, AO and SCA that has the strongest signal i.e. greatest influence on the variability in the SFP in clusters  $S^3$  and  $S^2$ . In the case of cluster  $S^1$ , the variability of the SFP is predominantly connected to NAO and SCA and it is the longer preferred oscillation period (6 to 8 years) that has the strongest signal. This shows that the variability of the SFP is clearly connected to the long-term variability of NAO. The short period variability is mostly connected to SCA up to 2 months before the season. This is probably due to the eastern placement of  $S^1$  that makes the Baltic Sea its main source of moisture.

Streamflows during the SFP are a combination of baseflow, lake out-flows and snowpack ablation. The strongest signal during this period is undeniably the amount of water released when the snowpack ablates during the spring. Positive (negative) AO and NAO indices have a positive (negatively) influence on temperatures and precipitation amounts during the winter. This, in turn raises (lowers) groundwater, lake, and snowpack storages which results in higher (lower) streamflow in the SFP. On the other hand, SCA negatively (positively) influences precipitation by hindering (allowing) mild and moist air masses to be transported over Sweden. This is due to the influences of associated blocking anticyclones over Fennoscandia.

## Multi modelling chain ensembles (ME)

In this section, the results related to the ME approach are presented. Initially, results that do not take advantage of the findings presented in the previous section are presented e.g. the sub-basins are not grouped into clusters and analogues are not selected using the periods for which the TCIs and SFV are most strongly correlated. These are then followed by results for MEs that do take those findings into account. The different ME models are differentiated by a subscript identifying which individual modelling chains are included in that ME e.g.  $ME_{hds}$  refers to a ME comprising the HE, DE, and SE modelling chains.

Table 10 gives performance results for two conceptually straightforward ME approaches: a median approach where the middle member in the ranked forecast ensemble is used as the multi-model deterministic forecast, and a weighted multi-model. The weighting scheme employed is simple set ratios based, for each forecast date, based on the individual model's performances during a historical period. The two MEs are one "optimized"  $ME_{ads}$  (referred to as NEW in paper III) that uses AE,

DE and SE (where the CP approach version of AE is used for the January and March forecasts and TCI version of AE for the May forecasts), and one “operational”  $ME_{hds}$  that substitutes AE for HE (referred to as OPE in paper III; the reader is referred to paper III for more details).

**Table 10.** Relative improvement RI (%) and frequency of years with a better performance  $FY^+$  (%) for the median and weighted multi-model approaches, as compared with the climatological ensemble HE (boldface indicates better performance than HE). The skill threshold is 0 for RI and 50 for  $FY^+$ .

|         |         | Median      |           |             |           | Weighted    |           |             |           |
|---------|---------|-------------|-----------|-------------|-----------|-------------|-----------|-------------|-----------|
|         |         | $ME_{ads}$  |           | $ME_{hds}$  |           | $ME_{ads}$  |           | $ME_{hds}$  |           |
|         |         | RI          | $FY^+$    | RI          | $FY^+$    | RI          | $FY^+$    | RI          | $FY^+$    |
| Jan     | Sorsele | <b>20.9</b> | 50        | <b>25.3</b> | <b>56</b> | <b>20.1</b> | <b>55</b> | <b>18.2</b> | <b>55</b> |
|         | Vindeln | <b>5.8</b>  | 50        | <b>12.5</b> | <b>56</b> | <b>15.7</b> | <b>64</b> | <b>12.9</b> | <b>55</b> |
| Mar     | Sorsele | <b>5.9</b>  | <b>60</b> | -4.2        | <b>56</b> | <b>13.3</b> | <b>64</b> | -7.2        | <b>55</b> |
|         | Vindeln | -0.1        | <b>60</b> | -10.7       | 43        | <b>3.8</b>  | <b>55</b> | -10         | <b>45</b> |
| May     | Sorsele | <b>3.7</b>  | <b>55</b> | <b>7.9</b>  | <b>67</b> | -5          | <b>55</b> | -0.6        | <b>64</b> |
|         | Vindeln | -15.6       | 36        | -5.2        | 33        | 23.3        | 36        | -13.5       | 27        |
| Average |         | <b>3.4</b>  | <b>52</b> | <b>4.3</b>  | <b>52</b> | <b>4.1</b>  | <b>55</b> | 0           | <b>50</b> |

Overall, the ME forecasts show some improvement over HE with the performance for individual forecast months and stations showing similar, at times better, results to the best performing individual methods (see paper III). This is due to the effect of single forecasts that are very wrong being either eliminated or minimised, depending on the multi-model modelling chain. The weighted  $ME_{ads}$  outperforms HE in all months and sub-basins except for forecasts initialised in May for Vindeln and has mixed RI results after the January forecast.  $ME_{ads}$  shows slightly better average performance over its median counterpart.  $ME_{hds}$  shows similar results with the median  $ME_{hds}$  having the best average RI while the weighted  $ME_{hds}$  has the best  $FY^+$ .

Although these results are from a preliminary feasibility study with limited data and overall basic versions of the modelling chains used, they do show that a multi-model approach has improved skill over any individual modelling chain. This suggests that a multi-model is preferable to any single modelling chain when making seasonal forecasts, at least for the spring flood period in Scandinavia.

Changing our focus from specific sub-basins to a more regional perspective. Figure 19 is a three dimensional plot showing the relative skills of the different modelling chains and possible ME combinations with respect to  $FY^+$ ,  $\Delta NSE$ , and MAESS averaged by cluster and over all initialisation dates used in paper V. These results show that, in general, the multi-models with fewer modelling chains tend to perform



worse than those with more, and that an ME that includes the full HE is often preferable to one that includes AE.

It is interesting to note that there appears to be a general neat differentiation between the different groups of models i.e. individual modelling chains, MEs with two modelling chains, and those with three modelling chains. However, in cluster  $S^2$  the DE performs significantly worse than the other individual models, so much so that it could not be plotted in the same frame as the rest in Figure 19, and all MEs that include it suffer accordingly. The only exception being  $ME_{hs}$ . The result is two general groups of models in skill space which suggests that it is not as clear that MEs with three modelling chains are preferred in cluster  $S^2$  as they are for clusters  $S^1$  and  $S^3$ . The results, going forward, are presented per cluster rather than by sub-basin. This is for the sake of brevity and that the sub-basins, within the same cluster, tend to have similar responses.

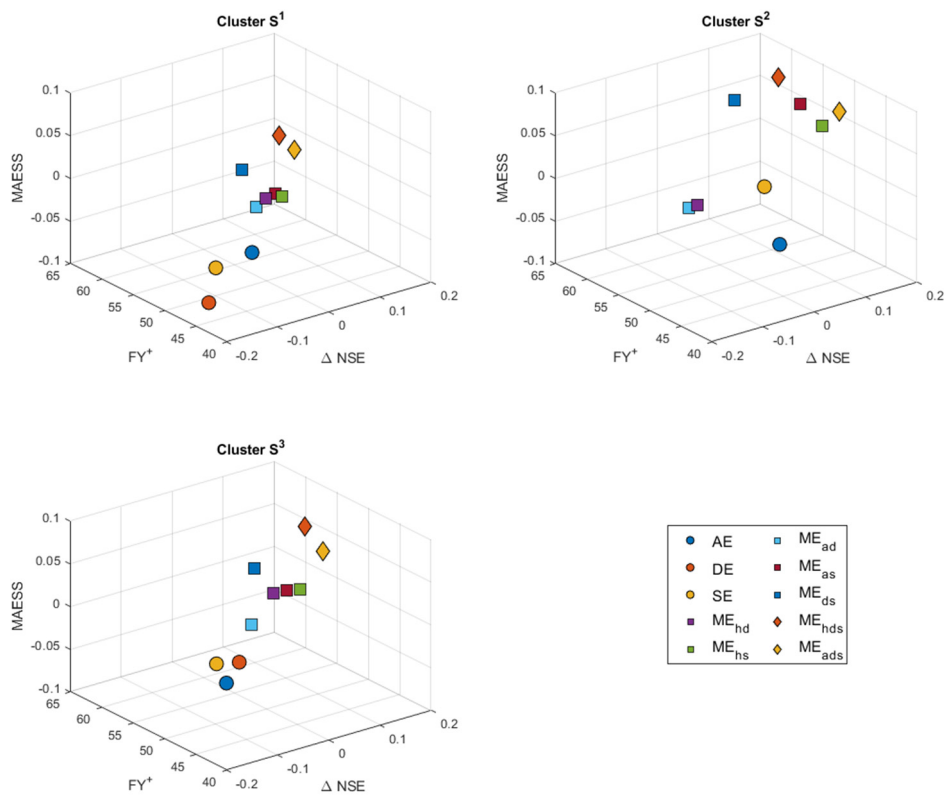


**Figure 19.** A 3D plot of the different skill scores for the different ME variants considered averaged across all forecast initialisation dates. The subscripts denote the modelling chains that comprise the ME; h = HE, a = AE, d = DE, and S = SE. Note that the DE is not shown in the panel for cluster  $S^2$  as it is outside the plot limits.

The naïve general skill (using climatology as a reference) of the two MEs,  $ME_{hds}$  and  $ME_{ads}$ , and HE to predict the SFV for the 84 sub-basins used in paper V are summarised in Table 11. These two MEs are those with three modelling chains and have been shown in Figure 19 to be those which perform best across all clusters. The results are aggregated across all sub-basins and clusters for each initialisation month. The percentage of sub-basins where the hindcasts outperform climatology is also shown ( $n^+$ ); the values in brackets are the percentage of sub-basins for which the results are statistically significant.

The performance measures for each of the three approaches are positively related to the relative timing of the hindcasts i.e. hindcasts initialised in any month are generally more (less) skilful than the hindcasts initialised in the preceding (following) months. This can be expected as the further away in time from the spring flood that the hindcast is initialised, increasing the lead time, the less the initial hydrological conditions contribute to predictability and the more uncertain the forcing data become (e.g. Wood et al., 2016; Arnal et al., 2017).

With respect to general skill and the ability to capture the interannual variation shown by the observations, the two multi-models tend to perform better than HE with  $ME_{hds}$  typically having the best performance. This is especially so when we consider the percentage of the sub-basins where this improved performance is statistically significant. The gap between HE and the two multi-models in MAESS, NSE, and percentage of sub-basins with improved performance over climatology tends to get smaller as the season progresses while the gap in the percentage of sub-basins where improved performance is statistically significant appears to grow, at least early in the season. However, when considering the forecast's ability to discriminate between below normal, near normal, and above normal SFVs then the HE holds an advantage over the two prototypes especially when it comes to identifying near normal events from all forecast initialisation dates and, to a lesser extent, below normal events for the later forecasts. The two multi-models are better at identifying above normal events for all forecasts except those initialised in May where the ability of the HE is comparable. The advantage displayed by the HE to identify near normal events is to be expected due to its climatological nature while the advantage with respect to the below normal events might again be attributed to the cold bias in the historical forcing data. These results suggest that the  $ME_{ads}$  is the preferred variant of ME.

**Table 11.** Cross-validated median skill scores, bootstrapped  $N = 10,000$ , for HE,  $ME_{ads}$ , and  $ME_{rds}$  with respect to climatology, aggregated by forecast initialisation month and cluster for the 84 sub-basin used in paper V. The  $n^+$  values indicate the percentage of sub-basins where the HE performs better than climatology averaged over all 84 sub-basins.  $n^+$  values in brackets show the percentages of the sub-basins for which these scores are statistically significant at the 0.1 level. The skill threshold is 0 for MAESS,  $\Delta NSE$ , and  $\Delta ROCSS$ , while the skill threshold for FY+ is 50.

|                              | MAESS     |       | $\Delta NSE$ |       | $\Delta ROCSS$ |           |          |           |         |           |          |
|------------------------------|-----------|-------|--------------|-------|----------------|-----------|----------|-----------|---------|-----------|----------|
|                              | $n^+$ (%) |       | $n^+$ (%)    |       | LT             |           | MT       |           | UT      |           |          |
|                              |           |       |              |       |                | $n^+$ (%) |          | $n^+$ (%) |         | $n^+$ (%) |          |
| <b>HE</b>                    | Jan       | -0.09 | 25 (1)       | -0.24 | 17 (0)         | 0.23      | 90 (21)  | 0.07      | 70 (0)  | 0.10      | 68 (11)  |
|                              | Feb       | 0.00  | 51 (6)       | -0.07 | 42 (5)         | 0.41      | 99 (52)  | 0.11      | 69 (1)  | 0.26      | 92 (27)  |
|                              | Mar       | 0.09  | 80 (17)      | 0.13  | 77 (23)        | 0.55      | 100 (87) | 0.10      | 73 (5)  | 0.44      | 99 (56)  |
|                              | Apr       | 0.15  | 85 (35)      | 0.22  | 85 (35)        | 0.62      | 100 (92) | 0.17      | 85 (7)  | 0.51      | 100 (75) |
|                              | May       | 0.21  | 90 (49)      | 0.32  | 90 (49)        | 0.68      | 100 (98) | 0.23      | 92 (10) | 0.61      | 100 (92) |
| <b><math>ME_{rds}</math></b> | Jan       | 0.00  | 50 (2)       | 0.00  | 55 (1)         | 0.31      | 99 (30)  | -0.01     | 48 (0)  | 0.20      | 80 (18)  |
|                              | Feb       | 0.06  | 73 (20)      | 0.11  | 76 (21)        | 0.39      | 99 (51)  | 0.08      | 74 (0)  | 0.36      | 96 (42)  |
|                              | Mar       | 0.11  | 86 (25)      | 0.20  | 87 (36)        | 0.47      | 100 (76) | 0.07      | 61 (4)  | 0.47      | 100 (60) |
|                              | Apr       | 0.20  | 95 (61)      | 0.32  | 94 (64)        | 0.60      | 100 (90) | 0.16      | 83 (5)  | 0.52      | 100 (79) |
|                              | May       | 0.22  | 96 (67)      | 0.36  | 98 (68)        | 0.66      | 100 (94) | 0.18      | 82 (8)  | 0.56      | 100 (76) |
| <b><math>ME_{ads}</math></b> | Jan       | 0.02  | 60 (6)       | 0.03  | 63 (5)         | 0.32      | 100 (31) | 0.00      | 51 (0)  | 0.22      | 83 (24)  |
|                              | Feb       | 0.08  | 80 (25)      | 0.14  | 85 (29)        | 0.41      | 99 (57)  | 0.07      | 69 (1)  | 0.38      | 99 (44)  |
|                              | Mar       | 0.14  | 90 (32)      | 0.24  | 92 (45)        | 0.51      | 100 (81) | 0.07      | 61 (5)  | 0.48      | 100 (64) |
|                              | Apr       | 0.19  | 94 (56)      | 0.32  | 93 (62)        | 0.60      | 100 (90) | 0.17      | 88 (5)  | 0.54      | 100 (80) |
|                              | May       | 0.24  | 98 (74)      | 0.39  | 96 (76)        | 0.67      | 100 (94) | 0.18      | 85 (10) | 0.60      | 100 (88) |

**Table 12.** Cross-validated median skill scores, bootstrapped  $N = 10\,000$ , for  $ME_{res}$  with respect to HE, aggregated by forecast initialisation month and cluster for the 84 sub-basin used in paper V. The  $n^+$  values indicate the percentage of sub-basins where the HE performs better than climatology averaged over all 84 sub-basins.  $n^+$  values in brackets show the percentages of the sub-basins for which these scores are statistically significant at the 0.1 level. The skill threshold is 0 for MAESS,  $\Delta NSE$ , and  $\Delta ROCSS$ , while the skill threshold for  $FY+$  is 50.

|                      | MAESS |           | FY*       |           | ANSE      |      | AROCSS    |       |           |       |           |       |         |
|----------------------|-------|-----------|-----------|-----------|-----------|------|-----------|-------|-----------|-------|-----------|-------|---------|
|                      |       | $n^+$ (%) | $n^+$ (%) | $n^+$ (%) | $n^+$ (%) | LT   |           | MT    |           | UT    |           |       |         |
|                      |       |           |           |           |           |      | $n^+$ (%) |       | $n^+$ (%) |       | $n^+$ (%) |       |         |
| <b>S<sup>1</sup></b> | Jan   | 0.04      | 68 (24)   | 55.7      | 76 (12)   | 0.15 | 76 (32)   | 0.02  | 68 (0)    | -0.05 | 40 (0)    | 0.06  | 68 (0)  |
|                      | Feb   | 0.05      | 72 (20)   | 56.0      | 72 (12)   | 0.14 | 92 (32)   | -0.03 | 32 (0)    | 0.02  | 60 (0)    | 0.07  | 84 (0)  |
|                      | Mar   | 0.02      | 80 (12)   | 55.0      | 72 (16)   | 0.08 | 80 (16)   | -0.06 | 16 (0)    | -0.04 | 32 (0)    | 0.01  | 48 (0)  |
|                      | Apr   | 0.04      | 72 (12)   | 57.5      | 84 (16)   | 0.09 | 76 (28)   | -0.01 | 44 (0)    | -0.01 | 56 (0)    | 0.04  | 80 (0)  |
|                      | May   | 0.02      | 64 (12)   | 53.7      | 64 (16)   | 0.06 | 84 (16)   | -0.07 | 28 (0)    | -0.05 | 24 (0)    | -0.01 | 32 (0)  |
| <b>S<sup>2</sup></b> | Jan   | 0.11      | 95 (47)   | 60.2      | 89 (37)   | 0.32 | 100 (53)  | 0.05  | 63 (0)    | -0.06 | 37 (0)    | 0.13  | 84 (16) |
|                      | Feb   | 0.12      | 95 (37)   | 61.4      | 100 (26)  | 0.31 | 100 (58)  | 0.00  | 53 (0)    | -0.04 | 42 (0)    | 0.14  | 89 (16) |
|                      | Mar   | 0.06      | 79 (26)   | 60.2      | 84 (37)   | 0.13 | 79 (26)   | -0.03 | 26 (0)    | -0.01 | 47 (0)    | -0.01 | 47 (0)  |
|                      | Apr   | 0.05      | 74 (21)   | 58.5      | 79 (21)   | 0.12 | 74 (47)   | -0.03 | 11 (0)    | 0.00  | 63 (0)    | 0.02  | 63 (0)  |
|                      | May   | 0.05      | 79 (26)   | 57.0      | 95 (5)    | 0.09 | 79 (42)   | 0.00  | 37 (0)    | -0.05 | 37 (0)    | 0.01  | 53 (0)  |
| <b>S<sup>3</sup></b> | Jan   | 0.12      | 100 (53)  | 61.2      | 98 (28)   | 0.33 | 63 (5)    | 0.14  | 95 (15)   | -0.07 | 23 (0)    | 0.13  | 85 (18) |
|                      | Feb   | 0.08      | 90 (15)   | 57.8      | 85 (23)   | 0.21 | 95 (45)   | 0.01  | 68 (0)    | -0.05 | 33 (0)    | 0.13  | 98 (10) |
|                      | Mar   | 0.05      | 68 (10)   | 54.7      | 75 (10)   | 0.12 | 92 (45)   | -0.04 | 15 (0)    | -0.04 | 35 (0)    | 0.07  | 85 (3)  |
|                      | Apr   | 0.04      | 65 (18)   | 55.1      | 75 (23)   | 0.10 | 93 (62)   | -0.01 | 35 (0)    | 0.01  | 57 (0)    | 0.01  | 57 (0)  |
|                      | May   | 0.04      | 73 (15)   | 56.1      | 73 (15)   | 0.06 | 96 (76)   | -0.01 | 43 (0)    | -0.02 | 35 (0)    | -0.02 | 25 (0)  |

Table 13 shows the skill scores for ME<sub>hds</sub> to predict the SFV for the 84 sub-basins used in paper V with respect to HE. The results are aggregated across all sub-basins per clusters for each initialisation month, similar to the previous table. The performance measures are negatively related to the relative timing of the hindcasts, i.e. hindcasts initialised in any month are generally more (less) skilful than the hindcasts initialised in the following (preceding) months. This too can be expected as the closer in time to the spring flood that the hindcast is initialised, decreasing the lead time, the more the initial hydrological conditions contribute to predictability and the more skilful the HE becomes. This means that the relative error on which any improvement can be made is reduced and thus the skill scores are expected to drop. With respect to MAESS, the median ME<sub>hds</sub> shows skill over HE in all clusters and for all forecast initialisation dates. The percentage of sub-basins where the ME<sub>hds</sub> has skill over the HE is well over 50%. The percentage of these sub-basins for which the skill is statistically significant at the 0.1 level range between 10 and 53%. The HE does not show any significant skill over the ME<sub>hds</sub>. Furthermore, the FY<sup>+</sup> scores show that the ME<sub>hds</sub> outperforms the HE more often than not for the majority of sub-basins in all clusters and for all forecast initialisation dates. The percentage of the sub-basins for which this is statistically significant 5% and 37%. This suggests that there is motivation to prefer the ME<sub>hds</sub> over the HE with respect to forecast volume errors.

Similarly, the NSE results suggest there is motivation to prefer that ME<sub>hds</sub> over the HE with respect to capturing the interannual variability. The ME<sub>hds</sub> outperforms the HE for the vast majority of the sub-basins with the percentage of sub-basins for which this result is statistically significant ranging between 5% and 76%.

The results considering the ME<sub>hds</sub> ability to discriminate between below normal, near normal, and above normal SFVs are very similar to those discussed from Table 11. The HE holds an advantage over ME<sub>hds</sub> when it comes to identifying near normal events and below normal events, while the ME<sub>hds</sub> is better at identifying above normal events for all forecasts except those initialised in May where the ability of the HE is comparable. The explanation for this, too, is the same i.e. the climatological nature of the HE and the cold bias in the historical forcing data accounting for the HEs better performance.

# The operational prototype

The findings of this work raises the prospect for an operational prototype for forecasting the spring flood inflow volumes to hydropower magazines in Sweden. With support from actors in the Swedish hydropower industry, namely the water regulation authority Vattenregleringsföretagen and the research funding group HUVU (hydrologiskt utvecklingsarbete, EnergiForsk), a prototype was developed using the methods discussed in the previous sections.

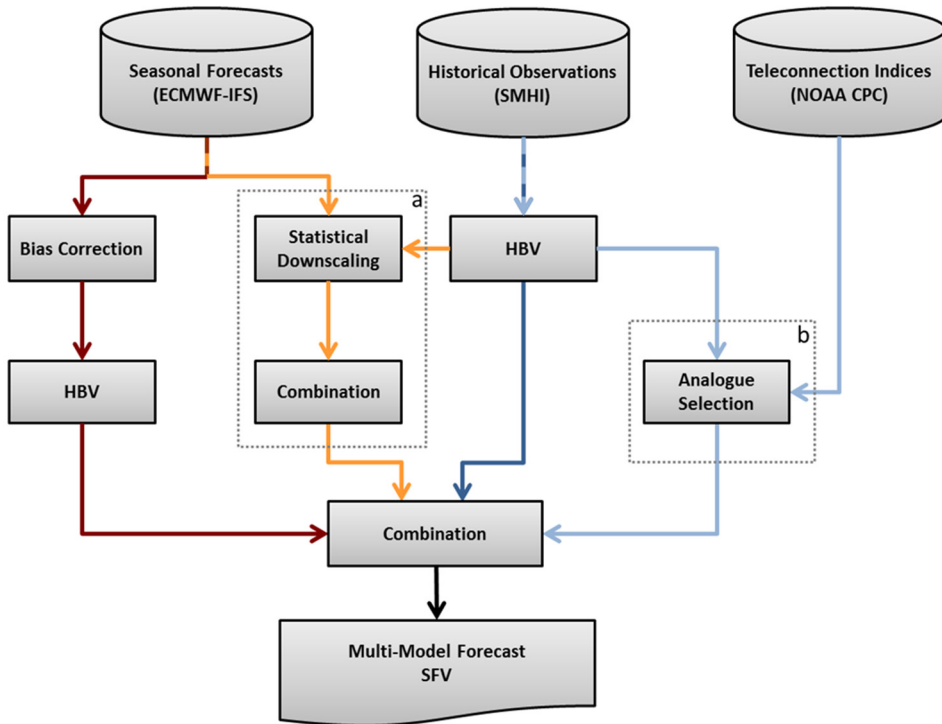


**Figure 20.** Schematic of the multi-model forecast system. The three individual model chains that are included in the multi-model are (from left to right) the DE model chain (red lines), the SE model chain (orange lines), and the HE (dark blue lines) or AE (light blue lines) model chain. The dashed boxes labelled (a) and (b) indicate the parts of the system that have non-trivial changes from the multi-model utilised in paper III.

The prototype is a three modelling chain multi-model which comprises the HE, DE, and SE modelling chains (Figure 20). The development of this ME prototype is based on the results presented above while making allowances for real world technical requirements and limitations. This means that the CP version of AE is excluded from the prototype due to the two month delay in the availability of some required data and that some steps still require manual intervention. The prototype is

a  $ME_{\text{hds}}$  variant of the ME but can be switched to the  $ME_{\text{ads}}$  if desired. The relatively similar performances between the two variants and the belief that the AE can be improved further made it clear that it is prudent to include such a switch to minimise cost changing the preferred variant in the future. This means that there will be limited resources needed and negligible impact on the operational aspects when such a change is made.

## Year-round forecasting: preliminary assessment

In light of the encouraging results already presented, and interest from the hydropower industry in Sweden, a preliminary assessment of whether adapting the seasonal forecasting methods developed in this work to making seasonal forecasts all year round is beneficial. This preliminary assessment concentrates on the AE approach as it offers an opportunity to further improve it. There is little scope for improving the performance of the HE approach, in this assessment, due to its performance being contingent on the model used and quality of the driving data. Additionally, the skill of year round seasonal forecasts using ECMWF driving data together with hydrological models in Sweden is already being investigated in a number of research projects e.g. EUPORIAS (FP7 Grant Agreement 308291) and S2S4E (Horizon 2020 Grant Agreement 776787). Assessing the SE approach is too large a task to be accommodated in the scope of this assessment.

The selection of analogues is performed in much the same way as described previously in this work, in particular the approach described in paper V. In the case of the TCI approach, a simple correlation analysis between seasonal inflow volumes and teleconnection indices identified NAO and SCA as the two teleconnection patterns that typically have the greatest impact on streamflow in the Ume River throughout the year. The former having a positive correlation with inflow volumes and the latter a negative correlation. This finding is in line with the findings reported in section Climate-streamflow connections. Although, a more thorough analysis would be needed before any future work in this direction is pursued. One non-trivial difference between these AE modelling chains and those described in earlier sections is that the AE and HE are pooled together to create an ensemble that retains the spread of the HE but which weights the ensemble to median towards that of the AE. The thinking is that this would harness the benefits of the different approaches while minimising their weaknesses. This new method is referred to as the modified AE approach going forward in this section.

Table 13 and Table 14 show the results of the impacts of modelled seasonal inflow volumes using the TCI version of the modified AE approach aggregated over all 12 sub-basins in the Ume River. The results for the CP version are not presented as

they are very similar to those for the TCI version and doing so would be redundant. The results show that the TCI version of the AE modelled inflow volumes conditioned using teleconnection analysis tend to show skill over the HE now. On average, modelled inflow volumes made using teleconnection index conditioned forcing data outperform the HE 62% of the time. Furthermore, the mean absolute error skill scores (MAESS) suggest that the modified AE shows skill at reducing error in inflow volumes too. The average MAESS is modest but positive for all initialisation months suggesting that the teleconnections have an impact on the inflow volumes for most of the sub-basins throughout the year.

**Table 13.** Cross-validated median MAESS, bootstrapped N = 10 000, for the modified TCI version of the AE forecasts with respect to HE averaged over all sub-basins in the Ume River. The threshold for skill is 0. (Blue shading) indicate the relative skill the AE exhibits over the HE i.e. darker = more skill and lighter = less skill. (Red shading) indicate the relative lack of skill the AE exhibits over the HE i.e. darker = less skill and lighter = more skill.

|     | Lead time (months) |        |        |        |        |        |        |        |        |
|-----|--------------------|--------|--------|--------|--------|--------|--------|--------|--------|
|     | 1                  | 2      | 3      | 4      | 5      | 6      | 7      | 8      | 9      |
| Jan | -0.013             | -0.022 | 0.002  | -0.033 | 0.002  | -0.033 | 0.005  | 0.004  | -0.003 |
| Feb | 0.004              | 0.003  | 0.002  | 0.006  | 0.007  | 0.002  | 0.007  | 0.007  | 0.006  |
| Mar | -0.041             | 0.045  | 0.002  | -0.013 | -0.009 | -0.014 | 0.010  | -0.006 | -0.008 |
| Apr | 0.025              | -0.008 | -0.001 | 0.014  | 0.000  | 0.011  | -0.010 | 0.004  | 0.011  |
| May | 0.060              | 0.025  | 0.036  | 0.021  | 0.044  | 0.054  | 0.005  | 0.009  | 0.025  |
| Jun | 0.048              | 0.025  | 0.018  | 0.025  | 0.022  | 0.029  | 0.022  | 0.031  | 0.023  |
| Jul | 0.015              | 0.007  | -0.002 | 0.003  | 0.002  | 0.029  | 0.004  | 0.026  | 0.011  |
| Aug | 0.016              | 0.007  | 0.009  | 0.010  | 0.008  | 0.009  | 0.013  | 0.011  | 0.010  |
| Sep | 0.009              | 0.008  | 0.003  | 0.013  | -0.007 | 0.001  | 0.012  | 0.015  | 0.011  |
| Oct | 0.003              | 0.004  | 0.006  | 0.003  | 0.002  | 0.004  | 0.005  | 0.000  | 0.005  |
| Nov | 0.009              | 0.008  | 0.014  | 0.018  | 0.017  | 0.016  | 0.011  | 0.012  | 0.012  |
| Dec | 0.008              | 0.009  | 0.008  | 0.010  | 0.007  | 0.002  | 0.005  | 0.009  | 0.008  |

**Table 14.** Cross-validated median FY\*, bootstrapped N = 10 000, for the modified TCI version of the AE forecasts with respect to HE averaged over all sub-basins in the Ume River. The threshold for skill is 50. (Blue shading) indicate the relative skill the AE exhibits over the HE i.e. darker = more skill and lighter = less skill. (Red shading) indicate the relative lack of skill the AE exhibits over the HE i.e. darker = less skill and lighter = more skill.

|     | Lead time (months) |      |      |      |      |      |      |      |      |
|-----|--------------------|------|------|------|------|------|------|------|------|
|     | 1                  | 2    | 3    | 4    | 5    | 6    | 7    | 8    | 9    |
| Jan | 44.4               | 50.0 | 50.0 | 44.4 | 50.0 | 50.0 | 50.0 | 50.0 | 50.0 |
| Feb | 55.6               | 50.0 | 50.0 | 55.6 | 55.6 | 50.0 | 55.6 | 55.6 | 55.6 |
| Mar | 44.4               | 55.6 | 50.0 | 50.0 | 50.0 | 50.0 | 55.6 | 50.0 | 55.6 |
| Apr | 50.0               | 50.0 | 50.0 | 55.6 | 50.0 | 50.0 | 50.0 | 50.0 | 50.0 |
| May | 55.6               | 55.6 | 55.6 | 55.6 | 55.6 | 61.1 | 55.6 | 55.6 | 55.6 |
| Jun | 61.1               | 55.6 | 55.6 | 55.6 | 55.6 | 55.6 | 55.6 | 55.6 | 55.6 |
| Jul | 50.0               | 55.6 | 50.0 | 50.0 | 50.0 | 55.6 | 50.0 | 55.6 | 50.0 |
| Aug | 55.6               | 55.6 | 55.6 | 55.6 | 55.6 | 55.6 | 55.6 | 61.1 | 55.6 |
| Sep | 61.1               | 55.6 | 55.6 | 55.6 | 50.0 | 55.6 | 61.1 | 61.1 | 61.1 |
| Oct | 61.1               | 61.1 | 72.2 | 66.7 | 61.1 | 61.1 | 61.1 | 55.6 | 66.7 |
| Nov | 66.7               | 66.7 | 72.2 | 77.8 | 83.3 | 77.8 | 77.8 | 77.8 | 77.8 |
| Dec | 66.7               | 66.7 | 66.7 | 72.2 | 72.2 | 61.1 | 66.7 | 72.2 | 66.7 |



The modified AE tends to outperform the HE least often for simulations initialised early in the year and most often in the later months of the year (see Table 14). This result is a surprise and the reason for it is not obvious, however one can speculate that the seasonal inflow volumes in the later part of the calendar year are more affected by variances in the antecedent climatic state than inflow volumes towards the beginning of the calendar year. This is especially true for the spring flood period, and to a lesser extent the following months, where the inflow volumes are almost entirely contingent on the snowpack i.e. initial conditions. The largest improvements in the volume error appear to be achieved for forecasts initialised around the middle of the year. This implies that the teleconnection impact of NAO and SCA on inflow volumes is greatest then. This is to be expected as previous results in this work connects these two TPs in the antecedent months and the spring flood period.

These results show that a modified AE approach has the potential to make skilful forecasts at other times of the year and suggests that some version of the multi-modelling approaches from this work would have added value outside of the scope of this study.

# Conclusions and Outlook

- *To investigate whether the seasonal forecasts can be improved by modifying the current approach or substituting it for another.* The skill of the hydrological seasonal forecasts of the SFV can be improved for specific sub-basins, initialisation date, and or modelling chain. However, of the three general individual modelling chains investigated in this work, none is able to show any general skill over the HE.
- *To investigate whether Sweden can be divided into sub regions to which the seasonal forecasts can be optimised.* Sweden's hydrology can be divided up into five regions of homogeneous hydrological variability. A northern group, consisting of three regions where the hydrology is dominated by snow processes, and a southern group, consisting of two regions where the hydrology is dominated by rain processes.
- *To investigate, identify, and understand the climatic drivers responsible for local hydrological variability.* It is shown that large scale climate patterns such as NAO, AO, SCA, EA, EAWR and POL are the drivers of the seasonal hydrological variability in the five different regions identified by the cluster analysis. The persistence of these large scale climate patterns either leading up to or concurrent with different hydrological periods have been connected with the variability in said hydrological period and the physical chain of causality identified. Additionally, using this information can successfully be used to improve the performance of seasonal forecasts.
- *To investigate whether there are any benefits of a multi-model approach to forecasting SFV in Sweden.* This work shows that a multi-model tends to perform better than an individual modelling chain. Furthermore, it shows that a multi-model comprising of all three of the alternative modelling chain types considered in this work i.e. AE/HE, DE, and SE, can improve the general skill of seasonal forecasts of the SFV. In addition to being able to improve general skill with respect to volume error and capturing interannual variability, a multi-model can also improve the forecast's ability to detect events that are above normal and, for forecasts initialised early in the season, those that are below normal.

- *To develop and evaluate a hydrological seasonal forecast prototype for operational forecasting of the SFV in Sweden.* A prototype forecast system has been developed to forecast the SFV in Sweden's seven largest hydropower producing river systems. Stakeholders in the hydropower industry have shown keen interest in the prototype.

Looking forward, using the results of this thesis as a datum, there are a couple of avenues of inquiry that should be pursued. The first is to try to improve the analogue modelling chain. In this work the analogues were selected on past knowledge of the climate state only. In paper **IV** it was shown that knowledge of the climate state leading all the way to the forecast date is required to maximise the explained variance. By using seasonal forecast data from NWP's such as ECMWF-IFS it should be possible to calculate climate indices for the period for which climate indices are lacking. These new forecasted climate indices can be used together with historical indices to calculate the persistence of the required climate pattern over the optimal periods identified in paper **IV**.

Secondly, in this thesis only one hydrological model was used, HBV. Future studies should investigate whether there is a benefit of adding other hydrological models. There are numerous other models that have differing modelling approaches that could improve these types of seasonal forecasts in general and the prototype in particular.

# References

- Álvarez-García, F.J., OrtizBevia, M.J., Cabos, W., Tasambay-Salazar, M. and RuizdeElvira, A., 2019. Linear and nonlinear links of winter European precipitation to Northern Hemisphere circulation patterns. *Climate Dynamics*, 52(11), pp.6533-6555.
- Ambaum, M.H., Hoskins, B.J. and Stephenson, D.B., 2001. Arctic oscillation or North Atlantic oscillation?. *Journal of Climate*, 14(16), pp.3495-3507.
- Angelin, S., 1981. Hydro power in Sweden. Vällingby: Swedish state power board [Statens vattenfallsverk].
- Arheimer, B., Lindström, G. and Olsson, J., 2011. A systematic review of sensitivities in the Swedish flood-forecasting system. *Atmospheric Research*, 100(2-3), pp.275-284.
- Arnal, L., Wood, A.W., Stephens, E., Cloke, H.L. and Pappenberger, F., 2017. An efficient approach for estimating streamflow forecast skill elasticity. *Journal of Hydrometeorology*, 18(6), pp.1715-1729.
- Barnett, T.P. and Preisendorfer, R., 1987. Origins and levels of monthly and seasonal forecast skill for United States surface air temperatures determined by canonical correlation analysis. *Monthly Weather Review*, 115(9), pp.1825-1850.
- Barnston, A.G. and Livezey, R.E., 1987. Classification, seasonality and persistence of low-frequency atmospheric circulation patterns. *Monthly weather review*, 115(6), pp.1083-1126.
- Barry, R.G., Barry, R.G., Perry, A.H. and Perry, A.H., 1973. *Synoptic climatology; methods and applications*. Routledge Kegan & Paul.
- Bastola, S., Misra, V. and Li, H., 2013. Seasonal hydrological forecasts for watersheds over the southeastern United States for the boreal summer and fall seasons. *Earth Interactions*, 17(25), pp.1-22.
- Beckers, J.V., Weerts, A.H., Tjiedeman, E. and Welles, E., 2016. ENSO-conditioned weather resampling method for seasonal ensemble streamflow prediction. *Hydrology and Earth System Sciences*, 20(8), pp.3277-3287.
- Bennett, J.C., Wang, Q.J., Li, M., Robertson, D.E. and Schepen, A., 2016. Reliable long-range ensemble streamflow forecasts: Combining calibrated climate forecasts with a conceptual runoff model and a staged error model. *Water Resources Research*, 52(10), pp.8238-8259.
- Berg, P., Bosshard, T. and Yang, W., 2015. Model consistent pseudo-observations of precipitation and their use for bias correcting regional climate models. *Climate*, 3(1), pp.118-132.

- Bergström, S., 1976. Development and application of a conceptual runoff model for Scandinavian catchments (No. 52). Department of Water Resources Engineering, Lund Institute of Technology, University of Lund.
- Bladé, I., Liebmann, B., Fortuny, D. and van Oldenborgh, G.J., 2012. Observed and simulated impacts of the summer NAO in Europe: implications for projected drying in the Mediterranean region. *Climate dynamics*, 39(3-4), pp.709-727.
- Bueh, C. and Nakamura, H., 2007. Scandinavian pattern and its climatic impact. *Quarterly Journal of the Royal Meteorological Society: A journal of the atmospheric sciences, applied meteorology and physical oceanography*, 133(629), pp.2117-2131.
- Candogan Yossef, N., Beek, R.V., Weerts, A., Winsemius, H. and Bierkens, M.F., 2017. Skill of a global forecasting system in seasonal ensemble streamflow prediction. *Hydrology and Earth System Sciences*, 21(8), pp.4103-4114.
- Cane, M.A., Zebiak, S.E. and Dolan, S.C., 1986. Experimental forecasts of EL Nino. *Nature*, 321(6073), p.827.
- Charney, J.G. and Shukla, J., 1981. Predictability of monsoons. *Monsoon Dynamics*, J. Lighthill and RP Pearce, Eds.
- Cheng, X. and Dunkerton, T.J., 1995. Orthogonal rotation of spatial patterns derived from singular value decomposition analysis. *Journal of Climate*, 8(11), pp.2631-2643.
- Choubin, B., Moradi, E., Golshan, M., Adamowski, J., Sajedi-Hosseini, F. and Mosavi, A., 2019. An Ensemble prediction of flood susceptibility using multivariate discriminant analysis, classification and regression trees, and support vector machines. *Science of the Total Environment*, 651, pp.2087-2096.
- Climate Prediction Center, 2005a. North Atlantic Oscillation (NAO). Available online from: [https://www.cpc.ncep.noaa.gov/data/teledoc/nao\\_map.shtml](https://www.cpc.ncep.noaa.gov/data/teledoc/nao_map.shtml). Last Accessed 12 August 2019.
- Climate Prediction Center, 2005b. East Atlantic (EA). Available online from: [https://www.cpc.ncep.noaa.gov/data/teledoc/ea\\_map.shtml](https://www.cpc.ncep.noaa.gov/data/teledoc/ea_map.shtml). Last Accessed 12 August 2019.
- Climate Prediction Center, 2005c. East Atlantic/Western Russia. Available online from: [https://www.cpc.ncep.noaa.gov/data/teledoc/eawruss\\_map.shtml](https://www.cpc.ncep.noaa.gov/data/teledoc/eawruss_map.shtml). Last Accessed 12 August 2019.
- Climate Prediction Center, 2005d. Scandinavia (Scand). Available online from: [https://www.cpc.ncep.noaa.gov/data/teledoc/scand\\_map.shtml](https://www.cpc.ncep.noaa.gov/data/teledoc/scand_map.shtml). Last Accessed 12 August 2019.
- Climate Prediction Center, 2005e. Polar/Eurasia. Available online from: [https://www.cpc.ncep.noaa.gov/data/teledoc/poleur\\_map.shtml](https://www.cpc.ncep.noaa.gov/data/teledoc/poleur_map.shtml). Last Accessed 12 August 2019.
- Climate Prediction Center, 2012a. The East Atlantic/ West Russia. Available online from: <http://www.cpc.ncep.noaa.gov/data/teledoc/eawruss.shtml>. Last Accessed 12 August 2019.
- Climate Prediction Center, 2012b. Polar/Eurasia. Available online from: <https://www.cpc.ncep.noaa.gov/data/teledoc/poleur.shtml>. Last Accessed 12 August 2019.

- Colman, A. and Davey, M., 1999. Prediction of summer temperature, rainfall and pressure in Europe from preceding winter North Atlantic Ocean temperature. *International Journal of Climatology: A Journal of the Royal Meteorological Society*, 19(5), pp.513-536.
- Comas-Bru, L. and McDermott, F., 2014. Impacts of the EA and SCA patterns on the European twentieth century NAO–winter climate relationship. *Quarterly Journal of the Royal Meteorological Society*, 140(679), pp.354-363.
- Córdoba-Machado, S., Palomino-Lemus, R., Gámiz-Fortis, S.R., Castro-Díez, Y. and Esteban-Parra, M.J., 2016. Seasonal streamflow prediction in Colombia using atmospheric and oceanic patterns. *Journal of Hydrology*, 538, pp.1-12.
- Crochemore, L., Ramos, M.H. and Pappenberger, F., 2016. Bias correcting precipitation forecasts to improve the skill of seasonal streamflow forecasts. *Hydrology and Earth System Sciences*, 20(9), pp.3601-3618.
- D'Aleo, J.S. and Easterbrook, D.J., 2016. Relationship of multidecadal global temperatures to multidecadal oceanic oscillations. In *Evidence-Based Climate Science* (pp. 191-214). Elsevier.
- Day, G.N., 1985. Extended streamflow forecasting using NWSRFS. *Journal of Water Resources Planning and Management*, 111(2), pp.157-170.
- DelSole, T. and Banerjee, A., 2017. Statistical seasonal prediction based on regularized regression. *Journal of Climate*, 30(4), pp.1345-1361.
- Deo, R.C., Kisi, O. and Singh, V.P., 2017. Drought forecasting in eastern Australia using multivariate adaptive regression spline, least square support vector machine and M5Tree model. *Atmospheric Research*, 184, pp.149-175.
- Déqué, M., Dreveton, C., Braun, A. and Cariolle, D., 1994. The ARPEGE/IFS atmosphere model: a contribution to the French community climate modelling. *Climate Dynamics*, 10(4-5), pp.249-266.
- Deser, C., 2000. On the teleconnectivity of the “Arctic Oscillation”. *Geophysical Research Letters*, 27(6), pp.779-782.
- Dias, D.F., Cayan, D.R. and Gershunov, A., 2018. Statistical prediction of minimum and maximum air temperature in California and Western North America. California’s Fourth Climate Change Assessment – Technical Reports. Available online from: [http://climateassessment.ca.gov/techreports/docs/20180827-Projections\\_CCCA4-CEC-2018-011.pdf](http://climateassessment.ca.gov/techreports/docs/20180827-Projections_CCCA4-CEC-2018-011.pdf). Last accessed 12 August 2019.
- Doblas-Reyes, F.J., 2010, September. Seasonal prediction over Europe. In *Proceedings of the ECMWF Seminar on Predictability in the European and Atlantic regions* (Vol. 6).
- Doblas-Reyes, F.J., García-Serrano, J., Lienert, F., Biescas, A.P. and Rodrigues, L.R., 2013. Seasonal climate predictability and forecasting: status and prospects. *Wiley Interdisciplinary Reviews: Climate Change*, 4(4), pp.245-268.
- Duan, Q., Ajami, N.K., Gao, X. and Sorooshian, S., 2007. Multi-model ensemble hydrologic prediction using Bayesian model averaging. *Advances in Water Resources*, 30(5), pp.1371-1386.
- Efron, B., 1992. Bootstrap methods: another look at the jackknife. In *Breakthroughs in statistics* (pp. 569-593). Springer, New York, NY.

- Forgy, E.W., 1965. Cluster analysis of multivariate data: efficiency versus interpretability of classifications. *biometrics*, 21, pp.768-769.
- Fuentes-Franco, R., Giorgi, F., Pavia, E.G., Graef, F. and Coppola, E., 2018. Seasonal precipitation forecast over Mexico based on a hybrid statistical–dynamical approach. *International Journal of Climatology*, 38(11), pp.4051-4065.
- Garen, D.C., 1992. Improved techniques in regression-based streamflow volume forecasting. *Journal of Water Resources Planning and Management*, 118(6), pp.654-670.
- Gerlitz, L., Vorogushyn, S., Apel, H., Gafurov, A., Unger-Shayesteh, K. and Merz, B., 2016. A statistically based seasonal precipitation forecast model with automatic predictor selection and its application to central and south Asia. *Hydrology and Earth System Sciences*, 20(11), pp.4605-4623.
- Greve, N., 2016. Skvaltkvarnarna i Ulvatorpsbäcken Byggnadsminnesutredning. Länsstyrelsens meddelande: 2016:09, Halmstad, Sweden.
- Grinsted, A., Moore, J.C. and Jevrejeva, S., 2004. Application of the cross wavelet transform and wavelet coherence to geophysical time series. *Nonlinear processes in geophysics*, 11(5/6), pp.561-566.
- Goddard, L., Mason, S.J., Zebiak, S.E., Ropelewski, C.F., Basher, R. and Cane, M.A., 2001. Current approaches to seasonal to interannual climate predictions. *International Journal of Climatology: A Journal of the Royal Meteorological Society*, 21(9), pp.1111-1152.
- Hamlet, A.F., Huppert, D. and Lettenmaier, D.P., 2002. Economic value of long-lead streamflow forecasts for Columbia River hydropower. *Journal of Water Resources Planning and Management*, 128(2), pp.91-101.
- Hay, L.E., McCabe Jr, G.J., Wolock, D.M. and Ayers, M.A., 1991. Simulation of precipitation by weather type analysis. *Water Resources Research*, 27(4), pp.493-501.
- Henriksen, A., Skjelvåle, B.L., Mannio, J., Wilander, A., Harriman, R., Curtis, C., Jensen, J.P., Fjeld, E. and Moiseenko, T., 1998. Northern European lake survey, 1995: Finland, Norway, Sweden, Denmark, Russian Kola, Russian Karelia, Scotland and Wales. *Ambio*, pp.80-91.
- Hotelling, H., 1933. Analysis of a complex of statistical variables into principal components. *Journal of educational psychology*, 24(6), p.417.
- Hotelling, H., 1936. Simplified calculation of principal components. *Psychometrika*, 1(1), pp.27-35.
- Hurrell, J.W., 1995. Decadal trends in the North Atlantic Oscillation: regional temperatures and precipitation. *Science*, 269(5224), pp.676-679.
- Hurrell, J.W., Kushnir, Y., Ottersen, G. and Visbeck, M., 2003. An overview of the North Atlantic oscillation. *Geophysical Monograph-American Geophysical Union*, 134, pp.1-36.
- Inwards, R. ed., 1898. *Weather lore: a collection of proverbs, sayings, and rules concerning the weather*. Elliot Stock.

- Ionita, M., 2014. The impact of the East Atlantic/Western Russia pattern on the hydroclimatology of Europe from mid-winter to late spring. *Climate*, 2(4), pp.296-309.
- Ionita, M., Lohmann, G. and Rimbu, N., 2008. Prediction of spring Elbe discharge based on stable teleconnections with winter global temperature and precipitation. *Journal of Climate*, 21(23), pp.6215-6226.
- Ionita, M., Boroneanț, C. and Chelcea, S., 2015. Seasonal modes of dryness and wetness variability over Europe and their connections with large scale atmospheric circulation and global sea surface temperature. *Climate dynamics*, 45(9-10), pp.2803-2829.
- Ionita, M., Tallaksen, L., Kingston, D., Stagge, J., Laaha, G., Van Lanen, H., Scholz, P., Chelcea, S. and Haslinger, K., 2017. The European 2015 drought from a climatological perspective. *Hydrology and Earth System Sciences*, 21, pp.1397-1419.
- Johansson, B., 2002. Estimation of areal precipitation for hydrological modelling (Doctoral dissertation, PhD thesis, Earth Sciences Centre, Report).
- Johansson, Å., Barnston, A., Saha, S. and van den Dool, H., 1998. On the level and origin of seasonal forecast skill in northern Europe. *Journal of the Atmospheric Sciences*, 55(1), pp.103-127.
- Johnson, S.C., 1967. Hierarchical clustering schemes. *Psychometrika*, 32(3), pp.241-254.
- Johnson, S.J., Stockdale, T.N., Ferranti, L., Balmaseda, M.A., Molteni, F., Magnusson, L., Tietsche, S., Decremer, D., Weisheimer, A., Balsamo, G. and Keeley, S.P., 2019. SEAS5: the new ECMWF seasonal forecast system. *Geoscientific Model Development*, 12(3), pp.1087-1117.
- Kim, J., Miller, N.L., Farrara, J.D. and Hong, S.Y., 2000. A seasonal precipitation and stream flow hindcast and prediction study in the western United States during the 1997/98 winter season using a dynamic downscaling system. *Journal of Hydrometeorology*, 1(4), pp.311-329.
- Kingston, D.G., Lawler, D.M. and McGregor, G.R., 2006a. Linkages between atmospheric circulation, climate and streamflow in the northern North Atlantic: research prospects. *Progress in Physical Geography*, 30(2), pp.143-174.
- Kingston, D.G., McGregor, G.R., Hannah, D.M. and Lawler, D.M., 2006b. River flow teleconnections across the northern North Atlantic region. *Geophysical Research Letters*, 33(14).
- Kingston, D.G., Hannah, D.M., Lawler, D.M. and McGregor, G.R., 2009. Climate–river flow relationships across montane and lowland environments in northern Europe. *Hydrological Processes: An International Journal*, 23(7), pp.985-996.
- Kleiven, A. and Steinsland, I., 2018, September. Inflow Forecasting for Hydropower Operations: Bayesian Model Averaging for Postprocessing Hydrological Ensembles. In *The International Workshop on Hydro Scheduling in Competitive Markets* (pp. 33-40). Springer, Cham.
- Koster, R.D., Mahanama, S.P.P., Yamada, T.J., Balsamo, G., Berg, A.A., Boisserie, M., Dirmeyer, P.A., Doblas-Reyes, F.J., Drewitt, G., Gordon, C.T. and Guo, Z., 2010. Contribution of land surface initialization to subseasonal forecast skill: First results from a multi-model experiment. *Geophysical Research Letters*, 37(2).



- Kohavi, R., 1995, August. A study of cross-validation and bootstrap for accuracy estimation and model selection. In *Ijcai* (Vol. 14, No. 2, pp. 1137-1145).
- Krumbein, W.C. and Graybill, F.A., 1965. An introduction to statistical models in geology. McGraw-Hill.
- Kyselý, J. and Huth, R., 2006. Changes in atmospheric circulation over Europe detected by objective and subjective methods. *Theoretical and Applied Climatology*, 85(1-2), pp.19-36.
- Landman, W.A. and Mason, S.J., 1999a. Operational long-lead prediction of South African rainfall using canonical correlation analysis. *International Journal of Climatology: A Journal of the Royal Meteorological Society*, 19(10), pp.1073-1090.
- Landman, W.A. and Mason, S.J., 1999b. Change in the association between Indian Ocean sea-surface temperatures and summer rainfall over South Africa and Namibia. *International Journal of Climatology: A Journal of the Royal Meteorological Society*, 19(13), pp.1477-1492.
- Li, H., Luo, L. and Wood, E.F., 2008. Seasonal hydrologic predictions of low-flow conditions over eastern USA during the 2007 drought. *Atmospheric Science Letters*, 9(2), pp.61-66.
- Lim, Y.K., 2015. The East Atlantic/West Russia (EA/WR) teleconnection in the North Atlantic: climate impact and relation to Rossby wave propagation. *Climate dynamics*, 44(11-12), pp.3211-3222.
- Lindström, G., Johansson, B., Persson, M., Gardelin, M. and Bergström, S., 1997. Development and test of the distributed HBV-96 hydrological model. *Journal of hydrology*, 201(1-4), pp.272-288.
- Lorenz, E.N., 1969. The predictability of a flow which possesses many scales of motion. *Tellus*, 21(3), pp.289-307.
- Lucatero, D., Madsen, H., Refsgaard, J.C., Kidmose, J. and Jensen, K.H., 2018. Seasonal streamflow forecasts in the Ahlergaard catchment, Denmark: the effect of preprocessing and post-processing on skill and statistical consistency. *Hydrology and Earth System Sciences*, 22(7), pp.3601-3617.
- Luo, L., Wood, E.F. and Pan, M., 2007. Bayesian merging of multiple climate model forecasts for seasonal hydrological predictions. *Journal of Geophysical Research: Atmospheres*, 112(D10).
- Ma, F., Ye, A., Deng, X., Zhou, Z., Liu, X., Duan, Q., Xu, J., Miao, C., Di, Z. and Gong, W., 2016. Evaluating the skill of NMME seasonal precipitation ensemble predictions for 17 hydroclimatic regions in continental China. *International Journal of Climatology*, 36(1), pp.132-144.
- Mackay, J.D., Jackson, C.R., Brookshaw, A., Scaife, A.A., Cook, J. and Ward, R.S., 2015. Seasonal forecasting of groundwater levels in principal aquifers of the United Kingdom. *Journal of Hydrology*, 530, pp.815-828.
- MacQueen, J., 1967, June. Some methods for classification and analysis of multivariate observations. In *Proceedings of the fifth Berkeley symposium on mathematical statistics and probability* (Vol. 1, No. 14, pp. 281-297).
- Maraun, D. and Kurths, J., 2004. Cross wavelet analysis: significance testing and pitfalls. *Nonlinear Processes in Geophysics*, 11(4), pp.505-514.

- Mason, S.J. and Tippett, M.K., 2015. Climate Predictability Tool version 15.2. Available online from: <https://academiccommons.columbia.edu/doi/10.7916/D8NK3DWJ>. Last accessed 12 August 2019.
- Melin, R., 1937. Forecasting Spring Run-off of the Forest-Rivers in North Sweden. *Geografiska Annaler*, 19(1-2), pp.118-125.
- Miller, D.E. and Wang, Z., 2019. Assessing Seasonal Predictability Sources and Windows of High Predictability in the Climate Forecast System, Version 2. *Journal of Climate*, 32(4), pp.1307-1326.
- Mo, K.C. and Lettenmaier, D.P., 2014. Hydrologic prediction over the conterminous United States using the national multi-model ensemble. *Journal of Hydrometeorology*, 15(4), pp.1457-1472.
- Mo, K.C., Shukla, S., Lettenmaier, D.P. and Chen, L.C., 2012. Do Climate Forecast System (CFSv2) forecasts improve seasonal soil moisture prediction?. *Geophysical Research Letters*, 39(23).
- Molteni, F., Buizza, R., Palmer, T.N. and Petroliagis, T., 1996. The ECMWF ensemble prediction system: Methodology and validation. *Quarterly journal of the royal meteorological society*, 122(529), pp.73-119.
- Molteni, F., Stockdale, T., Balmaseda, M., Balsamo, G., Buizza, R., Ferranti, L., Magnusson, L., Mogensen, K., Palmer, T. and Vitart, F., 2011. The new ECMWF seasonal forecast system (System 4) (Vol. 49). Reading, U. K: European Centre for Medium-Range Weather Forecasts.
- Morlet, J., Arens, G., Farge, E. and Gild, D., 1982a. Wave propagation and sampling theory—Part I: Complex signal and scattering in multilayered media. *Geophysics*, 47(2), pp.203-221.
- Morlet, J., Arens, G., Farge, E. and Gild, D., 1982b. Wave propagation and sampling theory—Part II: Sampling theory and complex waves. *Geophysics*, 47(2), pp.222-236.
- Grossmann, A. and Morlet, J., 1984. Decomposition of Hardy functions into square integrable wavelets of constant shape. *SIAM journal on mathematical analysis*, 15(4), pp.723-736.
- Grossmann, A. and Morlet, J., 1985. Decomposition of functions into wavelets of constant shape, and related transforms. In *Mathematics+ Physics: Lectures on Recent Results (Volume 1)* (pp. 135-165).
- Mutai, C.C., Ward, M.N. and Colman, A.W., 1998. Towards the prediction of the East Africa short rains based on sea-surface temperature–atmosphere coupling. *International Journal of Climatology: A Journal of the Royal Meteorological Society*, 18(9), pp.975-997.
- Nash, J. E., & Sutcliffe, J. V. (1970). River flow forecasting through conceptual models part I—A discussion of principles. *Journal of hydrology*, 10(3), 282-290.
- Olsson, J., Uvo, C.B., Foster, K. and Yang, W., 2016. Initial assessment of a multi-method approach to spring-flood forecasting in Sweden. *Hydrology and Earth System Sciences*, 20(2), pp.659-667.
- Orlove, B.S., Chiang, J.C. and Cane, M.A., 2000. Forecasting Andean rainfall and crop yield from the influence of El Niño on Pleiades visibility. *Nature*, 403(6765), p.68.

- Pearson, K., 1901. LIII. On lines and planes of closest fit to systems of points in space. *The London, Edinburgh, and Dublin Philosophical Magazine and Journal of Science*, 2(11), pp.559-572.
- Pagano, T.C., Garen, D.C., Perkins, T.R. and Pasteris, P.A., 2009. Daily updating of operational statistical seasonal water supply forecasts for the western US 1. *JAWRA Journal of the American Water Resources Association*, 45(3), pp.767-778.
- Palmer, T.N. and Anderson, D.L.T., 1994. The prospects for seasonal forecasting—A review paper. *Quarterly Journal of the Royal Meteorological Society*, 120(518), pp.755-793.
- Panagiotopoulos, F., Shahgedanova, M. and Stephenson, D.B., 2002, November. A review of Northern Hemisphere winter-time teleconnection patterns. In *Journal de Physique IV (Proceedings)* (Vol. 12, No. 10, pp. 27-47). EDP sciences.
- Polyakov, I.V. and Johnson, M.A., 2000. Arctic decadal and interdecadal variability. *Geophysical Research Letters*, 27(24), pp.4097-4100.
- Qian, S., Chen, J., Li, X., Xu, C.Y., Guo, S., Chen, H. and Wu, X., 2019. Seasonal rainfall forecasting for the Yangtze River basin using statistical and dynamical models. *International Journal of Climatology*.
- Rahmstorf, S., 2006. Thermohaline ocean circulation. *Encyclopedia of quaternary sciences*, 5. [Elsevier], Amsterdam.
- Robertson, D.E., Pokhrel, P. and Wang, Q.J., 2013. Improving statistical forecasts of seasonal streamflows using hydrological model output. *Hydrology and Earth System Sciences*, 17(2), pp.579-593.
- Roeckner, E., Arpe, K., Bengtsson, L., Christoph, M., Claussen, M., Dümenil, L., Esch, M., Giorgetta, M.A., Schlese, U. and Schulzweida, U., 1996. The atmospheric general circulation model ECHAM-4: Model description and simulation of present-day climate.
- Roeckner, E., Bäuml, G., Bonaventura, L., Brokopf, R., Esch, M., Giorgetta, M., Hagemann, S., Kirchner, I., Kornbluh, L., Manzini, E. and Rhodin, A., 2003. The atmospheric general circulation model ECHAM 5. PART I: Model description.
- Rogers, J.C., 1997. North Atlantic storm track variability and its association to the North Atlantic Oscillation and climate variability of northern Europe. *Journal of Climate*, 10(7), pp.1635-1647.
- Rosenberg, E.A., Wood, A.W. and Steinemann, A.C., 2011. Statistical applications of physically based hydrologic models to seasonal streamflow forecasts. *Water Resources Research*, 47(3).
- Rousseeuw, P.J., 1987. Silhouettes: a graphical aid to the interpretation and validation of cluster analysis. *Journal of computational and applied mathematics*, 20, pp.53-65.
- Rundgren, L. and Martna, J., 1989. Underground hydropower projects in Sweden. *Tunnelling and Underground Space Technology*, 4(2), pp.131-137.
- Sadeghi, S., Tootle, G., Elliott, E., Lakshmi, V., Therrell, M., Kam, J. and Bearden, B., 2019. Atlantic Ocean Sea Surface Temperatures and Southeast United States Streamflow Variability: Associations with the Recent Multi-decadal Decline. *Journal of Hydrology*.

- Saha, S., Moorthi, S., Wu, X., Wang, J., Nadiga, S., Tripp, P., Behringer, D., Hou, Y.T., Chuang, H.Y., Iredell, M. and Ek, M., 2014. The NCEP climate forecast system version 2. *Journal of Climate*, 27(6), pp.2185-2208.
- Schepen, A., Zhao, T., Wang, Q.J., Zhou, S. and Feikema, P., 2016. Optimising seasonal streamflow forecast lead time for operational decision making in Australia. *Hydrology and Earth System Sciences*, 20(10), pp.4117-4128.
- Seibert, M., Merz, B. and Apel, H., 2017. Seasonal forecasting of hydrological drought in the Limpopo Basin: a comparison of statistical methods. *Hydrology and Earth System Sciences*, 21(3), pp.1611-1629.
- Shamir, E., 2017. The value and skill of seasonal forecasts for water resources management in the Upper Santa Cruz River basin, southern Arizona. *Journal of Arid Environments*, 137, pp.35-45.
- Shirvani, A. and Landman, W.A., 2016. Seasonal precipitation forecast skill over Iran. *International Journal of Climatology*, 36(4), pp.1887-1900.
- Shukla, J., DelSole, T., Fennessy, M., Kinter, J. and Paolino, D., 2006. Climate model fidelity and projections of climate change. *Geophysical Research Letters*, 33(7).
- Sittichok, K., Djibo, A.G., Seidou, O., Saley, H.M., Karambiri, H. and Paturel, J., 2016. Statistical seasonal rainfall and streamflow forecasting for the Sirba watershed, West Africa, using sea-surface temperatures. *Hydrological Sciences Journal*, 61(5), pp.805-815.
- SMHI, 2016. HBV - Hydrologiska Byråns Vattenbalansavdelning. Available online from: (<https://www.smhi.se/en/research/research-departments/hydrology/hbv-1.90007>). Last accessed 12 August 2019.
- SMHI, 2017. Normal medelvattenföring. Available on line from: <https://www.smhi.se/data/hydrologi/vattenforing/normal-medelvattenforing-1.7999>. Last accessed 12 August 2019.
- SMHI, (2019). Nederbörd - NORMALVÄRDEN (1961-1990). Available online from: <https://www.smhi.se/data/meteorologi/nederbord>. Last accessed 12 August 2019.
- Smith, D.M., Scaife, A.A., Eade, R. and Knight, J.R., 2016. Seasonal to decadal prediction of the winter North Atlantic Oscillation: emerging capability and future prospects. *Quarterly Journal of the Royal Meteorological Society*, 142(695), pp.611-617.
- Statistiska centralbyrån (2018) El-, gas- och fjärrvärmeförsörjningen 2015, Slutliga uppgifter. Available online from: ([https://www.scb.se/contentassets/9a024e13098e4dc0b85feec1f288a68b/en0105\\_2015a01\\_sm\\_en11sm1601.pdf](https://www.scb.se/contentassets/9a024e13098e4dc0b85feec1f288a68b/en0105_2015a01_sm_en11sm1601.pdf)). Last accessed 12 August 2019.
- Sun, L., Ji, S., Yu, S. and Ye, J., 2009, June. On the equivalence between canonical correlation analysis and orthonormalized partial least squares. In *Twenty-First International Joint Conference on Artificial Intelligence*.
- Thober, S., Kumar, R., Sheffield, J., Mai, J., Schäfer, D. and Samaniego, L., 2015. Seasonal soil moisture drought prediction over Europe using the North American Multi-Model Ensemble (NMME). *Journal of Hydrometeorology*, 16(6), pp.2329-2344.
- Thompson, P.D., 1957. Uncertainty of initial state as a factor in the predictability of large scale atmospheric flow patterns. *Tellus*, 9(3), pp.275-295.

- Thompson, D.W. and Wallace, J.M., 1998. The Arctic Oscillation signature in the wintertime geopotential height and temperature fields. *Geophysical research letters*, 25(9), pp.1297-1300.
- Thompson, D.W. and Wallace, J.M., 2001. Regional climate impacts of the Northern Hemisphere annular mode. *Science*, 293(5527), pp.85-89.
- Torrence, C. and Compo, G.P., 1998. A practical guide to wavelet analysis. *Bulletin of the American Meteorological society*, 79(1), pp.61-78.
- Trambauer, P., Werner, M., Winsemius, H.C., Maskey, S., Dutra, E. and Uhlenbrook, S., 2015. Hydrological drought forecasting and skill assessment for the Limpopo River basin, southern Africa. *Hydrology and Earth System Sciences*, 19(4), pp.1695-1711.
- Tuel, A. and Eltahir, E.A.B., 2018. Seasonal precipitation forecast over Morocco. *Water Resources Research*, 54(11), pp.9118-9130.
- Uvo, C.B., 1998. Influence of Sea Surface Temperature on Rainfall and Runoff in Northeastern South America: Analysis and Modeling (Doctoral dissertation, Lund University).
- Uvo, C.B. and Berndtsson, R., 1996. Regionalization and spatial properties of Ceará State rainfall in northeast Brazil. *Journal of Geophysical Research: Atmospheres*, 101(D2), pp.4221-4233.
- Uvo, C.B. and Graham, N.E., 1998. Seasonal runoff forecast for northern South America: A statistical model. *Water Resources Research*, 34(12), pp.3515-3524.
- Uvo, C.B., Repelli, C.A., Zebiak, S.E. and Kushnir, Y., 1998. The relationships between tropical Pacific and Atlantic SST and northeast Brazil monthly precipitation. *Journal of Climate*, 11(4), pp.551-562.
- Vattenfall, 2019a. Before Vattenfall. Available online from: <https://historia.vattenfall.se/sv/the-revolution-of-electricity/innan-vattenfall-fanns>. Last accessed 12 August 2019.
- Vattenregleringsföretagen, 2016. Vattenhushållning. Available online from: <http://www.vattenreglering.se/>. Last accessed 12 August 2019.
- Wallace, J.M. and Gutzler, D.S., 1981. Teleconnections in the geopotential height field during the Northern Hemisphere winter. *Monthly Weather Review*, 109(4), pp.784-812.
- Wallace, J.M., Zhang, Y. and Lau, K.H., 1993. Structure and seasonality of interannual and interdecadal variability of the geopotential height and temperature fields in the Northern Hemisphere troposphere. *Journal of Climate*, 6(11), pp.2063-2082.
- Wanders, N., Thober, S., Kumar, R., Pan, M., Sheffield, J., Samaniego, L. and Wood, E.F., 2019. Development and evaluation of a pan-European multimodel seasonal hydrological forecasting system. *Journal of Hydrometeorology*, 20(1), pp.99-115.
- Ward Jr, J.H., 1963. Hierarchical grouping to optimize an objective function. *Journal of the American statistical association*, 58(301), pp.236-244.
- Ward, M.N. and Folland, C.K., 1991. Prediction of seasonal rainfall in the north Nordeste of Brazil using eigenvectors of sea-surface temperature. *International Journal of Climatology*, 11(7), pp.711-743.

- Weisheimer, A. and Palmer, T.N., 2014. On the reliability of seasonal climate forecasts. *Journal of the Royal Society Interface*, 11(96), p.20131162.
- Wetterhall, F., Bárdossy, A., Chen, D., Halldin, S. and Xu, C.Y., 2006. Daily precipitation-downscaling techniques in three Chinese regions. *Water Resources Research*, 42(11).
- Wilby, R.L. and Wigley, T.M.L., 1997. Downscaling general circulation model output: a review of methods and limitations. *Progress in physical geography*, 21(4), pp.530-548.
- Wilks, D.S., 2011. *Statistical methods in the atmospheric sciences* (Vol. 100). Academic press.
- Wood, A.W., Maurer, E.P., Kumar, A. and Lettenmaier, D.P., 2002. Long-range experimental hydrologic forecasting for the eastern United States. *Journal of Geophysical Research: Atmospheres*, 107(D20), pp.ACL-6.
- Wood, A.W., Kumar, A. and Lettenmaier, D.P., 2005. A retrospective assessment of National Centers for Environmental Prediction climate model-based ensemble hydrologic forecasting in the western United States. *Journal of Geophysical Research: Atmospheres*, 110(D4).
- Wood, A.W. and Lettenmaier, D.P., 2006. A test bed for new seasonal hydrologic forecasting approaches in the western United States. *Bulletin of the American Meteorological Society*, 87(12), pp.1699-1712.
- Wood, A.W. and Lettenmaier, D.P., 2008. An ensemble approach for attribution of hydrologic prediction uncertainty. *Geophysical Research Letters*, 35(14).
- Wood, A.W., Hopson, T., Newman, A., Brekke, L., Arnold, J. and Clark, M., 2016. Quantifying streamflow forecast skill elasticity to initial condition and climate prediction skill. *Journal of Hydrometeorology*, 17(2), pp.651-668.
- Wu, Z. and Yu, L., 2016. Seasonal prediction of the East Asian summer monsoon with a partial-least square model. *Climate dynamics*, 46(9-10), pp.3067-3078.
- Yang, W., Andréasson, J., Phil Graham, L., Olsson, J., Rosberg, J. and Wetterhall, F., 2010. Distribution-based scaling to improve usability of regional climate model projections for hydrological climate change impacts studies. *Hydrology Research*, 41(3-4), pp.211-229.
- Yang, W., Bárdossy, A. and Caspary, H.J., 2010. Downscaling daily precipitation time series using a combined circulation-and regression-based approach. *Theoretical and applied climatology*, 102(3-4), pp.439-454.
- Yang, X.Y., Yuan, X. and Ting, M., 2016. Dynamical link between the Barents-Kara Sea ice and the Arctic oscillation. *Journal of Climate*, 29(14), pp.5103-5122.
- Yarnal, B., 1984. A procedure for the classification of synoptic weather maps from gridded atmospheric pressure surface data. *Computers & Geosciences*, 10(4), pp.397-410.
- Yoon, J.H., Mo, K. and Wood, E.F., 2012. Dynamic-model-based seasonal prediction of meteorological drought over the contiguous United States. *Journal of Hydrometeorology*, 13(2), pp.463-482.
- Yossef, N.C., Winsemius, H., Weerts, A., van Beek, R. and Bierkens, M.F., 2013. Skill of a global seasonal streamflow forecasting system, relative roles of initial conditions and meteorological forcing. *Water Resources Research*, 49(8), pp.4687-4699.

- Yu, L., Wu, Z., Zhang, R. and Yang, X., 2018. Partial least regression approach to forecast the East Asian winter monsoon using Eurasian snow cover and sea surface temperature. *Climate dynamics*, 51(11-12), pp.4573-4584.
- Yuan, X., 2016. An experimental seasonal hydrological forecasting system over the Yellow River basin–Part 2: The added value from climate forecast models. *Hydrology and Earth System Sciences*, 20(6), pp.2453-2466.
- Yuan, X., Wood, E.F., Luo, L. and Pan, M., 2011. A first look at Climate Forecast System version 2 (CFSv2) for hydrological seasonal prediction. *Geophysical research letters*, 38(13).
- Yuan, X., Liang, X.Z. and Wood, E.F., 2012. WRF ensemble downscaling seasonal forecasts of China winter precipitation during 1982–2008. *Climate dynamics*, 39(7-8), pp.2041-2058.
- Yuan, X., Wood, E.F., Roundy, J.K. and Pan, M., 2013a. CFSv2-based seasonal hydroclimatic forecasts over the conterminous United States. *Journal of Climate*, 26(13), pp.4828-4847.
- Yuan, X., Wood, E.F., Chaney, N.W., Sheffield, J., Kam, J., Liang, M. and Guan, K., 2013b. Probabilistic seasonal forecasting of African drought by dynamical models. *Journal of Hydrometeorology*, 14(6), pp.1706-1720.
- Yuan, X., Roundy, J.K., Wood, E.F. and Sheffield, J., 2015. Seasonal forecasting of global hydrologic extremes: system development and evaluation over GEWEX basins. *Bulletin of the American Meteorological Society*, 96(11), pp.1895-1912.
- Yuan, X., Ma, F., Wang, L., Zheng, Z., Ma, Z., Ye, A. and Peng, S., 2016. An experimental seasonal hydrological forecasting system over the Yellow River basin–Part 1: Understanding the role of initial hydrological conditions. *Hydrology and Earth System Sciences*, 20(6), pp.2437-2451.
- Zadeh, L.A., 1965. Fuzzy sets. *Information and control*, 8(3), pp.338-353.
- Zaherpour, J., Mount, N., Gosling, S.N., Dankers, R., Eisner, S., Gerten, D., Liu, X., Masaki, Y., Schmied, H.M., Tang, Q. and Wada, Y., 2019. Exploring the value of machine learning for weighted multi-model combination of an ensemble of global hydrological models. *Environmental modelling & software*, 114, pp.112-128.
- Zorita, E. and Von Storch, H., 1999. The analog method as a simple statistical downscaling technique: comparison with more complicated methods. *Journal of climate*, 12(8), pp.2474-2489.







Lund University  
Faculty of Engineering  
Department of Building and Environmental Technology  
Water Resources Engineering  
ISBN 978-91-7623-986-5  
ISSN 1101-9824

